STUDIES IN SPORT, PHYSICAL EDUCATION AND HEALTH
232

Mika Silvennoinen

The Oxidative Capacity of Skeletal Muscle

Effects of Genotype, High-Fat Diet and Physical Activity

JYVÄSKYLÄN YLIOPISTO

STUDIES IN SPORT, PHYSICAL EDUCATION AND HEALTH 232

Mika Silvennoinen

The Oxidative Capacity of Skeletal Muscle

Effects of Genotype, High-Fat Diet and Physical Activity

Esitetään Jyväskylän yliopiston liikuntatieteellisen tiedekunnan suostumuksella
julkisesti tarkastettavaksi yliopiston vanhassa juhlasalissa (S212)
tammikuun 22. päivänä 2016 kello 12.

Academic dissertation to be publicly discussed, by permission of
the Faculty of Sport and Health Sciences of the University of Jyväskylä,
in building Seminarium, auditorium S212 on January 22, 2016 at 12 o'clock noon.

UNIVERSITY OF JYVÄSKYLÄ

JYVÄSKYLÄ 2016

The Oxidative Capacity of Skeletal Muscle

Effects of Genotype, High-Fat Diet and Physical Activity

STUDIES IN SPORT, PHYSICAL EDUCATION AND HEALTH 232

Mika Silvennoinen

The Oxidative Capacity of Skeletal Muscle

Effects of Genotype, High-Fat Diet and Physical Activity

UNIVERSITY OF JYVÄSKYLÄ

JYVÄSKYLÄ 2016

Editors
Taija Juutinen
Faculty of Sport Sciences, University of Jyväskylä
Pekka Olsbo
Publishing Unit, University Library of Jyväskylä

URN:ISBN:978-951-39-6519-8
ISBN 978-951-39-6519-8 (PDF)

ISBN 978-951-39-6518-1 (nid.)
ISSN 0356-1070

Jyväskylä University Printing House, Jyväskylä 2016

The characteristic of scientific progress is our knowing that we did not know

Gaston Bachelard, French philosopher (1884-1962)

ABSTRACT

Silvennoinen, Mika
The oxidative capacity of skeletal muscle: effects of genotype, high-fat diet and physical activity
Jyväskylä: University of Jyväskylä, 2016, 121 p.
(Studies in Sport, Physical Education and Health
ISSN 0356-1070; 232)
ISBN 978-951-39-6518-1 (nid.)
ISBN 978-951-39-6519-8 (PDF)

The primary purpose of the current dissertation was to investigate the effects of genotype, high-fat diet and physical activity on constituents of skeletal muscle oxidative capacity. More specifically we aimed to: 1) determine the characteristics of inherited oxidative capacity in rat skeletal muscle and investigate the gene expression profiles that could connect aerobic exercise capacity with metabolic disease risk factors; 2) investigate the effects of high-fat diet (HFD) and voluntary running on capillarization in skeletal muscle of mice; 3) to develop a system that is able to quantify the physical activity of sedentary and voluntary running mice; 4) to study skeletal muscle adaptation mechanisms after resistance exercise (RE) or endurance exercise (EE) by investigating acute gene expression responses of PGC-1 isoforms in humans. The rats with low inherited oxidative capacity (LCRs) had higher levels of metabolic disease risk factors. The rats with high inherited oxidative capacity (HCRs) had higher resting metabolic rate and levels of voluntary activity, as well as higher capillarization and mitochondrial area in their skeletal muscles. In addition, HCRs had higher expression of genes related to aerobic energy production pathways and branched chain amino acid degradation. Furthermore, the analyses showed that the expression of genes related to oxidative phosphorylation and lipid metabolism was associated with whole-body glucose balance. Both HFD and voluntary running induced capillarization in the skeletal muscle of mice. HFD increased protein level of angiogenic factor VEGF-A in muscle tissue and mRNA levels of VEGF-A and HIF-1α in endothelial cells. Calibration measurements and long-term activity measurements of mice showed that the developed activity measurement system is valid for its intended purpose. The assay of PGC-1 mRNA expression responses in human skeletal muscle confirmed that the alternative promoter originated transcripts are vastly upregulated after both EE and RE, whereas the proximal promoter originated transcripts are less inducible and were upregulated only after EE. Truncated PGC-1α transcripts were upregulated after both EE and RE. In conclusion, the current dissertation described the characteristics of inherited oxidative capacity in skeletal muscle and supported the significant role of aerobic metabolism in the development of metabolic diseases. Furthermore, HFD induces angiogenesis in skeletal muscle, which may be linked to increased expression of HIF-1α and VEGF-A in endothelial cells. The current dissertation supported the idea that PGC-1α isoforms may have an important role in exercise mode-specific muscle adaptations. The current results increase our knowledge of factors affecting the oxidative capacity of skeletal muscles, which may help to understand the pathogenic processes of physical inactivity-mediated disorders, as well as helping to develop new treatments or preventive therapies.

Keywords: exercise, high-fat diet, adaptation, angiogenesis, mitochondrial biogenesis, gene expression

Author's address Mika Silvennoinen
Department of Biology of Physical Activity
P.O. Box 35
FI-40014 University of Jyväskylä, Finland
mika.m.silvennoinen@jyu.fi

Supervisor Professor Heikki Kainulainen, PhD
Department of Biology of Physical Activity
University of Jyväskylä
Jyväskylä, Finland

Reviewers Professor Tara Haas, PhD
Faculty of Health
York University, UK

Adjunct professor Kari Kalliokoski, PhD
Turku PET Centre
University of Turku, Finland

Opponent Professor Philip Atherton, PhD
Faculty of Medicine & Health Sciences
University of Nottingham, UK

ACKNOWLEDGEMENTS

The main work described in this dissertation was carried out in the laboratories of the Neuromuscular Research Centre, Department of Biology of Physical Activity at the University of Jyväskylä. The facilities provided excellent tools to do the research. The financial support by the Academy of Finland, the Finnish Ministry of Education and Culture, Ellen & Artturi Nyyssönen foundation, LIKES Foundation, the TBDP national graduate school, and the University of Jyväskylä are acknowledged with gratitude.

I wish to express my biggest gratitude to my supervisor Prof. Heikki Kainulainen for his patience and belief in me. We travelled a long journey that occasionally seemed to be endless. You once said a long time ago in Tampere that you will help me to achieve my PhD, and you really did everything to keep your promise. The major part of the strength required to finish this journey came from my desire to honour your support. I would also like to thank Prof. Urho Kujala for his expertise and support.

I thank docent Juha Hulmi for his friendship, marvellous personality, and indispensable support. His support and guidance contributed to the extra boost that was needed to cross the finish line. Jussi Peltonen, PhD, I want to thank for his brotherhood. He is a great scientist who always has time for a good debate. Sira Torvinen, MSc, I would like to thank for being my roommate with whom I have spent most of my working hours during recent years. I think we started as rivals but ended up as colleagues and friends who appreciate each other a lot.

I also wish to thank all the co-authors of the original papers for their contributions to writing the manuscripts and performing the studies. I would like to especially thank Riikka Kivelä, PhD, Maarit Lehti, PhD and Rita Rinnankoski-Tuikka, PhD, for their friendship and the partnership that we shared, especially at the beginning of our PhD studies. In addition, the significant contributions of Timo Rantalainen, PhD and Juha Ahtiainen, PhD, are acknowledged.

I am thankful to my family, who supported me with their love and care. I would like to especially thank my father who has always believed in me, supported me and given me the freedom to find my own path. Finally, I thank my loving partner Laura. It is not easy to live with a scientist who likes to question nearly everything. However, I will never question my love for you and our incredible boys Veli and Samu.

Jyväskylä, November 2015
Mika Silvennoinen

LIST OF ORIGINAL ARTICLES

This thesis is based on the following original articles, which are referred to in the text by their Roman numerals.

I Kivelä R, **Silvennoinen M**, Lehti M, Rinnankoski-Tuikka R, Purhonen T, Ketola T, Pullinen K, Vuento M, Mutanen N, Sartor MA, Reunanen H, Koch LG, Britton SL, Kainulainen H. 2010. Gene expression centroids that link with low intrinsic aerobic exercise capacity and complex disease risk. The FASEB Journal 24 (11), 4565-74.

II **Silvennoinen M***, Rinnankoski-Tuikka R*, Vuento M, Hulmi JJ, Torvinen S, Lehti M, Kivelä R, Kainulainen H. 2013. High-fat feeding induces angiogenesis in skeletal muscle and activates angiogenic pathways in capillaries. Angiogenesis 16 (2), 297-307. (*equal contribution)

III **Silvennoinen M**, Rantalainen T, Kainulainen H. 2014. Validation of a method to measure total spontaneous physical activity of sedentary and voluntary running mice. Journal of Neuroscience Methods 235, 51-58.

IV **Silvennoinen M**, Ahtiainen J, Hulmi JJ, Pekkala S, Taipale R, Nindl B, Laine T, Häkkinen K, Selänne H, Kyröläinen H, Kainulainen H. 2015. PGC-1 isoforms and their target genes are expressed differently in human skeletal muscle following resistance and endurance exercise. Physiological Reports 3 (10), e12563.

ABBREVIATIONS

Aco1/2	aconitase 1/2
AMPK	5' adenosine monophosphate-activated protein kinase
Ang1/2	angiopoietin 1/2
ATF2	activating transcription factor 2
ATP	adenosine triphosphate
a-v O_2 difference	arteriovenous oxygen difference
CaMK	Ca2+/calmodulin-dependent protein kinase
CK	creatine kinase
CMJ	countermovement jump
CPT1a/b/2	carnitine palmitoyltransferase 1a/b/2
CREB	cAMP response element-binding protein
CV_{rms}	root-mean-square coefficient of variation
Cyc	cytochrome c
EDL	extensor digitorum longus
EE	endurance exercise
ES	enrichment score
ERK1/2	extracellular-regulated kinase 1/2
ERRα	estrogen-related receptor-α
FAK	focal adhesion kinase
Fat-%	body fat percentage
FDR q	false discovery rate q value
FOXO1	forkhead box protein O1
FWER *P*	familywise error rate *P* value
GAPDH	glyceraldehyde 3-phosphate dehydrogenase
Hadhb	hydroxyacyl-CoA dehydrogenase b
HCR	high capacity runner
HDAC	histone deacetylase
HFD	high-fat diet
HFS	high-fat sedentary
HFA	high-fat active
HIF-1α	hypoxia-inducible factor-1α
HOMA-IR	homeostatic model assessment of insulin resistance
HR_{max}	maximum heart rate
IGF-1	insulin-like growth factor 1
JNK	c-jun N-terminal kinase
LCM	laser capture microdissection
LCR	low capacity runner
LFD	low-fat diet
LFS	low-fat sedentary
LFA	low-fat active
LOA	limits of agreement
Lpl	lipoprotein lipase
MAFbx	muscle atrophy F-box

MAPK	mitogen-activated protein kinase
MEF2	myocyte enhancer binding factor-2
MHC	myosin heavy chain
MMP	matrix metalloproteinase
mTOR	mammalian target of rapamycin
MuRF1	muscle RING finger 1
MVC	maximal voluntary contraction
MQF	musculus quadriceps femoris
NAD^+	nicotinamide adenine dinucleotide (oxidized)
NADH	nicotinamide adenine dinucleotide (reduced)
NES	normalized enrichment score
NOM *P*	nominal *P* value
NRF-1/2	nuclear respiratory factor 1/2
NT-PGC-1α	N-truncated PGC-1α
PA	phosphatidic acid
PGC-1α/β	peroxisome proliferator-activated receptor gamma coactivator-1α/β
PHD	prolyl hydroxylase
P_iO_2	partial pressure of oxygen
PI3K	phosphatidylinositide 3-kinases
PPAR	peroxisome proliferator-activated receptor
p38 MAPK	p38 mitogen-activated protein kinase
p53	tumour protein p53
p70S6K	ribosomal protein S6 kinase
RE	resistance exercise
Rheb	ras homolog enriched in brain
ROS	reactive oxygen species
SDS-PAGE	sodium dodecyl sulphate polyacrylamide gel electrophoresis
SIRT1/2	sirtuin 1/2
SRF	serum response factor
TCA	tricarboxylic acid
TFAM	mitochondrial transcription factor A
Tie2	tyrosine kinase with immunoglobulin-like and EGF-like domains 2
TORC1/2	mTOR complex 1/2
TSC1/2	tuberous sclerosis complex 1/2
Ucp2/3	uncoupling protein 2/3
VEGF-A	vascular endothelial growth factor-A
VEGFR-2	vascular endothelial growth factor receptor-2
VL	musculus vastus lateralis
VO_{2max}	maximal oxygen uptake
1RM	one-repetition maximum
4E-BP1	eukaryotic initiation factor 4E-binding protein
10RM	ten-repetition maximum

CONTENTS

1 INTRODUCTION

Aerobic energy production is a principal element in the energy metabolism of the human body. Nowadays, it is very clear that adequate aerobic capacity is essential for human health. Numerous studies have shown that aerobic exercise capacity is a strong independent predictor of all-cause mortality (Blair et al. 1989; Blair et al. 1996; Kokkinos et al. 2008; Myers et al. 2002; Gulati et al. 2003; Kodama et al. 2009). Even small (3.5 mL/ Kg body weight per minute) increases in aerobic capacity have been reported to reduce mortality significantly (~13%) (Kokkinos et al. 2008). Furthermore, high aerobic capacity seems to provide significant protection from cardiovascular diseases (Blair et al. 1996), hypertension (Barlow et al. 2006), type 2 diabetes (Carnethon et al. 2009), and some cancers (Kampert et al. 1996).

Current evidence suggests that reduced mitochondrial content, mitochondrial function and reduced capacity for fatty acid oxidation in skeletal muscle are important contributors to the development of insulin resistance and type 2 diabetes (Simoneau & Kelley 1997; Kelley et al. 1999; Kim et al. 2000; Hulver et al. 2003; Toledo et al. 2007). This is further supported by the fact that insulin resistant individuals with a family history of type 2 diabetes have lower mitochondrial content and oxidative capacity in their skeletal muscles, suggesting that mitochondrial deficiency may be a cause, and not a consequence of insulin resistance (Petersen et al. 2004).

Although aerobic capacity is highly genetically determined (up to 50%), physical activity can significantly increase mitochondrial content and function in skeletal muscle (Holloszy & Coyle 1984; Toledo et al. 2007; Bouchard et al. 1998). However, the problem is that approximately 30% of adults and 80% of adolescents do not achieve the recommended levels of physical activity (Hallal et al. 2012). As Frank Booth has stated: "A sedentary life is now so prevalent that it has become common to refer to exercise as having "healthy benefits" even though the exercise-trained state is the biologically normal condition. It is a lack of exercise that is abnormal and causes health risks" (Booth et al. 2000). Epidemiological studies have shown that physical inactivity increases the incidence of at least 17 unhealthy conditions and related chronic diseases (Booth et

al. 2000). Ageing exacerbates inactivity-induced problems by reducing skeletal muscle mitochondrial density and function that may be caused by oxidative damage of DNA or age-induced reduction of physical activity (Short et al. 2005).

So far it is not clear how high aerobic capacity protects from premature death and development of metabolic diseases. However, it has been suggested that part of the development of insulin resistance, which is a major risk factor for metabolic diseases, could be caused by lipid accumulation in skeletal muscle that leads to insulin resistance of skeletal muscle fibers. Lipids accumulate in skeletal muscle when energy intake exceeds the storage capacity of adipose tissue, and when fatty acid oxidation capacity cannot cope with increased fatty acid uptake (Manco, Calvani & Mingrone 2004; Savage, Petersen & Shulman 2007). Thus, it is probable that individuals with high aerobic capacity are more able to cope with increased fatty acid uptake. Dube et al. have shown that moderate increases in physical activity increase insulin sensitivity of obese, previously sedentary insulin resistant people (Dube et al. 2008). Interestingly, the increase of physical activity increased intramuscular triglyceride content but decreased diacylglycerol and ceramide content. Thus, it seems that the triglyceride content of skeletal muscle is not a major player in insulin resistance development. Instead, the study of Dube et al. (Dube et al. 2008) and also other studies have suggested that other lipid metabolites like diacylglycerol and ceramide may be more directly linked to the development of insulin resistance (Yu et al. 2002; Turinsky, O'Sullivan & Bayly 1990; Chaurasia & Summers 2015).

Because aerobic capacity is important for human health and performance, it is very important to understand the physiological components of aerobic capacity and how they are affected by genotype and environmental factors. This knowledge could provide insight into the pathogenic processes of diseases that are influenced by aerobic capacity. Furthermore, this knowledge may help to develop new exercise or pharmaceutical treatments, or preventive therapies for the diseases in question. The primary aim of the current dissertation was to investigate the effects of genotype, high-fat diet and physical activity on constituents of skeletal muscle oxidative capacity. More specific aims of the dissertation were: 1) to determine the characteristics of inherited oxidative capacity in rat skeletal muscle and investigate the relationships that connect aerobic exercise capacity with metabolic disease risk factors; 2) to investigate the effects of high-fat diet and physical activity on capillarization in skeletal muscle of mice; 3) to develop and validate a system, which is able to quantify the total spontaneous activity of sedentary and voluntary running mice; 4) to study skeletal muscle adaptation mechanisms after a single bout of high-load resistance exercise or moderate intensity endurance exercise by investigating acute gene expression responses of different PGC-1 isoforms in human skeletal muscle. The thesis is a combination of a literature review and a summary of four original articles.

2 LITERATURE REVIEW

2.1 Overview of the energy metabolism of skeletal muscles

Like all animal cells, skeletal muscle fibers require energy to fuel their cellular processes. The energy can be derived from digested foods that contain fat, carbohydrate or protein. Before the cells can use this energy it has to be processed to ATP in energy production pathways.

2.1.1 Energy production pathways

The majority of ATP is produced in aerobic energy production pathways where either fat or carbohydrates (glucose) are oxidized. The fat oxidation starts in mitochondria where fatty acids are hydrolysed to acetyl groups in β-oxidation. In the following step, the acetyl groups are connected with Coenzyme A producing acetyl-CoA, which enters the tricarboxylic acid cycle (TCA) for further oxidation. In addition to carbon dioxide, TCA releases hydrogen ions and electrons that are combined with oxygen in oxidative phosphorylation. The process generates usable chemical energy in the form of ATP. The breakdown of glucose can be performed via aerobic or anaerobic pathways. Both pathways start in cytosol with glycolysis that converts glucose into pyruvate in ten enzyme-catalysed reactions. The energy released in this process is used to form ATP, and released hydrogen ions and electrons reduce NAD^+ to NADH (reduced nicotinamide adenine dinucleotide). From this stage, aerobic and anaerobic pathways separate. In the aerobic pathway, produced pyruvate molecules are transported into the mitochondria, where they are converted to acetyl-CoA, which enter the TCA and go through the same ATP-producing aerobic processes described earlier concerning fat oxidation. In contrast to aerobic glycolysis, anaerobic glycolysis does not need oxygen, because pyruvate, hydrogen ions and electrons do not enter TCA and oxidative phosphorylation. Instead, they react together in catalysed reactions and form lactic acid. The formation of lactic acid oxidizes NADH to NAD^+ that is needed in glycolysis. Thus, lactic acid

formation enables the continuation of ATP production using just the anaerobic glycolysis pathway. The rate of ATP production is faster in anaerobic glycolysis but the amount of produced ATP is much less compared to aerobic glycolysis. In addition to the described ATP production pathways, small amounts of ATP can be reproduced quickly by hydrolysing creatine phosphate.

2.1.2 Energy production in skeletal muscle during exercise

Skeletal muscles are able to rapidly modulate rate of energy production, blood flow, and substrate utilization in response to locomotion. Although resting intramuscular stores of ATP are small, the activation of energy production pathways maintains the intracellular levels of ATP. During acute exercise, the relative intensity and absolute power output determine which metabolic pathways are used in energy production. The partitioning of fuels used from extra- or intramuscular sources is coordinated quantitatively and temporally to meet the metabolic demands of exercise. Studies have shown that during low intensity exercise (25-40% VO_{2max}) the oxidation of fat (mostly plasma free fatty acids) provides the majority of required energy (Romijn et al. 1993; van Loon et al. 2001). As exercise intensity increases, the oxidation of circulating glucose and especially muscle glycogen increases in skeletal muscle. The oxidation of muscle triglycerides increases when the intensity of exercise increases from low to moderate (55-65% VO_{2max}) but thereafter further increments of intensity decrease fat oxidation. When moderate intensity exercise is prolonged (>60 min), an increasing proportion of energy is derived from circulating glucose and fatty acids (Romijn et al. 1993). At maximal intensity exercises of short duration like 100-m sprint or 25-m swim the required energy is derived almost exclusively from intramuscular ATP and creatine phosphate (McArdle, Katch & Katch 2014 ,169). The contribution of anaerobic glycolysis increases in the energy production when the duration of this type of exercise increases. However, when the exercise lasts over 2 min, the aerobic energy production pathways produce most of the energy (McArdle, Katch & Katch 2014 ,169).

2.1.3 Muscle fiber type characteristics

There are two primary muscle fiber types, which are type I and type II fibers. In human skeletal muscles type II fibers have two primary subclasses: type IIa and type IIx, while in rodent muscles significant amounts of type IIb fibers also exist (Schiaffino & Reggiani 2011). The fiber types are classified by the speed of contraction, their oxidative properties, and their staining properties. Type I muscle fibers contract slowly and they have greater aerobic metabolic capacity due to higher lipid, myoglobin, capillary, and mitochondrial content. On the contrary, type II muscle fibers have much faster contraction speeds, reduced oxidative capacity, lower myoglobin levels, fewer capillaries, and are better equipped for anaerobic metabolism. The oxidative capacity of type IIa fibers is higher compared to type IIx fibers, but less compared to type I fibers. Because type I fibers are slow, generate less mechanical power and use less ATP in relation to tension

development, they are more suitable for low-intensity and long-lasting activity (Schiaffino & Reggiani 2011). The corresponding characteristics of type II fibers are opposite and therefore type II fibers are best for short and strong muscle actions (Schiaffino & Reggiani 2011).

The four major fiber types are variously distributed in different muscles. Type I fibers are typically abundant in the muscles that maintain posture (e.g. soleus muscle). Type II fibers are more abundant in muscles that are needed in fast movements. Accordingly, human arm muscles contain more type II fibers than leg muscles (Harridge et al. 1996). There is also a significant amount of variation in the fiber type composition of skeletal muscles between individuals. For example, in a large cohort of Simoneau et al., the lowest proportion of type 1 fibers in vastus lateralis muscle was 15% and the highest 85% (Simoneau & Bouchard 1989). Based on data collected from American Caucasian men and women, it has been estimated that 45% of the total variance in proportion of type I muscle fibers is explained by inherited factors and 30% by differences in environmental factors (Simoneau & Bouchard 1995). Muscle fiber type is predominantly determined during early stages of post-natal development and it is still unclear how much adaptive transformation of muscle fibers from one type to another can occur. It has been shown that in rats type IIb fibers transform to IIx during ageing in fast muscles and from IIa to I in slow muscles (Larsson et al. 1995; Larsson et al. 1993). In human skeletal muscle, this type of fiber type profile change does not appear to happen during ageing, but the relative proportion of fast fibers seems to be reduced in the elderly due to greater atrophy of type II fibers (Lexell, Taylor & Sjöström 1988). Because muscle fiber type is controlled by innervating motoneurons, it has been speculated that the adaptive transformation of fiber types is limited by motor neuron plasticity (Schiaffino & Reggiani 2011). This would allow muscle fibers to transform from one fast fiber subclass to another (IIb↔IIX↔IIA) by altered activity of fast motor neurons during, for example, an endurance training protocol. However the transition between type I and II fibers would not be possible, because motor neurons cannot change their frequency pattern, which is specific for slow and fast motor units.

2.2 The cardiovascular system and skeletal muscle blood flow

The function of the cardiovascular system is to transport oxygen, hormones and nutrients to the tissues and waste products from the tissues, and in general to maintain optimal conditions in the cells. The main components of the system are the heart, blood and blood vessels and it includes systemic and pulmonary circulation. The pulmonary circulation is responsible for gas exchange in the lungs and the systemic circulation circulates oxygenated blood through the rest of the body. The circulatory system can be divided further into macrocirculation (arteries and veins) and microcirculation (arterioles, capillaries, venules). The macrocirculation manages the blood flow to and from organs and microcir-

culation controls blood flow in organ tissues. The arterioles are the last small branches of the arterial system, and they act as control conduits, which regulate the amount of blood released into the capillaries. The function of capillaries is to exchange fluid, gases, nutrients and other substances between the blood and the interstitial fluid. To be able to do this, the capillary walls are very thin and have numerous capillary pores that allow water and other small molecules to go through. When blood leaves the capillaries, it is collected by the venules, which coalesce into progressively larger veins, and finally the blood is transported back into the heart.

The blood flow to each tissue of the body is precisely controlled in relation to the tissue needs. The need for oxygen in skeletal muscle is highly variable depending on the level of contractile activity. At rest, the oxygen uptake by the muscle is approximately 1.5 ml of oxygen/min per 1 kg of tissue (Kalliokoski et al. 2001), whereas during intense contraction, oxygen uptake can increase 30-fold. To cope with a higher demand of oxygen, blood flow is increased in active muscles by opening a sufficient amount of arterioles. This happens because the muscles of arteriolar walls cannot maintain contraction when there is not enough oxygen available. Arterioles are also opened because of vasodilator substances, which are released when partial pressure of oxygen (PiO_2) is low. If oxygen demand and supply is not matched on a regular basis, the capillary network can adapt to this by reducing or increasing capillarization (Klausen, Andersen & Pelle 1981; Andersen & Henriksson 1977). Kalliokoski et al. have demonstrated skeletal muscle circulation adaptations by comparing endurance athletes with normal subjects (Kalliokoski et al. 2001). They found that endurance-trained subjects had higher oxygen extraction, longer blood transit time and their blood perfusion was more homogenous compared to untrained subjects at the same workload.

2.3 Aerobic capacity

The gold standard for aerobic capacity assessment is the measurement of maximum aerobic capacity (VO_{2max}) during a maximal graded exercise test to exhaustion. VO_{2max} is defined as the highest rate at which oxygen can be taken up and utilized in energy production by the body during severe exercise. It is one of the main variables in the field of exercise physiology, and is used to indicate the cardiorespiratory fitness of an individual.

2.3.1 Limiting factors of maximum oxygen uptake (VO_{2max})

VO_{2max} can be limited by central (pulmonary diffusing capacity, maximal cardiac output and oxygen carrying capacity of blood) and peripheral (skeletal muscle characteristics) factors (Figure 1) (Bassett & Howley 2000). In healthy humans the ability of the cardiorespiratory system to deliver oxygen to the exercising muscles is the primary limiting factor for VO_{2max} during whole-body

maximal exercises like bicycling or running tests. This is supported by three important facts: 1) when oxygen delivery is altered, VO_{2max} changes accordingly; 2) the increase in VO_{2max} induced by endurance training results primarily from an increase in maximal cardiac output (not an increase in the arteriovenous oxygen difference (a-v O_2 difference); and 3) when muscle is over perfused during exercise, it has a very high capacity for consuming oxygen (Bassett & Howley 2000). In spite of the important role of O_2 delivery, there is no single limiting factor to $VO_{2max,}$ because each step in the O_2 pathway contributes to determining VO_{2max}, and a reduction in the transport capacity of any of the steps will reduce VO_{2max} (Wagner 1992).

The lungs saturate the arterial blood with O_2 extremely well. Even during maximal work, the arterial O_2 saturation is stable and remains around 95% (Powers et al. 1989). Yet, the pulmonary system may limit VO_{2max} under certain circumstances. Dempsey et al. have shown that arterial O_2 desaturation during maximal work is more likely to occur in elite athletes compared with normal people (Dempsey, Hanson & Henderson 1984). Endurance-trained individuals have a much higher maximal cardiac output than untrained individuals. This may result in decreased transit time of blood in the pulmonary capillaries, which may not be enough to saturate the blood with O_2. Pulmonary limitations are also evident in people exercising at high altitudes or people with asthma or other types of pulmonary disease (Bassett & Howley 2000; Daniels & Oldridge 1970; Rooyackers et al. 1997).

Oxygen carrying capacity of blood can also limit VO_{2max}. It has been shown with highly trained endurance runners that reinfusion of 900 ml of blood elevates VO_{2max} on average by 5% (Buick et al. 1980).

It is clear that VO_{2max} is dependent on the interaction of O_2 transport and mitochondrial O_2 uptake. However, there is still controversy regarding whether peripheral diffusion of oxygen from capillary into muscle fibers is a limiting factor of VO_{2max} (Wagner 2015; Lundby & Montero 2015). The mitochondria are the organelles where O_2 is actually consumed in the final step of oxidative phosphorylation. In theory, doubling the number of mitochondria should also double the O_2 uptake capacity. However, Saltin et al. have shown that there is only a modest increase in VO_{2max} (20–40%) despite a 2.2-fold increase in mitochondrial enzymes after endurance training (Saltin et al. 1977). Thus, this supports the idea that at least during whole-body dynamic exercise, VO_{2max} is limited by oxygen delivery not muscle mitochondria. Why then does endurance exercise increase the amount of mitochondria if it does not improve VO_{2max}? Holloszy and Coyle have proposed that by mitochondrial adaptation 1) muscles will oxidize fat at a higher rate (thus sparing muscle glycogen and blood glucose) and 2) anaerobic energy production decreases during exercise (Holloszy & Coyle 1984). These muscle adaptations are important in explaining the improvement in endurance performance induced by training.

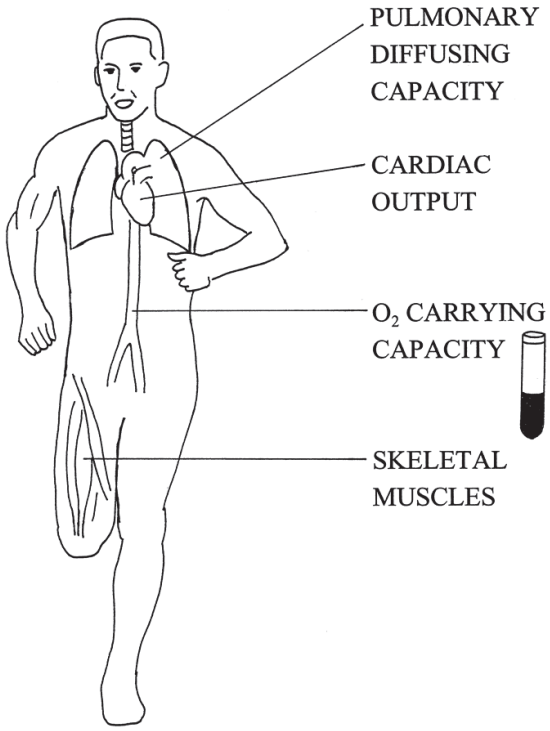

FIGURE 1 Limiting factors of $VO_{2max.}$ Pulmonary diffusing capacity determines the ability of the lungs to exchange gases between air and blood. Cardiac output is the amount of blood that the heart can pump through the circulatory system in one minute. O_2 carrying capacity is the total amount of oxygen that can be carried in the blood, which is dependent on the total amount of red blood cells and hemoglobin. Most of the oxygen utilised during maximal exercise is used in muscle fibers. The primary limiting factors of muscle oxygen uptake are capillary density and mitochondrion content of muscle. (Bassett & Howley 2000)

2.3.2 Exercise-induced adaptations in aerobic capacity

The aim of physical exercise is to disturb homeostasis of the body and certain organs like skeletal muscles or myocardium. When the exercise is progressive and regular, the affected tissues are forced to adapt to the challenge to minimize disruptions of homeostasis. Physical exercises consist of muscle actions that are generally combinations of concentric, isometric and eccentric contractions. The exercises normally consist of several modifiable variables including the modality, frequency, intensity, and duration of exercise sessions. All of these variables affect the metabolic and molecular responses elicited by exercise. Endurance and resistance exercises represent two extremes of the exercise continuum. Typical endurance exercise contains high volume repetitive muscle actions with low load, whereas in resistance exercise the volume of muscle actions is low and the load is rather high.

The purpose of endurance exercise programs is normally to improve endurance performance and aerobic capacity. Longitudinal studies have shown that endurance training induces an increase in VO_{2max} primarily by increasing maximal cardiac output rather than enhancing the systemic a-v O_2 difference. Ekblom et al. found that 16 weeks of endurance training increased VO_{2max} 17% (from 3.15 to 3.68 L/min) (Ekblom et al. 1968). This improvement in VO_{2max} resulted in an 8.0% increase in cardiac output (from 22.4 to 24.2 L/min) and a 3.6% increase in a-v O_2 difference (from 138 to 143 mL/L).

One of the main peripheral adaptations elicited by endurance exercise is the increase of mitochondrial content and respiratory capacity of muscle fibers both in humans and rodents. Underlying the increases in the respiratory capacity, endurance exercise increases the levels of the enzymes responsible for the activation, transport, and oxidation of fatty acids, the enzymes involved in ketone oxidation, the enzymes of TCA, and the components of the electron transport chain (Holloszy 1973; Holloszy & Coyle 1984).

There is no evidence that fast-twitch (type II) muscle fibers can be converted to slow–twitch fibers, or vice versa, by normal exercise training. However, it appears that strenuous endurance training can convert type IIb/IIx to type IIa fibers (Schiaffino & Reggiani 2011). Furthermore, the mitochondrial content of type II fibers tends to increase to a greater extent than that of type I fibers in response to strenuous endurance training (Holloszy & Coyle 1984).

It has been shown that endurance training also increases the capillarization of skeletal muscles (Brodal, Ingjer & Hermansen 1977; Andersen & Henriksson 1977; Ingjer 1979). In a study by Andersen at al., eight weeks of bicycle ergometer training (40 min/day, 4 times/week, 80% of VO_{2max}) resulted in a 16% increase in VO_{2max} and a 20% increase in capillary density (Andersen & Henriksson 1977). Saltin et al. have proposed that the main significance of the endurance training-induced increase in capillary density is to maintain or elongate mean transit time of blood in skeletal muscles (Saltin 1985). This enhances oxygen delivery by maintaining oxygen extraction (a-v O_2 difference) even at high rates of muscle blood flow.

Based on the studies of Sillanpää et al., long-term (21-weeks) resistance training does not significantly increase whole-body aerobic capacity (VO_{2max}) of men (40-65 years-old) or women (39-64 years-old) (Sillanpää et al. 2008; Sillanpää et al. 2009). Similar results have been found after ten weeks of resistance training in 19-45 year-old women (Keeler et al. 2001). In contrast, the study of Alvehus et al. has reported resistance training induced gains (~13%) in VO_{2max} after 8 weeks of heavy resistance training in young men (mean age: 25.3 ± 2.8 years) (Alvehus et al. 2014).

Early reports about muscle level adaptations suggested that skeletal muscle mitochondrial volume (MacDougall et al. 1979) and oxidative capacity (Chilibeck, Syrotuik & Bell 1999) are reduced by chronic resistance exercise training. Many studies have also shown that mitochondrial density (Luthi et al. 1986) and enzymes such as citrate synthase, β-hydroxyl-acyl-CoA dehydrogenase and succinate dehydrogenase, are largely unaltered by chronic resistance exercise

training (Tesch, Thorsson & Colliander 1990; Green et al. 1999; Tesch, Komi & Häkkinen 1987). These early studies mostly used measures of oxidative capacity, which reflect the abundance of mitochondrial proteins rather than mitochondrial function. Recently, Porter et al. studied the impact of a 12-week resistance exercise training program on skeletal muscle mitochondrial function in eleven young healthy men (Porter et al. 2015). Their study showed that resistance exercise training increased lean body mass and quadriceps muscle strength by 4 and 15%, respectively. In addition, they found that coupled mitochondria respiration was increased by ~2-fold. These results suggested that while resistance training does not induce significant mitochondrial biogenesis, it augments the intrinsic respiratory capacity and function of skeletal muscle mitochondria.

Studies have also shown that even though resistance training increases the area of muscle fibers, it does not compromise muscle tissue capillarization (Tesch, Thorsson & Colliander 1990; Green et al. 1999). In a study by Green et al., a 12-week resistance training program induced a 17% increase in the cross-sectional area of quadriceps femoris muscle (Green et al. 1999). However, because the number of capillaries increased (as indicated by increased capillary to fiber ratio), capillary density remained unchanged.

2.3.3 Inheritance and aerobic capacity

Bouchard et al. showed in their HERITAGE Family Study that there was significant familial aggregation for aerobic capacity (VO_{2max}) in sedentary humans, even when the data were adjusted for age, sex, body mass, and body composition (Bouchard et al. 1998). The study indicated that the maximal heritability of VO_{2max} among sedentary adults after adjustment for the above covariates could be as high as 50%. However, due to the presence of a significant spouse correlation, it seems that the genetic heritability is less than 50%. The data of the same study also revealed that maternal influence, perhaps mitochondrial inheritance, accounts for as much as 30% of the familial transmission (Bouchard et al. 1998).

Koch et al. have demonstrated inheritance of aerobic capacity by developing rat strains that contrast in inherent maximal running capacity (Koch & Britton 2001). Rat strains called high running capacity (HCR) and low running capacity (LCR) rats were produced by selective breeding. Selection for low and high capacity was based upon distance run to exhaustion on a motorized treadmill using a velocity-ramped running protocol. In each generation, within-family selection was practiced using 13 families for both the low and high lines. Six generations of selection produced lines that differed in running capacity by 171%. In generation 6 the low line ran 310 ± 8 m and the high line 839 ± 21 m at exhaustion. Moreover, selection generated 30% higher VO_{2max} in HCR versus LCR (Hoydal et al. 2007).

Studies have shown that there are considerable individual differences in the response of maximal aerobic capacity to endurance training (Bouchard et al. 1999). Among adults, some individuals exhibit a pattern of high response, whereas others present a pattern of no or minimal response, with a broad range of response phenotypes between the extremes. Bouchard et al. showed in their

study that the trainability of VO_{2max} is highly familial and includes a significant genetic component (Bouchard et al. 1999). Based on their data, the maximal heritability estimate for VO_{2max} response was 47%.

2.3.4 Effects of high-fat diet on aerobic capacity

It is well known that carbohydrate loading increases muscle and liver glycogen stores, simultaneously improving endurance performance and increasing the rate of glycogen utilization. Because sparing of glycogen is important in prolonged endurance performances, different dietary strategies have been tested that would diminish glycogen utilisation while increasing fat oxidation. For this purpose, low carbohydrate high-fat diets (HFD) have also been tested, which are known for their effectiveness in weight loss (Foster et al. 2003; Dashti et al. 2004). Studies have indicated that on a ketogenic HFD, fatty acid oxidation is significantly enhanced and carbohydrate utilisation is markedly reduced during moderate intensity exercises (Burke & Hawley 2002; Yeo et al. 2011; Brinkworth et al. 2009). In spite of these favourable changes in energy metabolism, the majority of studies indicate that HFD does not improve the performance of endurance athletes (Erlenbusch et al. 2005; Helge 2002). In fact, in some studies, HFD even impaired endurance performance (Zajac et al. 2014). It has been reported that HFD decreases absolute $VO_{2max,}$ but it does not decrease or it even increases body mass normalised VO_{2max} (Brinkworth et al. 2009; Walberg et al. 1988; Wycherley et al. 2014). In human studies, the levels of absolute and relative VO_{2max} values after HFD are highly dependent on HFD-induced changes in body mass, fat mass and muscle mass, which complicates the interpretation of results. In rats, HFD increases submaximal running endurance and $VO_{2max,}$ especially when combined with submaximal endurance training (Boyadjiev 1996; Simi et al. 1991).

The results of studies investigating the effects of HFD on oxidative capacity of skeletal muscle have been conflicting. It has been reported that HFD decreases mRNA levels of peroxisome proliferator-activated receptor γ coactivator-1α (PGC-1α), the central mediator of mitochondrial biogenesis, and the mRNA levels of various mitochondrial components in human (Sparks et al. 2005) and rodent skeletal muscles (Crunkhorn et al. 2007; Koves et al. 2005). In contrast, a number of other studies have shown that HFD induces increases in mitochondrial enzymes (Hancock et al. 2008; Miller, Bryce & Conlee 1984; Nemeth et al. 1992; Garcia-Roves et al. 2007; Boyadjiev 1996; Simi et al. 1991), mitochondrial biogenesis and fatty acid oxidative capacity in rodent skeletal muscles (Hancock et al. 2008; Garcia-Roves et al. 2007; Turner et al. 2007).

2.4 Regulation mechanisms of muscle adaptation

Skeletal muscle has an outstanding capability to adapt to a variety of external stimuli including level of muscle activation, substrate availability, and envi-

ronmental conditions (Fluck & Hoppeler 2003). This phenomenon of plasticity explains, in part, the marked differences observed in physical performance (e.g. endurance and strength) and health profiles between individuals (Schiaffino & Reggiani 1996). The question is, what are the specific mechanisms by which different types of challenges such as endurance and resistance training exert their effects on skeletal muscles?

2.4.1 Molecular basis of muscle adaptation

Muscle contractions induce changes in mechanical tension, ATP turnover, calcium flux, redox balance, reactive oxygen species (ROS) production, and intracellular partial pressure of oxygen (P_iO_2), all of which have been linked to activation of signal transduction cascades regulating skeletal muscle adaptation (Egan & Zierath 2013). Muscle fibers have various cellular sensors that transduce these homeostatic perturbations to muscle adaptation via transcriptional processes. The major sensing pathway for intracellular P_iO_2 is regulated through hypoxia-inducible factor (HIF), a heterodimeric transcription factor composed of two subunits, HIF-1α and HIF-1β. Under normoxic conditions, HIF-1α is hydroxylated by prolyl hydroxylase enzymes which act as sensors of P_iO_2. The hydroxylation triggers a reaction cascade that leads to the proteosomal degradation of HIF-1α (Maxwell et al. 1999). During conditions of reduced P_iO_2, prolyl hydroxylase enzymes are inhibited, allowing stabilization of HIF-1α, which translocates to the nucleus to form an active complex with HIF-1β. Activation of HIF induces transcription of target genes involved in, for example, angiogenesis and energy metabolism (Semenza 2001; Forsythe et al. 1996).

AMP-activated protein kinase (AMPK) is a serine/threonine kinase that regulates cellular energy metabolism through phosphorylation of metabolic enzymes and via transcriptional regulation. AMPK is activated allosterically during energy deficit by increased ratios of AMP/ATP and creatine/creatine phosphate (Hardie et al. 1999; Ponticos et al. 1998). The activation of AMPK inhibits biosynthetic pathways and anabolic pathways, while simultaneously stimulating catabolic pathways to restore energy stores (Kahn et al. 2005). For example acute AMPK activation decreases glycogen synthesis (Carling & Hardie 1989) and protein synthesis (Bolster et al. 2002), but enhances glucose uptake and fatty acid oxidation in skeletal muscles (Merrill et al. 1997). Chronic AMPK activation induces mitochondrial biogenesis by altering gene expression via induced activity of transcription factors including nuclear respiratory factor 1 (NRF-1), histone deacetylases (HDACs) and myocyte enhancer binding factor-2 (MEF2) (Bergeron et al. 2001; McGee et al. 2009; Egan & Zierath 2013).

Sirtuins are protein deacetylases that are dependent on redox balance. The deacetylase activity of sirtuins is sensitive to increases in NAD^+ concentration and NAD^+/NADH ratio (Schwer & Verdin 2008). The deacetylation of transcriptional regulators and mitochondrial enzymes allows the coupling of alterations in the cellular redox state to the adaptive changes in gene expression and cellular metabolism (Lagouge et al. 2006).

Growth factors, cytokines, and cellular stress can affect muscle fiber adaptation through mitogen-activated protein kinases (MAPKs). Through a variety of biochemical and biophysical processes, muscle contractions activate three main MAPK subfamilies: the extracellular-regulated kinase (ERK1/2), p38 MAPK, and c-jun N-terminal kinase (JNK) (Egan & Zierath 2013). MAPKs regulate gene expression by phosphorylation of transcription factors and coactivators. For example, during muscle contractions, p38 MAPK can stimulate upstream transcription factors of the peroxisome proliferator-activated receptor gamma coactivator-1α (PGC-1α) gene, such as activating transcription factor 2 (ATF2) and MEF2, which leads to upregulation of PGC-1α expression (Akimoto et al. 2005). Muscle contractions increase production of ROS that can induce gene expression changes by activating MAPK and JNK signalling pathways (Whitham et al. 2012; Petersen et al. 2012; Powers et al. 2010).

Calcium-ion flux is an essential part of muscle contraction. It facilitates crossbridge interaction between myosin and actin during myofibrillar contraction. The calcium-ion concentration oscillates during contraction, and the amplitude and duration of these oscillations are dependent on the force output of the muscle (Egan & Zierath 2013). The calcium fluxes modulate the activity of calmodulin-dependent protein kinases (CaMKs), of which CaMKII is the most important isoform in human skeletal muscle (Hook & Means 2001). Exercise increases its activity by phosphorylation in an exercise intensity-dependent manner (Rose, Kiens & Richter 2006). Thus, calcium signalling is sensitive to different types of contractions and based on the relative amplitude and frequency of calcium transients, it can result in differential activation of transcription factors, and thus differential adaptation responses (Dolmetsch et al. 1997). Calcium signalling is involved in the regulation of glucose transport, lipid uptake and lipid oxidation (Raney & Turcotte 2008; Wright et al. 2004). The main mechanism is transcriptional regulation that occurs by modulating the activity of transcription factors such as cAMP response element-binding protein (CREB), MEF2 and HDACs (Egan & Zierath 2013; Liu, Randall & Schneider 2005).

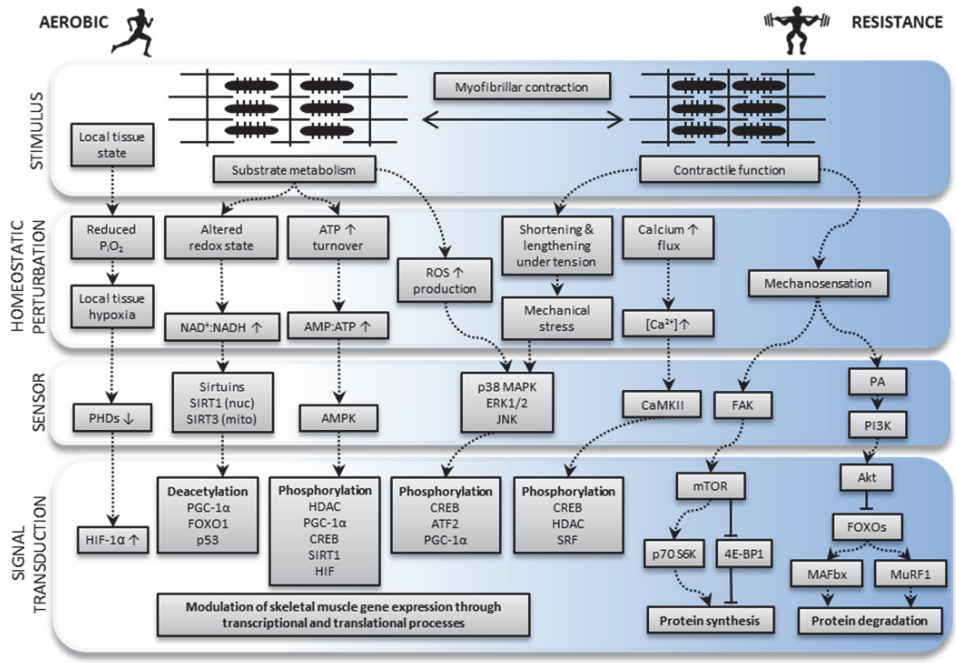

FIGURE 2 Excitation-transcription coupling in skeletal muscles. Muscle contractions result in biochemical and biophysical changes in the contracting muscle. This kind of perturbation in skeletal muscle homeostasis leads to the activation of networks of signalling molecules such as protein kinases, phosphatases, and deacetylases. These molecules are integrated into physiological adaptation processes by their downstream targets, including transcription factors and transcriptional coregulators. The relative activation and contribution of the described pathways are dependent on the intensity, duration, and mode of the exercise stimulus, and on imposed environmental factors. The presented pathways demonstrate dependence, crosstalk, interference, and redundancy in their regulation that allows the fine-tuning of the adaptive responses. AKT, ATF2, activating transcription factor 2; AMPK, 5' adenosine monophosphate-activated protein kinase; CaMK, Ca2+/calmodulin-dependent protein kinase; CREB, cAMP response element-binding protein; ERK1/2, extracellular-regulated kinase 1/2; FAK, focal adhesion kinase; FOXO1, forkhead box protein O1; HDAC, histone deacetylase; HIF-1α, hypoxia-inducible factor-1α; JNK, c-jun N-terminal kinase; MAFbx, muscle atrophy F-box; mTOR, mammalian target of rapamycin; MuRF1, muscle RING finger 1; PA, phosphatidic acid, PGC-1α, peroxisome proliferator-activated receptor gamma coactivator-1α; PHDs, prolyl hydroxylases; PI3K, phosphatidylinositide 3-kinases; p38, p38 mitogen-activated protein kinase; p53, tumour protein p53; p70S6K, ribosomal protein S6 kinase; ROS; reactive oxygen species; SIRT1/2, sirtuin 1/2; SRF, serum response factor; 4E-BP1, eukaryotic initiation factor 4E-binding protein. (The figure is modified from Egan & Zierath 2013)

All types of muscular contractions produce tension (force) through the muscle. The tension can be sensed by the mechanosensory system. In this system, high-force contractions transiently disrupt the sarcolemma (cell membrane of the muscle fibre), which increases the concentration of membrane phospholipid

phosphatidic acid (PA) in cytosol (Egan & Zierath 2013; O'Neil et al. 2009). Finally, PA activates mammalian target of rapamycin (mTOR) resulting in increased muscle protein synthesis. Mechanosensory regulation of muscle protein synthesis also includes focal adhesion kinases (FAK), which are transmembrane receptors with tyrosine kinase activity. They are important elements in the transmission of contractile force through the skeletal muscle structures and are a central component of integrin signalling. The role of FAK proteins in load-activated muscle adaptation was originally suggested because it was shown that the activity of FAK proteins was increased during stretch-induced muscle hypertrophy (Fluck et al. 1999). Thereafter FAK-activation has also been demonstrated in practice after an acute bout of resistance training (Wilkinson et al. 2008), and it has been verified as an upstream regulator of the mechanosensory pathway (Klossner et al. 2009).

In summary, the exercise challenge causes perturbations in skeletal muscle homeostasis, which can be translated to long-term physiological adaptations via cellular censors that are integrated to signalling pathways regulating gene expression. This framework is known as excitation-transcription coupling (Egan & Zierath 2013). The framework and its components are illustrated in Figure 2.

2.4.2 Molecular regulation of angiogenesis

The capillary network of skeletal muscles is able to adapt according to the need for oxygen. Adaptation is needed especially when the level of muscular activity is significantly changed from previous levels, which can result in either angiogenesis or capillary regression. Muscle activity can affect capillarization by inducing mechanical or chemical signalling. Mechanical signals that can be sensed by the endothelial cells of capillaries are shear-stress and tensile forces. Shear-stress is caused by the blood flowing through the capillaries, and the tensile forces are generated by the stretch of muscle fibers that surround capillaries. It has been shown with rodent models that both shear-stress and stretch can induce angiogenesis separately in skeletal muscle, and they have an additive effect in chronically stimulated muscles (Egginton et al. 1998; Ziada, Hudlicka & Tyler 1989; Egginton et al. 2001). Furthermore, human studies have indicated that passive leg movements increase capillary density in skeletal muscle by inducing blood flow (shear-stress) and muscle stretch with a negligible increase in oxygen uptake and without muscle activity (Hoier et al. 2010b). Based on these findings, it has been concluded that mechanical factors play an important role in exercise-induced angiogenesis (Hellsten & Hoier 2014). Animal studies have indicated that passive muscle stretch induces capillary growth primarily by sprouting, whereas shear-stress induces capillary growth mainly by longitudinal splitting (intussusception), and electrically stimulated muscle contractions elicit angiogenesis through both of these mechanisms (Egginton et al. 2001).

The signals induced by mechanical factors are mediated by pro- and anti-angiogenic factors, whose formation are increased after stimuli. They can be produced in endothelial cells or other cells present in the surrounding tissue. The most well-studied pro-angiogenic factors that may be involved in exercise-

induced skeletal muscle angiogenesis are vascular endothelial growth factor-A (VEGF-A), matrix metalloproteinases (MMPs), angiopoietins (Ang1 and Ang2) and endothelial nitric oxide synthase (eNOS), whereas anti-angiogenic factors include tissue inhibitor of MMPs (TIMPs), endostatin and thrombospondin-1 (Haas & Nwadozi 2015).

VEGF-A is probably the most studied pro-angiogenic factor. In skeletal muscle tissue VEGF-A is expressed in pericytes, endothelial cells and muscle fibers, but muscle fibers seem to be the primary source of VEGF-A (Hoier et al. 2010a; Jensen, Schjerling & Hellsten 2004; Hellsten & Hoier 2014). VEGF-A is involved in both shear-stress- and stretch-stress-induced angiogenesis and it is important for both basal and exercise-induced skeletal muscle angiogenesis (Olfert et al. 2009; Tang et al. 2004). VEGF-A exerts its pro-angiogenic effects in skeletal muscles primary through VEGFR-2 receptors located in the endothelial cells. The activation of this receptor leads to the activation of signalling pathways that enhance endothelial cell survival, proliferation, migration and expression of numerous angiogenesis related genes (Koch & Claesson-Welsh 2012). MMPs are needed in proteolytic degradation of the extracellular matrix, which is an essential step in sprouting angiogenesis (Hellsten & Hoier 2014). Haas et al. have shown that MMPs are essential in muscle activity-induced angiogenesis. Their study indicated that the inhibition of MMP activity prevented angiogenesis in rat muscle in response to prolonged electrically stimulated muscle activity (Haas et al. 2000). Ang1 and Ang2 are competing ligands of receptor Tie2 (tyrosine kinase with immunoglobulin-like and EGF-like domains 2) (Augustin et al. 2009). Ang2 is involved in degradation of the basement membrane and is therefore important in stretch-induced sprouting angiogenesis, whereas Ang 1 opposes the effects of Ang2 and thereby promotes stability of the capillary network (Hellsten & Hoier 2014). Endothelial nitric oxide synthase (eNOS) is an enzyme, which catalyses the production of nitric oxide in endothelial cells. The activity of eNOS is increased by elevated shear-stress and by growth factor receptors that use Akt as part of their signalling pathway (Haas & Nwadozi 2015). The resulting increase in the levels of nitric oxide can promote angiogenesis in different ways. It can happen indirectly by increased blood flow through capillaries due to arteriolar vasodilation, which is stimulated by nitric oxide, or nitric oxide can directly stimulate skeletal muscle VEGF-A production and endothelial cell proliferation and migration (Haas & Nwadozi 2015; Uchida et al. 2015; Morbidelli et al. 1996).

TIMPs are proteins that inhibit MMPs and can thus reduce the remodelling of extracellular matrix proteins (Brew & Nagase 2010). It has been shown that elevated shear-stress increases the production of TIMP1, which may indicate that it assists in maintaining capillary integrity during elevated hemodynamic stress (Milkiewicz et al. 2008; Uchida & Haas 2014). Endostatin is an anti-angiogenic factor formed of small fragments of collagen XVIII. It inhibits VEGF-A signalling and reduces endothelial cell proliferation and migration (O'Reilly et al. 1997). Migration is disrupted because endostatin competes with collagen to bind to integrins (Faye et al. 2009). There are several isoforms of thrombos-

pondin, but in skeletal muscle, thrombospondin-1 is believed to be the most important. It is an important negative regulator of angiogenesis that prevents excessive capillarization in skeletal muscles (Malek & Olfert 2009). Thrombospondin-1 may also play this role during exercise-induced angiogenesis because acute endurance exercise increases its mRNA expression (Hoier et al. 2012; Olfert et al. 2006).

Capillarization changes are determined by the balance of pro- and anti-angiogenic factors. Because these multiple factors exert positive and negative influences on the capillarization of muscle, they have to be coordinated. There are transcription factors that have potential to act in this role, because they can simultaneously regulate the transcription of numerous genes related to angiogenesis. PGC-1α and HIF-1 are important regulators of VEGF-A expression. During conditions of reduced P_iO_2, HIF-1 accumulates and translocates into the nucleus, where it increases the expression of VEGF-A and numerous other genes needed for angiogenesis (Semenza 2001). A study by Chinsomboon et al. demonstrated that, in skeletal muscle, PGC-1α is the most significant mediator of exercise-induced angiogenesis and it is not dependent on the HIF-1 pathway (Chinsomboon et al. 2009). They showed that exercise activates β-adrenergic signalling, leading to robust induction of PGC-1α, which then acts through the estrogen-related receptor-α (ERRα) to activate a program of angiogenesis, including the induction of VEGF-A. However, recent studies have shown that an important step in exercise-induced angiogenesis is the release of VEGF-A from the vesicles of skeletal muscle fibers to the extracellular fluid, where it can activate the VEGFR-2 receptors located in the endothelial cells (Figure 3) (Hoier et al. 2013). It seems that the acute release of VEGF-A does not require synthesis of VEGF-A, because the release starts rapidly after the onset of exercise and continues throughout the activity, whereas the upregulation of VEGF-A mRNA does not occur until the termination of exercise (Gavin et al. 2004; Gustafsson et al. 1999; Hellsten & Hoier 2014). It has been suggested that VEGF-A mRNA is upregulated after exercise to allow faster replenishment of the VEGF-A stores in the muscle fibres (Hellsten & Hoier 2014).

A single exercise stimulus can increase the production of both pro- and anti-angiogenic factors, but generally it is not strong or long enough to induce angiogenesis (Egginton 2009; Haas & Nwadozi 2015). However, it has been shown that repeated exercise bouts can lead to accumulation of pro-angiogenic proteins (e.g. VEGF-A and Ang2) and to a restrained pro-angiogenic (e.g. thrombospondin-1) response (Gustafsson et al. 2007; Slopack et al. 2014). It has been suggested that this type of sustained alteration in intracellular signalling would eventually lead to endothelial cell proliferation and angiogenesis (Haas & Nwadozi 2015).

In some disease states there is not adequate blood flow in skeletal muscle. This has been observed for example in type 2 diabetes and peripheral artery disease (Haas & Nwadozi 2015). Although there can be significant hypoxia in skeletal muscle tissue, the angiogenic processes seem not to work efficiently in these diseases. It has been suggested that this could be caused by increased lev-

els of anti-angiogenic factors that restrain the actions of pro-angiogenic factors (Haas & Nwadozi 2015).

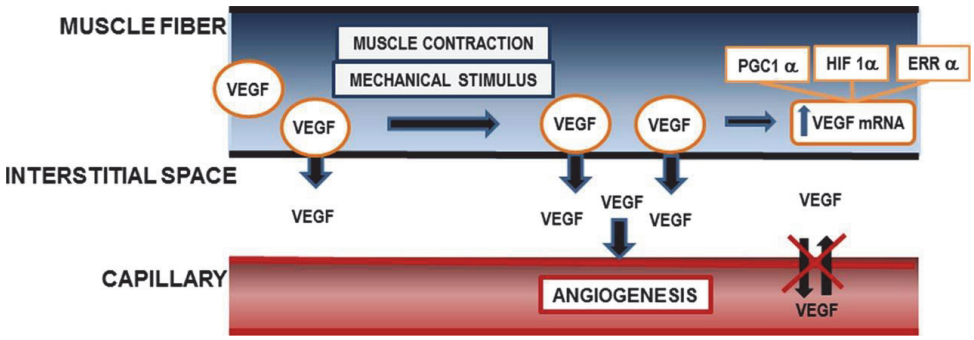

FIGURE 3 Proposed mechanism of VEGF-induced angiogenesis in skeletal muscle. An important step in physiological angiogenesis in skeletal muscle tissue is VEGF (VEGF-A) secretion from skeletal muscle fibres into the extracellular space. In this process, muscle contraction or mechanical stimulus induce transport of intramyofibrillar VEGF-containing vesicles into the sarcolemma where the vesicles release their content into the interstitial space. VEGF initiates angiogenesis by binding VEGFR-2 located on endothelial cells that activates its downstream signalling pathways. The level of VEGF in blood does not appear to contribute to the interstitial VEGF concentration. VEGF mRNA levels are upregulated after termination of exercise, possibly through PGC1-α, HIF-1α and ERRα pathways. ERRα, estrogen-related receptor α; HIF-1α, hypoxia-inducible factor-1α; PGC-1α, peroxisome proliferator-activated receptor gamma coactivator-1α; VEGFR-2, vascular endothelial growth factor receptor-2. (Hellsten & Hoier 2014)

2.4.3 Molecular regulation of mitochondrial biogenesis

It has been suggested that cumulative effects of transient increases in expression of a broad range of specific genes are the most important mechanism behind mitochondrial adaptations to repeated physical activity (Perry et al. 2010). Mitochondrial biogenesis requires the coordination of multiple cellular events, including transcription of nuclear and mitochondrial genomes encoding mitochondrial proteins, synthesis of lipids and proteins, and the assembly of multisubunit protein complexes into a functional electron transport chain (Hood et al. 2006; Hawley et al. 2014).

Nuclear genes encoding mitochondrial proteins are regulated by nuclear respiratory factors 1 and 2 (NRF-1, NRF-2) that bind to the promoters and activate transcription of genes that encode mitochondrial electron transport chain proteins (Kelly & Scarpulla 2004). Furthermore, NRF-1 activates the expression of mitochondrial transcription factor A (TFAM), which translocates into the mitochondria and regulates transcription of the mitochondrial genome. There are also other transcription factors that are needed in exercise-induced mitochondrial biogenesis, including the estrogen-receptor-related receptor α (ERRα) and the peroxisome proliferator-activated receptors (PPARs), which regulate expression of the mitochondrial fatty acid oxidative enzymes (Kelly & Scarpulla

2004). The main signalling pathways regulating mitochondrial biogenesis are presented in Figure 4.

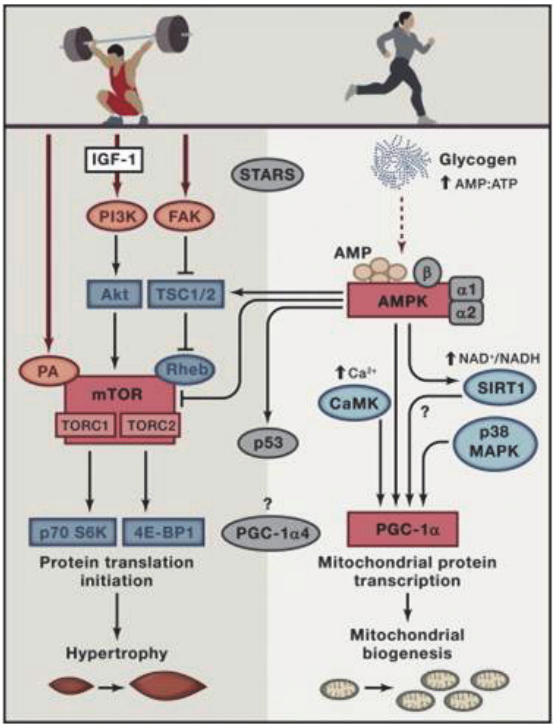

FIGURE 4 Major signalling pathways involved in the regulation of skeletal muscle hypertrophy and mitochondrial biogenesis. AMPK, 5' adenosine monophosphate-activated protein kinase; CaMK, Ca^{2+}/calmodulin-dependent protein kinase; FAK, focal adhesion kinase; IGF-1, insulin-like growth factor 1; mTOR, mammalian target of rapamycin; PGC-1α, peroxisome proliferator-activated receptor gamma coactivator-1α; PI3K, phosphatidylinositide 3-kinases; p38 MAPK, p38 mitogen-activated protein kinase; p70S6K, ribosomal protein S6 kinase; Rheb, ras homolog enriched in brain; SIRT1, sirtuin 1; TORC1/2, mTOR complex 1/2; TSC1/2, tuberous sclerosis complex 1/2; 4E-BP1, eukaryotic initiation factor 4E-binding protein. (Hawley et al. 2014)

One major breakthrough in unravelling the cellular events that promote mitochondrial biogenesis was the discovery of PGC-1α. PGC-1α was originally discovered in 1998 and it was identified as a coactivator of PPARγ in brown adipose tissue and a factor in adaptive thermogenesis (Puigserver et al. 1998). Since then it has been identified as a master regulator of mitochondrial biogenesis, but also been shown to regulate proteins involved in exercise-induced angiogenesis and the anti-oxidant defence (Olesen, Kiilerich & Pilegaard 2010). PGC-1α can regulate simultaneously large set of genes by working as a coactivator of numerous transcription factors e.g. PPARs, NRFs, myocyte enhancing factors, ERRα and forkhead box O1 (Lin, Handschin & Spiegelman 2005; Rodgers et al. 2008). Moreover, transcriptional regulation by PGC-1α involves the recruitment

of coactivators with histone acetyl transferase activity as well as interaction with proteins involved in RNA processing and transcriptional initiation (Wallberg et al. 2003). A single bout of endurance exercise transiently increases PGC-1α transcription and mRNA content in human (Pilegaard, Saltin & Neufer 2003) and rodent (Baar et al. 2002) skeletal muscle. Furthermore, other types of physical activity (e.g. sprint and resistance exercise) also result in an increase in the mRNA and protein levels of PGC-1α (Gibala 2009; Ydfors et al. 2013; Burgomaster et al. 2008). The study of Lin et al. showed that transgenic expression of PGC-1α at physiological levels in fast type muscle led to activation of genetic programs characteristic of slow-twitch muscle fibers, and thereby to conversion of muscle fiber type from fast to slow (Lin et al. 2002).

There are several intracellular signalling pathways that may contribute to eliciting the exercise-induced PGC-1α mediated adaptation response. It has been shown that PGC-1α gene expression can be regulated in skeletal muscle by calcium signalling, AMPK signalling, ROS-mediated regulation, β-adrenergic signalling and substrate availability. Because all of these factors may change during exercise, they can potentially contribute to exercise-induced PGC-1α gene regulation (Olesen, Kiilerich & Pilegaard 2010). In addition to gene expression regulation, PGC-1α is regulated by covalent modifications including phosphorylation (Jager et al. 2007; Puigserver et al. 2001), acetylation (Dominy et al. 2010; Lerin et al. 2006) and methylation (Teyssier et al. 2005). In vitro experiments have shown that p38 MAPK phosphorylates PGC-1α resulting in a more active and a more stable PGC-1α protein (Puigserver et al. 2001), and similarly that AMPK phosphorylates PGC-1α leading to a more active protein (Jager et al. 2007). Acetylation turns PGC-1α into a transcriptionally inactive protein that translocates from promoter regions to nuclear foci (Lerin et al. 2006), while the NAD+-dependent sirtuin 1 (Sirt1) deacetylates PGC-1α, maintaining it in an active form bound to chromatin (Gerhart-Hines et al. 2007). Methylation potentiates the activity of PGC-1α (Teyssier et al. 2005).

Recently the existence of several different splice variants of PGC- 1α has been reported in skeletal muscle. In skeletal muscle of mice the following splice variants have been detected: PGC-1α-a, PGC-1α-b, PGC-1α-c, NT- PGC-1α-a, NT- PGC-1α-b and NT- PGC-1α-c (Miura et al. 2008; Wen et al. 2014). Additionally, Ruas et al. characterized four PGC-1α splice variants in skeletal muscle of mice: PGC-1α1, α2, α3, and α4 (Ruas et al. 2012), which have partial overlap with the above mentioned splice variants. The splice variants differ from starting exon (exon 1a, exon 1b and exon 1c) and via alternative 3′ splicing which produce either full-length PGC-1α protein (PGC-1α) or shorter N-truncated protein (NT- PGC-1α) (Ruas et al. 2012; Zhang et al. 2009). Exon 1a-derived PGC-1α-a mRNAs are transcribed from the canonical proximal promoter, while Exon 1b- and 1c-derived mRNAs are transcribed from an alternative promoter ~14kb upstream from the canonical one. Compared to full-length PGC-1α, the structure of the N-truncated-PGC-1α proteins seems to have distinct patterns of protein stability, subcellular localization, transcription factor interaction and target gene activation (Chang et al. 2010; Zhang et al. 2009; Shen, Liu & Schnei-

der 2012). Based on recent human studies, PGC-1α-a, PGC-1α-b, PGC-1α-c and NT- PGC-1α (may include one or more different NT-PGC-1α splice variants) are expressed in human skeletal muscle (Ydfors et al. 2013; Popov et al. 2014; Norrbom et al. 2011; Gidlund et al. 2015).

2.4.4 Molecular regulation of muscle hypertrophy

Systematic and progressive resistance training leads to skeletal muscle hypertrophy and improves maximal force production (Häkkinen et al. 2001; Luthi et al. 1986; Hubal et al. 2005). When skeletal muscle is subjected to an overload stimulus, it causes perturbations in myofibers and the extracellular matrix. This induces myogenic processes that lead to expansion of the extracellular matrix, increase in the size and amounts of the contractile proteins actin and myosin, and an increase in the total number of sarcomeres in parallel. This in turn augments the diameter of individual fibers and thereby leads to the enlargement of whole muscle cross-sectional area and volume (Häkkinen et al. 2001; McCall et al. 1996; Ahtiainen et al. 2003). There is no clear evidence that hyperplasia, an increase in the number of fibers, plays a significant role in muscle hypertrophy. Furthermore, muscle hypertrophy seems to be a fiber-type specific event. Studies have shown that traditional resistance training programs increase the size of fast type II fibers more than slow type I fibers (Häkkinen et al. 2001; Kosek et al. 2006).

What are the molecular mechanisms involved in muscle hypertrophy and its regulation? Muscle hypertrophy takes place by positive muscle protein balance and satellite cell addition to the pre-existing fibers. Positive muscle protein balance occurs when the rate of new muscle protein synthesis exceeds that of breakdown (Hawley et al. 2014). In addition to resistance exercise, postprandial hyper-aminoacidemia stimulates muscle protein synthesis. It is known that the synergistic effects of these stimuli leads to the net gain of muscle proteins, and thereby muscle hypertrophy takes place (Phillips 2014).

It has been suggested that there are three primary factors that are responsible for initiating the hypertrophic response to resistance exercise: mechanical tension, muscle damage, and metabolic stress (Schoenfeld 2010). Mechanically induced tension produced both by force generation and stretch is considered essential to muscle growth. It is believed that tension induces muscle hypertrophy by causing mechano-chemically transduced molecular and cellular responses in myofibers and satellite cells (Toigo & Boutellier 2006). The upstream signalling of these events occurs through a cascade of events that involve growth factors, cytokines, stretch-activated channels, and focal adhesion complexes (Schoenfeld 2010). Evidence suggests that the downstream processes are regulated via the AKT/mTOR pathway (Figure 2 and 4). This pathway seems to be crucial because hypertrophic responses and protein synthesis have been shown to be significantly attenuated by mTOR inhibitor rapamycin (Bodine et al. 2001). The mTOR pathway controls protein synthesis by increasing the translation of numerous specific mRNAs (Terada et al. 1994; Egan & Zierath 2013). It affects downstream regulators of protein synthesis working as a part of two

complexes: TORC1 and TORC2. However, most of the effect on downstream regulators is achieved through TORC1 (Philp, Hamilton & Baar 2011). When activated by Akt, TORC1 induces protein synthesis by phosphorylating ribosomal protein S6 kinase (p70S6K) and eukaryotic initiation factor 4E-binding protein (4E-BP1) (Hawley et al. 2014). The phosphorylation of p70S6K and subsequent activation of ribosomal protein S6 enhances translation of mRNAs, encoding elongation factors and ribosomal proteins that leads to enhanced translational capacity.

Some studies have suggested that muscle damage caused by resistance training can have a significant role in the hypertrophic response (Hill & Goldspink 2003). Muscle damage causes an acute inflammatory response that is needed to maintain the fiber's ultrastructure and produce cytokines that activate myoblasts, macrophages and lymphocytes. This is believed to lead to the release of growth factors that regulate satellite cell proliferation and differentiation (Schoenfeld 2010; Vierck et al. 2000). Satellite cell activation has the potential to facilitate muscle hypertrophy in the following ways: they can donate extra nuclei to muscle fibers that increase protein synthesis capacity; they can serve as a pool of new myonuclei, which are essential for muscle growth; they express various myogenic regulatory factors that may help in muscle repair, regeneration and growth (Schoenfeld 2010).

Numerous studies have supported the important role of metabolic stress in exercise-induced muscle hypertrophy (Rooney, Herbert & Balnave 1994; Schott, McCully & Rutherford 1995; Smith & Rutherford 1995). However, metabolic stress does not seem to be an essential component of muscular hypertrophy (Folland et al. 2002). Metabolic stress is produced typically as a result of anaerobic exercises and during muscle ischemia, which both result in the subsequent accumulation of metabolites such as lactate, hydrogen ions, inorganic phosphate and creatine (Suga et al. 2009; Tesch, Colliander & Kaiser 1986). It has been suggested that metabolic stress could induce a hypertrophic response via alterations in hormonal milieu, cell swelling, free-radical production, and increased activity of growth promoting transcription factors (Schoenfeld 2010).

Ruas et al. recently found a novel splice variant of PGC-1α, which was named PGC-1α4 (Ruas et al. 2012). It is highly expressed in skeletal muscle and appears to play a role in the adaptive response to resistance exercise. PGC-1α4 protein does not regulate the same set of oxidative genes as PGC-1α. Instead, it induces the expression of IGF-1 and represses the expression of myostatin, an inhibitor of muscle hypertrophy. The study of Ruas et al. suggests that PGC-1α4 could be a new piece in the puzzle of exercise-induced muscle hypertrophy (Ruas et al. 2012).

2.5 Summary of literature review

Aerobic energy production pathways produce the majority of the ATP required for cellular metabolism. Aerobic capacity determines how effectively ATP can

be produced in these oxygen dependent pathways. Aerobic capacity is limited mainly by oxygen delivery capacity, but all steps of the O_2 pathway are integrated and can affect aerobic capacity. Capillary density and mitochondria content of skeletal muscle are primary determinants of oxidative capacity of skeletal muscle. High oxidative capacity of skeletal muscle allows efficient fat oxidation, which is known to be important for endurance performance. The fiber type composition and oxidative capacity of skeletal muscles are highly genetically determined but they can be significantly affected by environmental factors such as level of physical activity. In addition, skeletal muscles are able to adapt specifically for different types of muscle activities. Endurance training generally leads to improved oxidative capacity and resistance training results in muscle hypertrophy. There are still gaps in our understanding of the mechanisms of this specificity but it has been suggested that different types of external challenges disrupt homeostasis of specific physiological factors (e.g. AMP/ATP ratio, calcium concentration, redox balance and PiO2), and these disturbances stimulate specific sensors. Activated sensors activate down-stream signalling pathways that generally lead to induction of transcription or translation of a certain set of genes. When the stimulus is repeated it can eventually lead to structural adaptation that will increase the resistance of muscle to the original stimulus.

Because skeletal muscle oxidative capacity is important for health and endurance performance, it is important to know how the physiological components of aerobic capacity are affected by genotype and environmental factors. In the current thesis, the effects of genotype were investigated with rat strains contrasting in their inherent aerobic capacity. If the oxidative capacity of skeletal muscle is not adequate in relation to fatty acid uptake, it may lead to fat metabolism disturbances, which have been linked to the development of insulin resistance. Skeletal muscle adaptation to HFD has been studied earlier but the results regarding the effects of HFD on skeletal muscle oxidative capacity are controversial, and there is a lack of information about the effects of HFD on skeletal muscle capillary density. To extend knowledge of these issues, the effect of HFD, physical activity and their interactions on capillarization of skeletal muscle was investigated in genetically homogenous C57BL/6J mice. PGC-1α is a known regulator of mitochondrial biogenesis and angiogenesis in skeletal muscle. There are many isoforms of this protein and some studies have suggested that certain isoforms mediate responses typical of endurance exercise and others typical of resistance exercise. To get further information about this proposed novel, exercise mode-dependent adaptation mechanism, the acute gene expression responses of different PGC-1α isoforms were measured in human skeletal muscle after a single bout of endurance exercise or resistance exercise.

3 AIMS AND HYPOTHESIS

The aim of this dissertation was to study characteristics of inherited aerobic exercise capacity, and to investigate physical activity and high-fat diet elicited skeletal muscle adaptations related to skeletal muscle hypertrophy and aerobic capacity. Furthermore, for the voluntary running experiments in mice, we aimed to develop and validate a system that is able to quantify the total spontaneous activity of mice.

The specific aims were to study:

1. The differences in skeletal muscle characteristics of rat strains with low (LCR) and high (HCR) inherited aerobic exercise capacity, and to investigate gene-phenotype relationships that connect aerobic exercise capacity with metabolic disease risk factors in skeletal muscle. (I)

   Hypothesis:

   LCR rats have lower levels of determinants of skeletal muscle aerobic capacity e.g. capillary density, mitochondrial content, and higher levels of risk factors for complex metabolic diseases in comparison to HCR rats. There are also differences in mRNA expression of genes linked to aerobic capacity that can explain the higher risk of metabolic syndrome in LCR rats.

2. The effects of high-fat diet on capillarization and angiogenic factors in skeletal muscle of mice that were either active or sedentary. (II)

   Hypothesis:

   It is known that a high-fat diet increases fatty acid oxidation in skeletal muscle. We hypothesized that this would lead to increased oxygen de-

mand and thus to increased capillarization. Increased physical activity increases the capillary density of skeletal muscle in both high-fat diet and low-fat diet fed mice. The effects of high-fat diet and physical activity are accompanied by increased gene expressions of angiogenic factors.

3. The validity of the developed physical activity measuring system and its variables in calibration measurements and in situ by measuring the activity of mice both with and without running wheels. In addition, the study aimed to quantify the stimulating effect of running wheels on the cage activity of mice. (III)

   Hypothesis:

   The activity index and activity time variables are valid measures for long-term spontaneous activity measurements of mice with or without running wheels. Distance analysis is acceptable when there is no running wheel in the cage.

4. The acute gene expression responses of different PGC-1 isoforms after a single bout of high-load resistance exercise (leg press protocol) or moderate intensity endurance exercise (uphill walking on treadmill) in human skeletal muscle. In addition, we aimed to determine how these two different exercise protocols affect the expression of a selection of known PGC-1α target genes related to mitochondrial biogenesis, angiogenesis, and muscle hypertrophy. (IV)

   Hypothesis:

   Both exercise modes significantly increase the expression of alternative promoter originated PGC-1α isoforms, whereas the expression of proximal promoter originated PGC-1α exon 1a-derived isoforms is not significantly changed. Truncated PGC-1α isoforms are upregulated preferentially after resistance exercise. Endurance exercise induces expression of genes related to mitochondrial biogenesis and angiogenesis, while resistance exercise decreases the expression of genes linked to inhibition of muscle hypertrophy.

4 MATERIALS AND METHODS

4.1 Subjects

4.1.1 Animals

All experimental procedures for the animal studies (I,II,III) were approved by the Animal Care and Use Committee of the University of Jyväskylä, Finland. In study I, the experimental procedures were also approved by the Animal Care and Use Committee of the University of Michigan, United States.

To achieve the aims of **study I**, rat strains contrasting in inherent aerobic capacity were investigated. High running capacity (HCR) and low running capacity (LCR) rat strains were produced by artificial selective breeding, starting with a founder population of 186 genetically heterogeneous rats (N:NIH stock). The procedure is described in detail previously (Koch & Britton 2001). Briefly, endurance running capacity was assessed on a treadmill and the maximal distance run during the test was used as a measure of maximal aerobic exercise capacity (Figure 5).

Using the criterion of single best day running test result, the 13 lowest and 13 highest capacity rats of each sex were selected from the founder population and randomly paired for mating within selection groups (low or high capacity). At 10 weeks of age the offspring were tested for maximal running capacity. Next, one female and one male offspring representing HCR and LCR were selected from each family and they became parents for the next generation. The breeding was continued from generation to generation and at each subsequent generation, within-family selection from 13 mating pairs was practiced because it decreases the rate of inbreeding to yield retention of genetic variation and thus increases the overall response to selection. The schedule of matings is presented in Table 1.

A subsample of female rats (12 HCR and 12 LCR) from generation 18 was used in **study I**. In **study II**, the study questions were investigated using 58 5-week-old male C57BL/6J mice (Taconic Europe, Denmark). To test the activity

measuring system in situ in **study III**, we conducted an experiment with 12 6-month-old male C57BL/6 mice (Harlan Laboratories, Inc., The Netherlands).

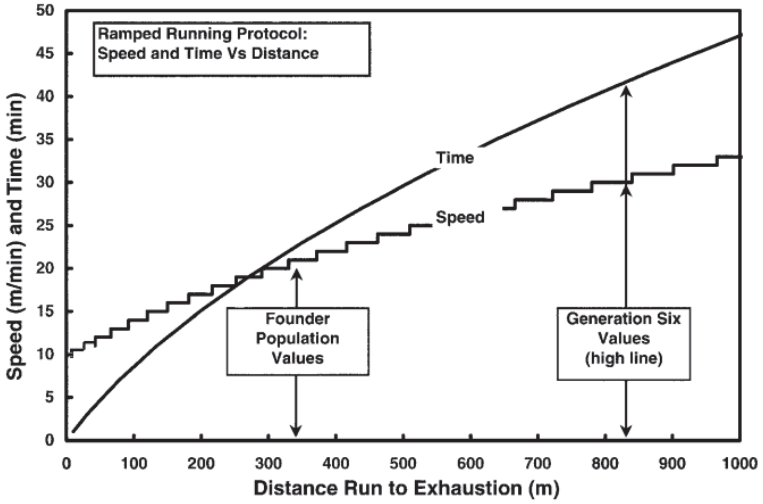

FIGURE 5 Nomogram relating speed and time to distance run to exhaustion for the speed-ramped maximal running test protocol. The starting speed was 10 m/min and the speed was increased 1 m/min every 2 minutes. Average distances run by the founder population and by the high-line rats (HCR) in generation 6 are indicated by the vertical arrows. (Koch & Britton 2001)

TABLE 1 The prearranged schedule of matings followed a simple sequence based on assigned family number (1 to 13, F = female, M = male). When the rotation has completed one entire cycle (i.e., generation 13), the 1 × 1, 2 × 2, etc. matings are skipped to avoid mating of siblings. (Koch & Britton 2001)

Family Number	*Founder* F × M = family	*Generation 1* F × M = family	*Generation 2* F × M = family	*Generation 3...n* → F × M = family
1	1 × 1 = 1	1 × 2 = 1	1 × 3 = 1	1 × 4 = 1
2	2 × 2 = 2	2 × 3 = 2	2 × 4 = 2	2 × 5 = 2
3	3 × 3 = 3	3 × 4 = 3	3 × 5 = 3	3 × 6 = 3
Continue	Continue	Continue	Continue	Continue
↓	↓	↓	↓	↓
13	13 × 13 = 13	13 × 1 = 13	13 × 2 = 13	13 × 3 = 13

4.1.2 Human subjects

In **study IV** two different experimental setups were included in the study: resistance and endurance exercise. The studies were linked to a larger military research project. A total of 22 healthy male reservists, who were physically active but not endurance or strength athletes, were recruited for the present investigation. Two subjects withdrew from the endurance exercise group and one subject was excluded from this group because of inadequate muscle samples.

Therefore, the final study groups included 11 subjects in the resistance exercise group (RE) and eight in the endurance exercise group (EE). The general characteristics of the groups are presented in Table 2. Each subject was carefully informed of all potential risks and discomforts and, thereafter, signed an informed consent document. The study was conducted according to the declaration of Helsinki, and ethical approval was granted by the ethics committees of the University of Jyväskylä and the Central Finland Health Care District, Jyväskylä, Finland.

TABLE 2. General characteristics of the subjects in study IV.

	EE (n = 8)	RE (n = 11)
Age (years)	27.0 ± 3.6	26.0 ± 4.6
Height (cm)	181 ± 9	182 ± 8
Body mass (kg)	72.5 ± 11.5	78.6 ± 11.7
BMI (kg/m^2)	22.0±2.6	23.8 ± 2.4
Fat-%	14.4 ± 3.6	12.1 ± 4.8
MVC (Kg)	221.8 ± 33.2	339.7 ± 99.7
CMJ (cm)	30.9 ± 3.6	34.0 ± 3.8
1 RM (kg)	167.3 ± 33.6	207.0 ± 26.6
VO_{2max} (ml/kg/min)	65.3 ± 5.2	59.9 ± 5.3

Data are presented as mean ± SD. EE, Endurance exercise; RE, Resistance exercise; BMI, body mass index; Fat-%, body fat percentage; MVC, maximal voluntary contraction (isometric knee extension); CMJ, countermovement jump; 1 RM, One-repetition maximum (bilateral leg press); VO_{2max}, maximal oxygen consumption.

4.2 Experimental design

4.2.1 Study I

The study was performed using 12 HCR and 12 LCR rats from generation 18. At the beginning of study I, the maximal running capacity of the rats was measured at the University of Michigan using the same running protocol as applied for artificial selection (Koch & Britton 2001). Next the rats were shipped via overnight flight to the University of Jyväskylä. In Jyväskylä the animals were housed two per cage in standard conditions (temperature 22˚C, humidity 50 ± 10%, light from 8.00 am to 8.00 pm) and they had free access to tap water and food pellets (R36, Labfor, Stockholm, Sweden). To analyse the voluntary activity of the rats, they were housed individually for three weeks in a cage with a running wheel, which was connected to a computer. Daily voluntary running activity was measured during these 21 days with a computerized recording system. Energy intake was measured during the three weeks in a cage with a running wheel and during six weeks in a normal cage. Intraperitoneal glucose tol-

erance test was performed on all rats. Energy consumption of rats was measured in a post absorptive stage (access to food was restricted 12 h prior to measurements) with an open flow respirometer system. At 9 months of age, the rats were killed. Blood and muscle samples were taken and stored at -80 °C. The timeline of the measurements, which were performed on living rats, is presented in Figure 6. The stored muscle samples were analysed later for mitochondrial content, lipid droplet content, capillary density, muscle fiber type, myosin heavy chain composition and mRNA level gene expression profiles.

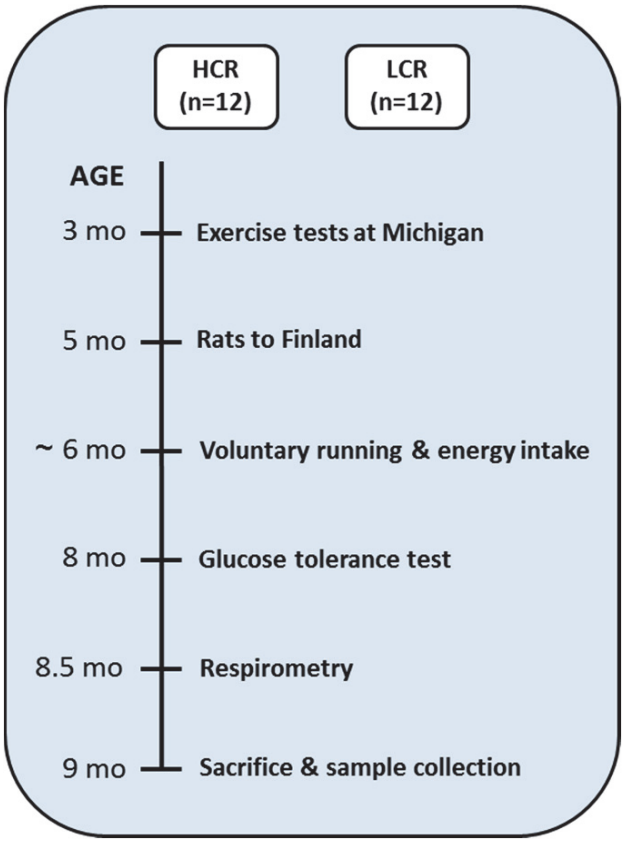

FIGURE 6 Time course of the measurements in study I.

4.2.2 Study II

Sixty body weight-matched mice were allocated evenly to one of the four intervention groups: low-fat diet / sedentary (LFS), low-fat diet / active (LFA), HFD / sedentary (HFS), and HFD / active (HFA). One mouse died during the experiment from group LFS and one from HFS. The mice were housed individually in standard conditions (temperature 22 °C, humidity 50 ± 10%, 12:12-h light–darkness cycle) and received food pellets and tap water ad libitum. The high-fat diet (HFD, 60 E% fat, 20 E% carbohydrate, 20 E% protein, 5,24 kcal/g, D12492-

Euro, Purina Mills TestDiet®, Richmond, IN, USA) and low-fat diet (LFD, 10% fat, 70% carbohydrate, 20% protein, 3,85 kcal/g, D12450-Euro) differed only in fat and carbohydrate content. The active mice groups LFA and HFA were housed in cages where they had free access to custom-made vertical running wheels (diameter 24 cm, width 8 cm) 24 h/day. Total wheel revolutions were recorded daily and the total running distance per day was determined by multiplying the number of wheel rotations by the circumference of the wheel. Sedentary animals were housed in similar cages without the running wheel. Body mass and food consumption were measured at three-week intervals throughout the study. The glucose balance of the mice was determined at week 18 of the intervention by analysing fasting glucose and fasting insulin concentrations. At week 19 of the intervention, the mice were sacrificed, after 3 hours fasting and 12 hours running restraint, by cervical dislocation and decapitation. Blood samples and skeletal muscle samples were collected and stored at -80 °C. Next the muscle samples were analysed for capillary density, muscle fiber cross-sectional area, protein levels of angiogenic factors and cytochrome C. In addition, mRNA level gene expressions of angiogenic factors were analysed separately in muscle homogenate, muscle fiber and capillary samples. The study design is illustrated in Figure 7.

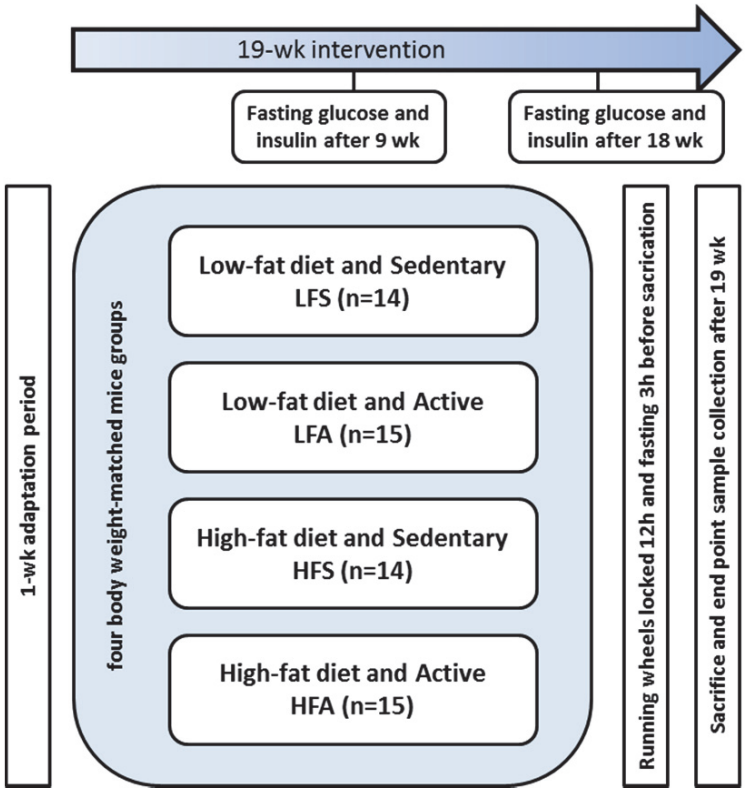

FIGURE 7 The experimental design of study II.

4.2.3 Study III

For analysis of total activity of mice housed in normal cages or cages with running wheels, a ground reaction force measurement system (described later in chapter 4.12.1) was developed in our laboratory. In study III we validated the system and its variables with calibration measurements, and tested the function of the system in practice with mice.

The accuracy and repeatability of activity index and activity time analyses were measured by producing triangle wave shaped force changes onto the force plate with a solenoid (electromagnet). The solenoid was fixed to its own rigid support, which did not have any contact with the base of the force plate. The magnetic force (amplitude) was adjusted to 0.94 N by tuning the distance between the solenoid and the iron cylinder that was affected on the plate. The frequency was regulated by a low frequency oscillator set to 4 Hz. Each validation measurement lasted 65 minutes. Four different durations of force changes were used in separate measurements: 3600, 900, 225 and 57 seconds (each repeated 3 times). Activity indexes and activity times were then analysed and the results were compared to true values. The true activity times were known (described above). For the activity index true values, activity index analyses were performed on synthetic triangle wave signals with the same amplitude, frequency and duration as the induced force changes.

The validation of distance analysis was performed by using a custom made device that can move a certain amount of water from one measuring glass to another and back without external force affecting the force plate (Figure 8). Measuring glasses were fixed exactly 125 mm apart from each other and they were connected by a tube from the lowest part of the glasses. The outfall of one glass was open but the outfall of the other glass was sealed with a tubed lid. One tube was attached to an air compressor and the other tube was in the water bottle. Just before the measurement, water was added to the glass system so that both glasses contained 200 ml water. Then all sensors of the force plate were set to zero and 40 ml (simulating the weight of a mouse) of extra water was added to the system. Next, the air compressor was turned on and the tube in the water bottle was fixed to the depth where hydrostatic pressure equals the pressure needed to shift exactly 40 ml of water from the sealed glass to the other. When the air compressor was turned off, the water volumes returned to normal. During the described cycle, 40 g of water travelled a distance of 250 mm. In validation measurements, four different travelling distances were induced during a 65 minute reaction force measurement: 1.5, 5.5, 11.25 and 44.5 meters. The measurements were repeated three times with all four distances. Distances were analysed from reaction force data and the results were compared to known theoretical distances.

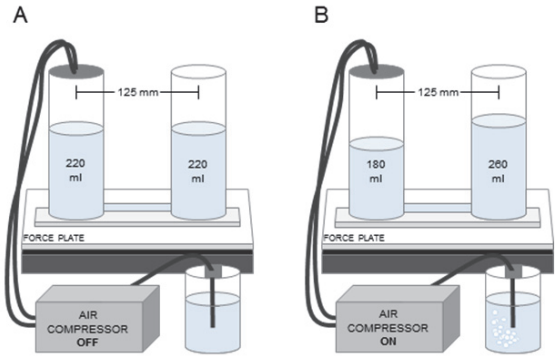

FIGURE 8 Distance analysis was tested with a calibration device that transferred water from one measuring glass to another using air pressure. A. When the air compressor was off there was an equal amount of water in both glasses. B. When the air compressor was turned on, 40 ml of water moved from the left glass into the right glass. When the air compressor was turned off again, the water volumes returned to normal. In validation measurements, the water was transferred back and forth inducing four different travelling distances during a 65 minute reaction force measurement: 1.5, 5.5, 11.25 and 44.5 meters. All the measurements were repeated three times.

To test the activity measuring system in situ, we conducted an experiment with 12 mice. Before the experiment, the mice were housed in groups of four in standard conditions (temperature 22 °C, humidity 50 ± 10%, lights on from 8 AM to 8 PM) and received food pellets ((R36, 4% fat, 55.7% carbohydrate, 18.5% protein, 3 kcal/g; Labfor, Stockholm, Sweden) and tap water ad libitum. Two weeks before the start of activity measurements, the mice housed in the same cage were separated into individual cages (Makrolon 3, Tecniplast, Varese, Italy) and they were also allocated to two groups: control group (C, n=4) and running group (R, n=8). In the first experiment week all the mice were housed in similar cages where they had aspen nesting material as a stimulus (Tapvei, Kaavi, Finland). During this week, a basal activity measurement of each animal was performed. The measurement was conducted in the animal's own cage and in the same room with the other mice in this experiment. The measurement protocol was as follows: the cage without the mouse was positioned on top of the force plate, and the force levels of all force sensors were adjusted to zero. The mouse was inserted into the cage and the activity measurement of a 48 hour period was collected. After the basal measurement, custom made vertical running wheels (diameter 24 cm, width 8 cm) were added into the cages of the running group. The mice had continuous free access to running wheels. Total wheel revolutions were recorded daily and the total running distance per day was determined by multiplying the number of wheel rotations by the circumference of the wheel. For the next four weeks, the same activity measurement protocol was repeated once a week for all animals. After the final measurements, the running wheels were removed and, one week after that, post-exercise activity measurements were performed. The final results of activity index, activity time

and intensity were calculated from the mean of the first and second halves of the 48h-measurement. The distance result was analysed from the first 24 hours. The design of the in situ testing is summarized in Figure 9.

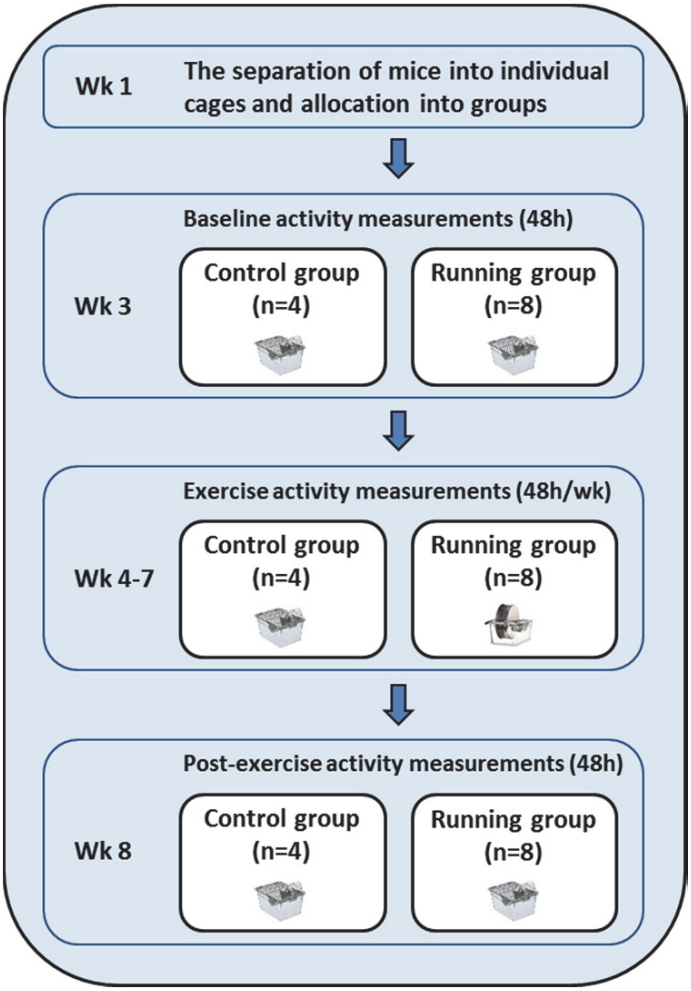

FIGURE 9 The design of in situ testing in study III.

4.2.4 Study IV

The experimental setup consisted of two separate groups: a resistance exercise group (RE, n=11) and an endurance exercise (EE, n=8) group. The subjects were familiarized to the upcoming measurements 4-5 days before the actual experiment day. They were instructed about correct performance techniques in all performed tests. In addition, 1RM leg press (David 210, David Health Solutions Ltd, Helsinki, Finland) and maximal endurance capacity test on a treadmill were performed to assess individual starting loads for subjects. The actual experiment day started at 7.15 a.m. with measurements of height, body mass and

body composition (InBody 720 body composition analyser, Biospace Co. Ltd, Seoul, South Korea). At 8.10 a.m. the first (PRE) muscle biopsy was obtained from musculus vastus lateralis (right leg). The biopsy was cleaned of any visible connective and adipose tissue as well as blood and frozen immediately in liquid nitrogen (-180 °C) and stored at -80 °C. More detailed descriptions of biopsy procedures are given in chapter 4.6. Three hours after the first biopsy, RE performed a single high-load hypertrophic type of resistance exercise using a bilateral leg press machine and EE a single strenuous walking exercise on a treadmill (the exercise protocols are described in more detail in chapter 4.3). To assess basal strength characteristics and muscular fatigue produced by the exercise protocols, the following measurements were performed just before and after exercise: maximal voluntary bilateral isometric force (MVC) of leg extensor muscles (electromechanical dynamometer, Department of Biology of Physical Activity, University of Jyväskylä, Jyväskylä, Finland), maximal dynamic bilateral 1RM leg press and countermovement jump (CMJ). The post exercise biopsy samples were taken from musculus vastus lateralis (left leg) after 30 (12.30 p.m.) and 180 min (15.00 p.m.) of passive recovery. To control effects of pre-loading nutrition and hydration status, the subjects fasted for 12 hours before the first (PRE) biopsy, and immediately after the first biopsy the subjects ate an energy bar (170 kcal, protein 7 g, carbohydrate 21 g and fat 5.5 g) and drank 0.5 litre of water. After the exercise loading, the subjects were again allowed to eat an energy bar and drink water (ad libitum). Finally, the following PGC-1 transcripts were analysed from stored muscle samples: PGC-1α exon 1a-, 1b- and 1b' -derived mRNAs, total NT-PGC-1α, total PGC-1α, and PGC-1β. The measured *PGC-1*α target genes were related to mitochondrial biogenesis (Cytochrome C), angiogenesis (VEGF-A), and muscle hypertrophy (myostatin). In addition, the responses of known PGC-1α regulators p38 MAPK$^{Thr180/Tyr182}$ and p-AMPKα^{Thr172} were measured from the samples. The experimental design of study IV is summarized in Figure 10.

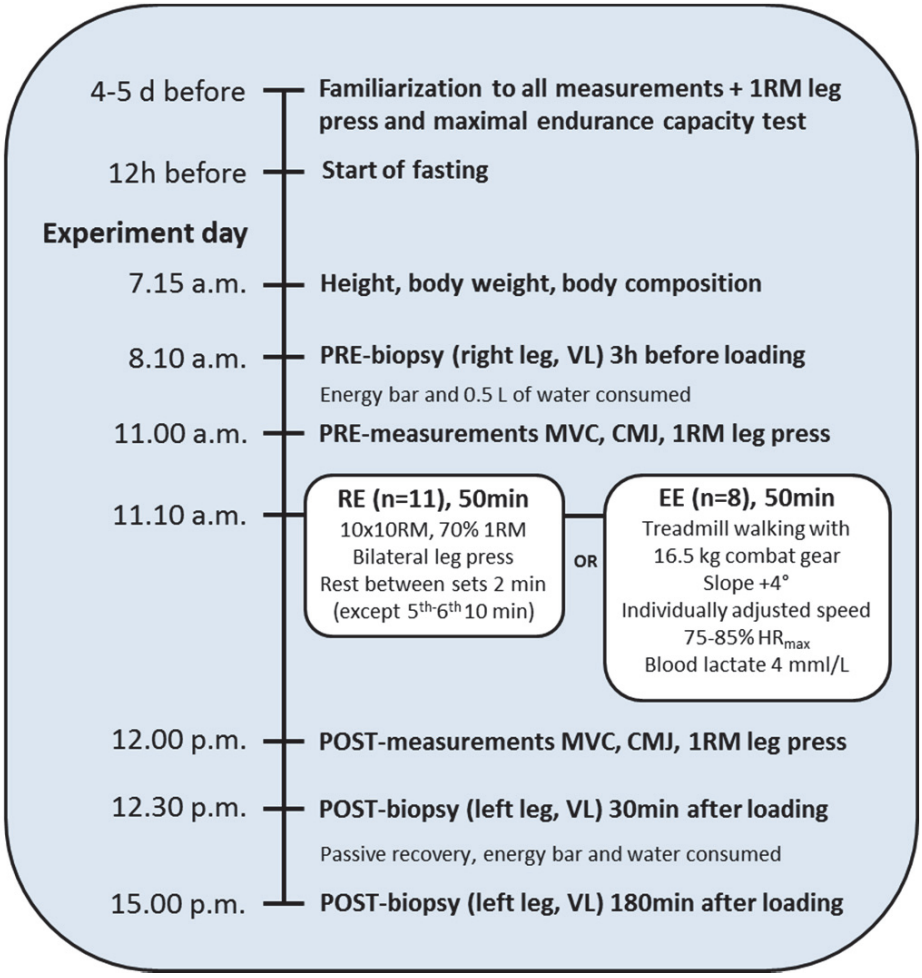

FIGURE 10 The experimental design of study IV (CMJ, countermovement jump; EE, endurance exercise; HR_{max}, maximum heart rate; MVC, maximal voluntary contraction in bilateral isometric force test for leg extensor muscles; RE, resistance exercise; VL, musculus vastus lateralis; VO_{2max}, maximal oxygen consumption; 1RM, one-repetition maximum; 10RM, ten-repetitions maximum).

4.3 Exercise protocols

4.3.1 Voluntary running (I,II,III)

In voluntary running groups, mice or rats were living in cages, which were equipped with running wheels 24h/day. The cages were otherwise similar to those that housed the sedentary animals without the running wheels. During the studies, the total wheel revolutions were recorded daily and the total running distance per day was determined by multiplying the number of wheel ro-

tations by the circumference of the wheel. The voluntary running systems were constructed in our laboratory.

4.3.2 Resistance exercise (IV)

RE was a high-load hypertrophic type of resistance exercise consisting of 10 sets of 10 repetition maximum (10 x 10RM) using a bilateral leg press device (David 210, David Health Solutions Ltd, Helsinki, Finland). The starting load was 70% of 1RM, which was assessed during a familiarization session 4-5 days before exercise loading. Thereafter, the loads were adjusted so that each subject would be able to perform a maximum of 10 repetitions for each set. The recovery between the sets was 2 min, except a 10 min rest that was applied between the 5th and 6th set.

4.3.3 Endurance exercise (IV)

EE consisted of 50 min of strenuous walking on a treadmill with military combat gear weighing 16.5 kg (OJK-1, Telineyhtymä, Kotka, Finland). At minutes 0:00-5:00 and 40:00-45:00 the speed of the treadmill was 4.5 km·h^{-1} and the slope 4.0 degrees. At minutes 5:00-10:00 and 45:00-50:00 the speed was 7.0 km·h^{-1} and the slope 4.0 degrees. During the minutes 10:00-40:00, the walking speed was individually controlled and adjusted in 5-minute intervals based on heart rate (HR) and blood lactate measurements. The criteria for walking speed included: (1) blood lactate concentration approximately 4.0 mmol·L^{-1}, and (2) HR between 75-85% of the individual HR maximum (HR_{max}) that was determined in the maximal endurance capacity test performed during a familiarization session 4-5 days before exercise loading.

4.4 Intraperitoneal glucose tolerance test (I)

Rats were fasted for 12 hours before the test. First the rats were weighed, fasting blood glucose was measured, and 2 g/kg of glucose was injected into the peritoneal cavity. Blood was drawn from the tail vein (5µl) and glucose concentration was measured at 0, 30, 60 and 90 min after the injection with HemoCue B-Glucose Analyser (HemoCue AB, Sweden). The area under the curve (AUC) was used to assess in vivo glucose clearance.

4.5 Respirometry (I)

At first, temperature controlled (22 °C) air from an air conditioning channel was led to a multi-channel mass flow meter (Flow bar 8, Sable systems, Las Vegas, NV, USA), which controlled the steady air flow (3100 ml min^{-1}) to four meas-

urement chambers (1728 cm^3) and one control chamber. After the chambers, air was sub sampled from the particular chamber by a respirometer multiplexer (RM-8, Sable systems, Las Vegas, NV, USA) and led to analysers. Prior to entering a carbon dioxide analyser (LI-6252, LI-COR, Lincoln, Nebraska, USA), moisture was removed from the air (Drierite, Hammond Drierite, Xenia, Ohio, USA). Steady airflow through the analyser was controlled by the gas analyser sub sampler (Sable systems, Las Vegas, NV, USA). The multichannel mass flow meter, respirometer multiplexer and CO_2 analyser were interfaced (Universal interface, Sable systems, Las Vegas, NV, USA) to a PC that controlled the respirometer multiplexer and recorded data from the equipment. This data acquisition was conducted using Datacan V software (Sable Systems, Henderson, Nevada, USA). Each day we initiated measurements by placing weighed individuals (rats) into their chambers 1 h prior to the measurements. The measurements were performed during the daytime (light period of the day), and the chambers were covered with a blanket to prevent visual contact between individuals and to reduce external disturbances. CO_2 levels of each chamber were followed for 20 minutes, after which recordings were done for the next chamber. Before and after the full cycle of 4 chambers (totalling 80 minutes), we obtained baseline values for CO_2 over 20 minutes. The whole measurement cycle was repeated two or three times. After drift correction we picked values of minimum CO_2 production from the data when the animals were not moving, to resemble minimal energy use requirements.

4.6 Tissue collection and preparation (I, II, IV)

In study I, rats were killed at nine months of age. Soleus, extensor digitorum longus (EDL), gastrocnemius and quadriceps femoris muscles and the heart were excised, dissected free from visible fat and connective tissue, and blood samples were taken. For histology, the middle section of the muscles was transversally oriented, mounted in an O.C.T. embedding medium (Tissue Tek, Sakura Finetek Europe) under a microscope to orientate the muscle fibers vertically and snap-frozen in isopentane cooled with liquid nitrogen. The rest of the muscle samples were snap frozen in liquid nitrogen and stored at -80 °C. Serum was separated from the whole blood and stored at -20 °C for later analyses.

After the sacrification of mice used in study II, the gastrocnemius and quadriceps femoris muscles (MQF) were removed from both hind limbs and dissected free from visible fat and connective tissue. The histological samples were prepared from the middle section of the left MQF with the procedure described above. The remaining part of MQF and the other muscle samples were snap-frozen in liquid nitrogen and stored at -80 °C for further analysis. Serum was separated and stored as described above.

In study IV, the first (PRE) muscle biopsy was obtained from VL (right leg) three hours before exercise, and post exercise biopsy samples from VL (left leg) after 30 and 180 min of recovery. Biopsies were taken with a 5-mm Bergström

biopsy needle together with suction, midway between the patella and greater trochanter. Muscle depth was kept constant through markings on the needle. The muscle sample was cleaned of any visible connective and adipose tissue as well as blood, frozen immediately in liquid nitrogen (-180 °C) and stored at -80 °C.

4.7 Blood analyses (I, II, IV)

Blood glucose concentration was analysed with a HemoCue B-Glucose Analyser (HemoCue AB, Ängelholm, Sweden) and serum insulin with an Ultra-Sensitive Rat Insulin ELISA Kit according to the manufacturer's protocol (Crystal Chem Inc., Downers Grove, IL, USA). The HOMA-IR index (homeostasis model assessment of insulin resistance) was calculated as follows: HOMA-IR = fasting blood glucose (mmol/L) x fasting plasma insulin (mU/L) / 22.5 (Matthews et al. 1985). Serum-free fatty acids were determined by an enzymatic colorimetric method of the Wako NEFA C test kit (Wako Chemicals GmbH, Neuss, Germany) scaled down to a microplate format. Triglycerides, total cholesterol and HDL-cholesterol were measured from the serum using VITROS DT60 II Chemistry System (Ortho-Clinical Diagnostics, Rochester, NY, USA). The LDL-cholesterol (LDL-C) concentration was estimated using Friedewald's equation (Friedewald, Levy & Fredrickson 1972). In study IV, fingertip blood lactate samples were collected before and immediately after exercises into capillary tubes, which were placed in a 1 mL hemolysing solution and analysed automatically (EKF diagnostic, Biosen, Barleben, Germany).

4.8 Electron microscopic analysis of mitochondrial content (I)

Pieces of soleus muscle were fixed with 3% glutaraldehyde in 0.1 M phosphate buffer (pH 7.4) for 2-3 h at 4 °C, and post-fixed with 1% osmiumtetroxide in the same buffer at 4 °C. The specimens were then stained en block in 2% uranyl acetate, dehydrated in ethanol and embedded in LX-112 (Ladd). Semi thin sections of tissue blocks were first examined with light microscope to optimize the transverse orientation and thin sections were thereafter cut with ultramicrotome and mounted on formvard-coated copper grids. Double staining on grids was performed with uranyl acetate and lead citrate. Thin sections were examined with a Jeol JEM-1200 electron microscope at an accelerating voltage of 60 kV. The best section of each block was chosen and 10-15 micrographs were taken at 1500-2500 x primary magnification. It was carefully checked that micrographs were taken from different cells and that sarcolemmal areas were included in micrographs. Micrographs were analysed using AnalySIS software from Olympus. The amount of subsarcolemmal mitochondria was expressed as mitochondrial area (μm^2) and related to the length of the sarcolemma (1000 μm) un-

der which it was measured. Intermyofibrillar mitochondrial content was expressed as a percentage of mitochondrial area of the cytoplasm.

4.9 Immunohistochemistry and ATPase staining (I, II)

Cross-sections (8 µm) were cut from the studied muscles (Study I: Soleus, EDL and Gastrocnemius; Study II: MQF) in a cryomicrotome (-25 °C). Capillaries were visualized by staining with Isolectin-GS-IB_4 containing fluorescent Alexa Fluor 488 label (Molecular Probes, Eugene, OR, USA; 1:200 dilution in 1% BSA/PBS). This was combined with antidystrophin staining (Novocastra, Newcastle on Tyne, UK; 1:500 dilution in 1% BSA/PBS) with Alexa Fluor 555 secondary antibody (Molecular Probes; 1:300 dilution in 1% BSA/PBS) to visualize muscle fibers. Double-stained sections were visualized with Olympus BX-50 fluorescent microscope (Olympus Optical, Tokyo, Japan) and analysed using TEMA image analysing software (TEMA Image-Analysis System, Scan Beam, Denmark) in a blinded manner. Muscle fiber cross-sectional area (CSA), capillary density (number of capillaries per mm^2) and capillary-to-fiber ratio were calculated. The number of muscle fibers analysed per sample ranged from 300 to 500.

For light microscopy (study I), EDL muscle sections were stained with dystrophin antibody (1:500 dilution) and DAB as a substrate for fiber size analysis. ATPase staining with acidic (4.3) and alkalic (10.4) pH was used to analyse type I and type II fiber type proportions (Brooke & Kaiser 1970). TEMA image analysis software (Tema, Scanbeam, Hadsund, Denmark) was used to calculate the fiber type proportions, cross-sectional areas and fiber type proportions.

4.10 Protein measurements (II, IV)

4.10.1 Western blotting (II,IV)

The MQF muscle samples of study II were hand-homogenized with dounce homogenizer in ice-cold buffer [10% SDS (w/v), 40 mM DTT, 5 mM EDTA, 0.1 M Tris-HCl (pH 8), 40 µg/ml aprotinin, 80 µg/ml PMSF and 40 µg/ml leupeptin] at a dilution of 25 µl/mg of wet weight muscle. The muscle biopsy specimens of study IV were homogenised with the same method but using different buffer (20mM HEPES (pH 7.4), 1mM EDTA, 5mM EGTA, 10mM MgCl2, 100mM b-glycerophosphate, 1mM Na_3PO_4, 2mM DTT, 1% Triton X-100, 0.2% sodium deoxycholate, 30 mg·mL^{-1} leupeptin, 30 mg·mL^{-1} aprotinin, 60 mg·mL^{-1} PMSF, and 1% phosphatase inhibitor cocktail [P 2850; Sigma, St Louis, Missouri, USA)] at a dilution of 15 µl/mg of wet weight muscle. Homogenates were rotated for 30 min at 4 °C, centrifuged at 10,000 *g* for 10 min at 4 °C to remove cell debris, and stored at −80 °C. Total protein was determined using a bicincho-

ninic acid protein assay (Pierce Biotechnology, Rockford, IL, USA). Aliquots of muscle lysate (Study II: 20 µg; Study IV: 30 µg of total protein) were solubilised in Laemmli sample buffer and heated at 95 °C for 10 min to denature proteins, and were then separated by SDS-PAGE for 90 min at 200 V using 4–20% gradient gels on Criterion electrophoresis cell (Bio-Rad Laboratories, Hercules, California, USA). Proteins were transferred to PVDF membranes at 300-mA constant current for 3 h on ice at 4 °C. Membranes were blocked in TBS with 0.1% Tween 20 (TBS-T) containing 5% non-fat dry milk for 1 h and then incubated overnight at 4 °C with commercially available primary antibodies. In study II, the following primary antibodies were used: PGC-1α (1:1000, Calbiochem, Merck KGaA, Darmstadt, Germany), ERRα (1:3000 Novus Biologicals, Littleton, CO, USA), VEGF-A (1:500, Santa Cruz Biotechnology, Santa Cruz, CA,USA) Cytochrome C (1:2000, Santa Cruz Biotechnology, Santa Cruz, CA,USA) and HIF-1α (1:300, Novus Biologicals). PGC-1α, ERRα, VEGF-A and Cytochrome C antibodies were diluted in TBS-T containing 2.5% non-fat dry milk. HIF-1α antibody was diluted in TBS-T containing 2.5% BSA. In study IV, antibodies recognizing phosphorylated p38MAPK$^{Thr180/Tyr182}$ and AMPKα^{Thr172} were purchased from Cell Signalling Technology (Danvers, Massachusetts, USA) and these primary antibodies were diluted 1:2000 in TBS-T containing 2.5% non-fat dry milk. PGC-1α antibody (Calbiochem, Merck KGaA, Darmstadt, Germany) was diluted 1:3000 in the same buffer solution.

After primary antibody incubations, the membranes were washed in TBS-T (5 x 5min), incubated with secondary antibody (horseradish peroxidase-conjugated IgG; Jackson ImmunoResearch Laboratories, PA, USA) diluted 1:25000 in TBS-T with 2.5% milk for 1 h and washed in TBS-T. Proteins were visualized by ECL according to the manufacturer's protocol (SuperSignal West femto maximum sensitivity substrate, Pierce Biotechnology) and quantified using a ChemiDoc XRS in combination with Quantity One software (version 4.6.3. Bio-Rad Laboratories). The uniformity of protein loading was confirmed by staining the membrane with Ponceau S. The earlier studies and preliminary experiments in our laboratory had confirmed a proportional linear relation between the protein loaded and the strongest band in Ponceau S at ~42 kDa in quantification between 5 and 60 µg of total protein loaded (Hulmi et al. 2012). A less proportional and linear relationship was found between GAPDH , α-actin and staining of myosin heavy chain left in the gel after blotting. Therefore, all of the results were normalised to the corresponding Ponceau S staining value at ~42 kDa.

4.10.2 Myosin heavy chain composition analysis (I)

The MHC isoform composition of the soleus, EDL and gastrocnemius muscle samples collected in study I was determined by SDS-PAGE according to a previously described method with slight modifications (Andersen & Aagaard 2000). For the analysis, 15-25 serial cryosections (10µm) from the histology samples were placed into lysing buffer (10% glycerol, 5% 2-mercaptoethanol, 2.3% SDS in 62.5 mM Tris-HCl buffer) and heated for 10 min at 60 °C. A small amount of

muscle extract (5-10 µl) was loaded into each lane of the SDS-PAGE gel system consisting of stacking gel with 3% acrylamide and separating gel with 6% acrylamide and 30% glycerol. The gels were run at a constant voltage of 70 for 42 h at 4 °C. After the run, the gels were fixed, stained with Coomassie blue, and destained in 7.5% acetic acid and 5% methanol. In the stained gels three distinct protein bands could be separated and identified as MHC I, IIb, and IIa+x according to their migration characteristics in the gel. The IIa and IIx bands were too close to each other to be analysed separately. The relative proportion of each MHC isoform was determined by densitometric analysis using Quantity One software (Bio-Rad).

4.11 Messenger RNA expression

4.11.1 Laser capture microdissection (II)

LCM was used to collect capillaries and pure muscle fibers from the MQF muscles in study II. Samples were collected from eight randomly selected mice from all intervention groups, comprising a total of 64 LCM samples (capillaries and muscle fibers from each animal). The procedures were adapted from Milkiewicz & Haas (2005) (Milkiewicz & Haas 2005). Cryosections (8 µm) were cut on uncoated glass slides and fixed immediately with cold acetone. Capillaries were stained with Isolectin GS-IB4 from Griffonia simplicifolia Alexa Fluor 488 conjugate (Molecular Probes), which was diluted in sterile PBS with SUPERaseIn RNAase inhibitor (Ambion, Austin, USA). After a brief wash, the samples were dehydrated and debris was removed with PrepStrip (Arcturus Engineering, Molecular Devices Corporation, Sunnyvale, USA). LCM was performed with a Veritas microdissection system (Arcturus Engineering). From each cryosection 500–1000 capillaries and muscle fiber samples were randomly collected from all parts of the muscle, including both the deep oxidative and the superficial glycolytic portions. Capillary and muscle fiber samples were attached to CapSure LCM caps (Arcturus Engineering) with similar laser pulses. Capillaries were distinguished by size (<10 µm) from larger blood vessels.

4.11.2 RNA extraction (I,II,IV)

Total RNA was isolated from muscle samples (I,II,IV) with Trizol Reagent (Life Technologies, Carlsbad, California, USA) according to the manufacturer's instructions. Muscle samples were homogenised with a FastPrep FP120 (Thermo Fisher Scientific, Waltham, Massachusetts, USA) tissue homogeniser using Lysing Matrix D FP120 (Thermo Fisher). The concentration and purity of RNA was determined by spectrophotometry (NanoDrop; Thermo Fisher Scientific) at wavelengths 260 and 280 nm. Integrity was checked with agarose gel electrophoresis. From capillary and muscle fiber samples (II), RNA was extracted with

a PicoPure RNA isolation kit (Arcturus Engineering) according to the manufacturer's protocol.

4.11.3 cDNA synthesis (I,II,IV)

In study I, 1 µg of total RNA was reverse-transcribed to cDNA with a High Capacity cDNA Archive Kit (Applied Biosystems, Foster City, USA). In studies II and IV, reverse transcription of muscle sample-derived mRNA was performed from total RNA (5 µg) using anchored oligo$(dT)_{20}$ primers (Oligomer, Helsinki, Finland) and a SuperScript III Reverse Transcriptase kit (Life Technologies) according to the manufacturer's instructions. RNA extracted from capillary and muscle fibers samples was reverse-transcribed to cDNA with a Sensiscript reverse transcription kit (Qiagen, Hilden, Germany) according to the manufacturer's instructions, and using both random and oligo (dT) primers (Ambion). The cDNA samples were stored at -20 °C.

4.11.4 Microarray analysis (I)

RNA samples from gastrocnemius muscle of all 24 rats (study I) were analysed with genome-wide Illumina Sentrix RatRef-12 BeadChip (BD-27-303, Illumina Inc., San Diego, CA, USA) that contained 22,523 probes. The microarray hybridizations were performed by the Finnish DNA Microarray Centre at Turku Centre for Biotechnology according to the manufacturer's instructions. Hybridization was detected with Cyanin-3-streptavidin (1 µg/ml, Amersham Biosciences, GE Healthcare, Uppsala, Sweden) using Illumina Bead Array Reader (Illumina Inc.) and BeadStudio v2.3.41 software (Illumina Inc.). Data analyses were performed with R software environment for statistical computing, including Bioconductor development software. The data were normalized with quantiles-normalization from affy package of Bioconductor (Gautier et al. 2004).

The clustering of differentially expressed genes into functional groups and their significance of over-representation among the groups was estimated with DAVID Functional Annotation Tool (http://david.abcc.ncifcrf.gov/home.jsp) (Dennis et al. 2003; Huang da, Sherman & Lempicki 2009). Genes were clustered according to enrichment of Gene Ontology terms (GO-terms) within differentially expressed genes. In addition, Gene Set Enrichment Analysis (GSEA; www.broad.mit.edu/gsea/) (Subramanian et al. 2005) was applied for functional clustering of all genes without a priori filtering of the expression data. In the analysis, predetermined curated and motif gene sets of MSigDB database (www.broad.mit.edu/gsea/msigdb/) were utilized to compare HCR and LCR phenotypes. In order to compare pheno- and genotypes, the most significant gene clusters obtained from the GSEA analysis were further correlated to physiological and biochemical parameters. For this purpose, leading-edge subsets (i.e. genes producing the GSEA enrichment score) were determined. Common leading-edge genes of several clusters were determined using the leading-edge analysis feature of GSEA (Subramanian et al. 2005). The mean centroid of each

leading-edge subset was computed by normalizing the expression levels of all subset genes to a mean of 0.

4.11.5 Real-time Quantitative PCR (I,II,IV)

The microarray data of study I was verified and supplemented with RT-qPCR measurements for selected genes involved in energy metabolism. These genes were selected both to validate microarray results and also to determine whether other genes important to lipid metabolism were changed. In addition to gastrocnemius muscle, which was studied with microarray, we analysed slow soleus and fast EDL muscles with qPCR. In study II, the expression of angiogenesis regulating genes were measured from mouse gastrocnemius muscle samples, muscle fibers and capillary samples. In addition, in study IV we investigated the expression of different PGC-1 isoforms in human skeletal muscle (VL) before and after RE and EE. Two different RT-PCR methods were used in these measurements. The ABI Prism 7300 Sequence Detection System was used to perform TaqMan probe-based RT-qPCR reactions (Life Technologies), and CFX96 Real-Time PCR Detection System (Bio-Rad Laboratories) in performing SYBR green (Bio-Rad Laboratories) based RT-qPCR reactions. The following PCR cycle parameters were used: +50 °C for 2 min, +95 °C for 10 min, 40 cycles at +95 °C for 15 s, and +60 °C for 1 min (TaqMan); and +95 °C for 10 min, 40 cycles at +95 °C for 10 s, at gene specific annealing temperature (~60 °C) for 30 s and at +72 °C for 30 s, followed by 5 s at +65 °C (SYBR green). TaqMan primers and probe sets were designed and synthesized by Applied Biosystems (Life Technologies). The primer pairs for SYBR green based RT-qPCR were synthesized by Invitrogen (Life Technologies). The primer sequences recognising total NT-PGC-1α and PGC-1α exon 1a-derived transcripts were copied from Ruas et al. (Ruas et al. 2012) and myostatin from Kim et al. (Kim et al. 2007). Other primers were designed with Primer3 (web version 4.0.0) software (Koressaar & Remm 2007; Untergasser et al. 2012). When possible, the primer pairs were designed so that they overlapped an exon-exon boundary to avoid interference from possible genomic DNA contamination. Following pilot RT-qPCR runs performed with the SYBR green method, the specificity of each primer set was monitored by the melting curves and by agarose gel (3%) electrophoresis. In addition, optimal gene specific annealing temperatures were determined. The amplification efficiencies for each gene were 100 ± 5%. The primers and probes used are presented in Table 3. The structure of 5′-region of the human PGC-1α gene is illustrated in Figure 11a. In addition, a detailed description of exon structure and the design of primers used in detecting different isoforms of PGC-1α are presented in Figure 11b.

To correct for variation in RNA loading and reverse transcription efficiency, the expression data of study I was normalized to the levels of 18S mRNA, which showed no difference between groups when related to the amount of total RNA or another commonly used reference gene GAPDH. In study II GAPDH was used as a reference gene. The stability of GAPDH was confirmed by the fact that there were no differences between groups in the GAPDH ex-

pression of the muscle homogenate samples when normalized to cDNA-RNA hybrid concentrations. cDNA-RNA hybrid concentrations were measured using a Quant-iT™ PicoGreen® assay (Invitrogen) according to the manufacturer's recommendations. In study IV, mRNA expression data was normalised using cDNA-RNA hybrid concentrations. This method of normalisation has been validated especially for human exercise studies and muscle biopsy samples (Lundby et al. 2005). The stability of cDNA-RNA hybrid concentrations was compared to stability of GAPDH. The average differences between time points in both exercise modes were similar in GAPDH and cDNA-RNA hybrid concentrations. However, variation within time points for both exercise modes was lower in cDNA-RNA hybrid concentrations compared to GAPDH levels. Each sample was analysed in triplicate, and a nontemplate control was included in each run. Relative gene expression levels of all target transcripts were calculated with the ΔΔCt method.

TABLE 3 Primers and probes used for RT-qPCR. [1](Ruas et al. 2012); [2](Kim et al. 2007)

Transcript	Species	TaqMan primers and probes	SYBR Green primers (5´-3´)
Aco1	Rat	Rn00569045_m1	
Aco2	Rat	Rn00577876_m1	
Cpt1a	Rat	Rn00580702_m1	
Cpt1b	Rat	Rn00566242_m1	
Cpt2	Rat	Rn00563995_m1	
Cyc	Human	Hs01588974_g1	
ERRα	Mouse	Mm00433142_m1	
GAPDH	Human	Hs03929097_g1	
GAPDH	Mouse	Mm99999915_g1	
GAPDH	Rat	Rn99999916_s1	
Hadhb	Rat	Rn00592435_m1	
HIF-1α	Mouse	Mm00468875_m1	
Lpl	Rat	Rn00561482_m1	
Total NT-PGC-1α[1]			F: TCACACCAAACCCACAGAGA
			R: CTGGAAGATATGGCACAT
Total PGC-1α	Human		F: AGCCTCTTTGCCCAGATCTT
			R: GGCAATCCGTCTTCATCCAC
Total PGC-1α	Mouse	Mm01208833_m1	
Myostatin[2]			F: CTACAACGGAAACAATCATTACCA
			R: GTTTCAGAGATCGGATTCCAGTAT
PGC-1α ex1a-derived[1]	Human		F: ATGGAGTGACATCGAGTGTGCT
			R: GAGTCCACCCAGAAAGCTGT
PGC-1α ex1b-derived	Human		F: CTATGGATTCAATTTTGAAATGTGC
			R: CTGATTGGTCACTGCACCAC
PGC-1α ex1b'-derived	Human		F: TGAAAGTGAGTATCAGGAGGCA
			R: CTGATTGGTCACTGCACCAC
PGC-1β			F: GAGTCAAAGTCGCTGGCATC
			R: AACTATCTCGCTGACACGCA
Ucp2	Rat	Rn01754856_m1	
Ucp3	Rat	Rn00565874_m1	
VEGF-A	Human	Hs00900055_m1	
VEGF-A	Mouse	Mm00437304_m1	
18S	Rat	Rn01428915_g1	

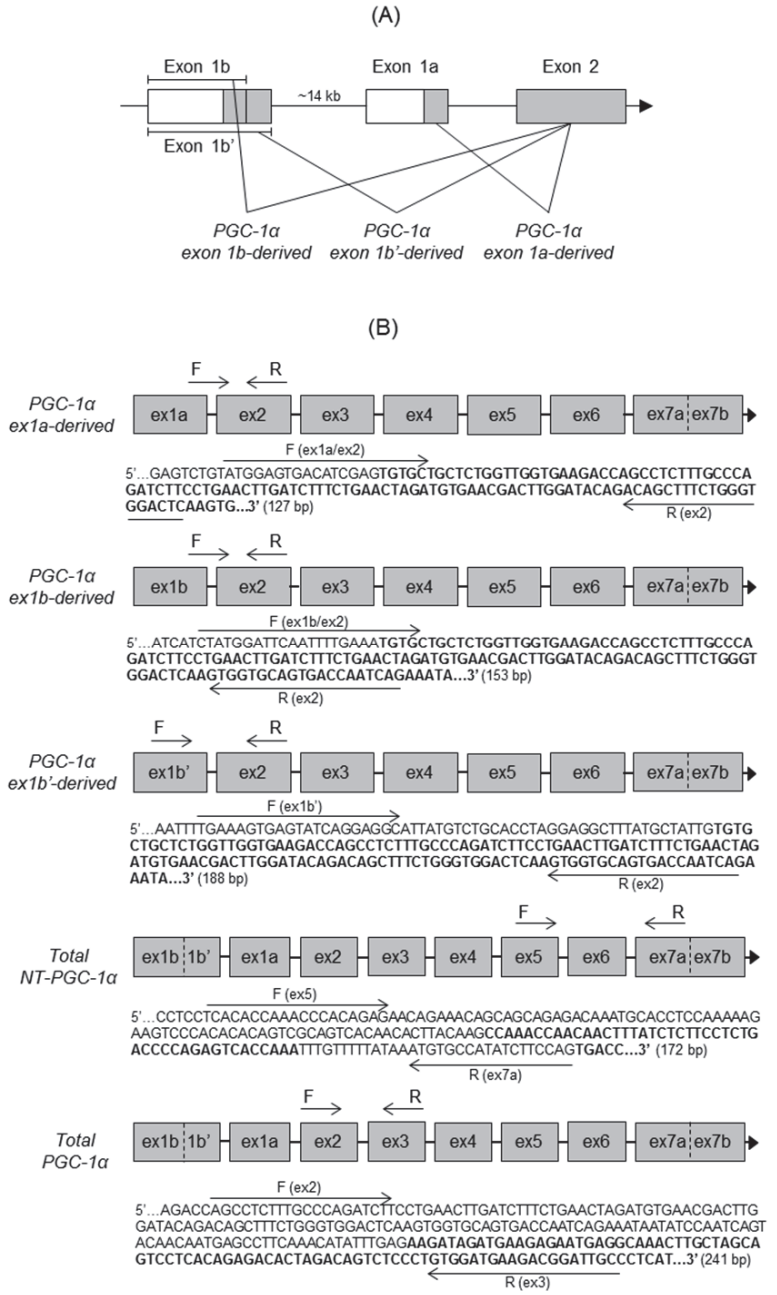

FIGURE 11 (A) The schematic structure of the 5′-region of the human PGC-1α gene (Miura et al. 2008). White boxes indicate untranslated exon regions and grey boxes translated coding regions. Straight lines between boxes indicate introns. When mRNA is formed from the gene, two completely distinct first exons of PGC-1α (exon 1a and 1b) can be spliced to the common exon 2. Furthermore, exon 1b can be spliced to the common exon 2 in two different ways producing either PGC-1α exon 1b- or 1b′-derived transcripts. In addition to differences in the starting exon, the splice variants of PGC-1α differ via alternative 3′ splicing. The exon subsequent to exon 6

may be either exon 7a (ex7a) or exon 7b (ex7b). Ex7a is the exon insert, which contains an in-frame stop codon resulting in the shorter N-truncated proteins (NT-PGC-1α). Ex7b is present in nontruncated full length PGC-1α proteins, which are translated using all 13 exons of PGC-1α. The proximal promoter drives the transcription of PGC-1α exon 1a-derived transcripts (truncated and nontruncated) and the alternative promoter the transcription of PGC-1α exon 1b and 1b′-derived transcripts (truncated and nontruncated). (B) Detailed descriptions of primer pairs and their possible cDNA targets. Primer pairs for detecting PGC-1α exon 1a-, 1b-, 1b′-derived transcripts are specific for different first exons but do not separate truncated and nontruncated PGC-1α splice variants. Primer pair for Total NT-PGC-1α is specific for truncated PGC-1α splice variants but does not separate differences in the first exon. The total PGC-1α primer pair was designed to detect all truncated and nontruncated splice variants of PGC-1α. The possible exon structures of mRNA targets for each primer pair are illustrated with grey boxes. The structure is presented only from the first exon to Ex7a or Ex7b because the mRNA structure is common in the following exons (Ex8-Ex13). Binding sites of target specific forward (F) and reverse (R) primers are pointed out by arrows drawn next to the cDNA sequence in question. The sequences of all primers are also listed in Table 3. The sequences are amplicon sequences plus 5 nucleotides in the 3′- and 5′-end. The sequences of every other exon are in bold to separate subsequent exons from each other. The sequences were constructed by using human PGC-1α cDNA sequence (Ensembl: ENST00000264867), human PGC-1α gene sequence with its upstream regions (NCBI, Gene ID: 10891), and published cDNA structures of murine PGC-1α splice variants (Wen et al. 2014; Ruas et al. 2012).

4.12 Spontaneous activity measurements (IV)

4.12.1 Force-plate system

For the home cage activity analysis, a ground reaction force measurement system was developed in our laboratory. The plates were located on their own shelves (damping rubber sheets between the legs and ground) to avoid cross talk between the plates. To minimize vibration from the surroundings, cellular plastic sheets (thickness 15 mm) were placed between the shelf and the base of the force plate. A granite plate (thickness 35 mm, width 255 mm, length 580 mm, weight 14.3 kg) was used as a stabilizing base on top of which the four force sensors were attached in a rectangular formation (Figure 12). The core of the force sensor is the bridge formed by a stainless steel sheet fixed from both of its ends. There are two strain gauges (1-LY41-6/700; HBM, Darmstadt, Germany) attached on both the lower and upper surface of the sheet. The strain gauges are connected so that a classical Wheatstone bridge is formed. The output voltage from the sensor is directly related to the vertical force bending the strain gauges. The forces are mediated by a pin (diameter 4 mm) that is attached to the top of the steel bridge in the middle of two strain gauges. The pins of the four sensors form a rectangle (width 120 mm and length 280 mm) and a glass plate (thickness 5 mm, width 250 mm, length 450 mm) lies on top of them. Horizontal movement of the glass plate is prevented by rubber ring adapters that are attached underneath the glass plate. Similar rubber rings, on the other side of the

glass, fix the cage in place on top of the glass. The force plates can measure ground reaction forces from all cage types regardless of the equipment inside the cage. In the present study, the model of the cage was 1284L Eurostandard Type II L (365x207x140 mm, Tecniplast, Italy). The output voltages from the sensors were pre-amplified (AD620, Analog Devices, Norwood, MA, USA) before data collection. The amplifications were adjusted to 0.077 Kg/V in each sensor. After amplification, the signals pass through the controller unit that has the capability to zero all sensors. A 14 bit A/D converter (DI-710, DATAQ Instruments, Akron, Ohio, USA) was used for digitizing the data at a sampling rate of 80 Hz. The converter was operated and the data stored with WinDaq/Lite (DATAQ Instruments, Akron, Ohio, USA) data acquisition software. A measurement range of ±192.5 g was used, while the digitization precision was <0.02 g.

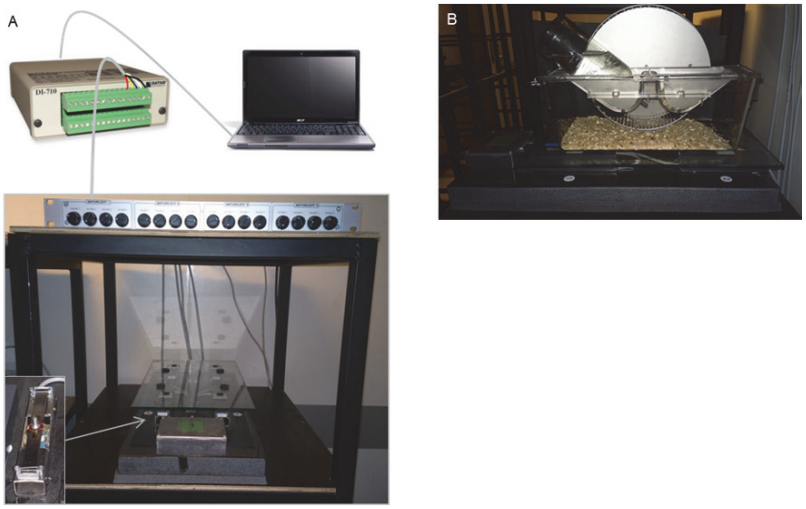

FIGURE 12 (A) The main components of the activity measurement system: rack, cellular plastic sheet cushioning, granite base, strain gauge based sensors (enlarged picture in the lower left corner), sensor amplifier, glass plate with rubber ring adapters, controller unit, A/D converter and computer. B. Side view of the plate with a cage.

4.12.2 Activity index

Activity index was originally developed by Biesiadecki et al. 1999 (Biesiadecki et al. 1999) for using laboratory balance as an activity measurement device. It was developed and tested for measuring the activity of rats. The activity index is simple to calculate and it is insensitive to evaporation-induced mass changes. We modified the analysis of activity index for our system that was developed for measuring mice. The most significant modifications are the body mass correction of the index value and the background subtraction. In detail, the meas-

ured force values were summed from four sensors. The sum signal was then smoothed by a 2nd order 10 Hz zero lag low pass Butterworth filter. The filtering cut-off was selected based on pilot experimentation. After filtering, the activity index was calculated as follows: the absolute values of the differences between consecutive force values were calculated. The mean of the absolute values were calculated from every second (from 80 values per second). To obtain a single value for total spontaneous activity, the 1-second means were summed for the total measurement time and the sum was divided by the body mass (kg) of the measured mice. The lowest activity index value for a 5 minute interval was analysed from the data (background activity) and then this value was scaled to the whole measurement time to produce an estimate of the contribution of inactivity to the index (including measurement noise, and forces caused by an inactive animal, e.g. breathing, heart beat). The contribution of background activity was then subtracted from the activity index to produce the index reported in the present paper.

4.12.3 Activity time

The activity time calculation was based on identifying and summing the active seconds from the activity index data. Each second when the activity index value was higher than 3 times the level of background activity was classified as an active second.

4.12.4 Intensity of the activity

The intensity of the activity was calculated by summing the final activity indexes from active seconds and dividing the sum by activity time.

4.12.5 Horizontal distance

Before the determination of instantaneous position and distance calculations, the raw data from all individual force sensors was smoothed by a 2nd order 0.75 Hz zero lag low pass Butterworth filter. The filtering cut-off was selected based on pilot experimentation. The coordinates of the instantaneous position of the animal (or water in validation measurement) were calculated as:

$$x = \frac{\mathrm{f2} + \mathrm{f3}}{\mathrm{f1} + \mathrm{f2} + \mathrm{f3} + \mathrm{f4}} \times \mathit{Distance\ between}\ \mathrm{f1}\ \mathit{and}\ \mathrm{f2} \quad (1)$$

$$y = \frac{\mathrm{f3} + \mathrm{f4}}{\mathrm{f1} + \mathrm{f2} + \mathrm{f3} + \mathrm{f4}} \times \mathit{Distance\ between}\ \mathrm{f1}\ \mathit{and}\ \mathrm{f4} \quad (2)$$

where f1. . .4 are the instantaneous force readings of a given strain gauge.

The horizontal distance was calculated as:

$$Distance = \sum_{i=1}^{n-1} \sqrt{(x_{i+1} - x_i)^2 + (y_{i+1} - y_i)^2} \times \frac{1}{dt}, \quad (3)$$

where n is the total number of coordinate pairs, x_i and y_i are the x- and y-coordinates in mm of the *i*th instantaneous position, and dt is the interval between consecutive samplings, i.e. 0.0125 s.

4.12.6 Horizontal distance correction and background subtraction

When long-lasting measurements (>10 hours) are performed with mice, evaporation induces mass change that generate an error in the distance results. The error can be seen as a significant drift in minimum minute distances per hour. Assuming that the minimum distance covered in a minute in any given hour is inactivity, these values should be similar and stable. The distance data was corrected minute by minute using correction coefficients derived from a formula describing a second order regression line fitted to minimum distance values (minimum minutes per hour). The median of minimum minute distances, analysed hour by hour from corrected data, was used as the background value and it was finally subtracted from the data.

4.13 Statistical methods

In all studies (I-IV), conventional statistical methods were used to obtain means, standard deviations (SD), standard errors (SE), medians, interquartile ranges, and percentiles when needed. The Shapiro-Wilk test was used to test the normality of the variables and Levene's test was used to analyse the homogeneity of variances. All statistical analyses were carried out using IBM SPSS statistics 20.0 software (IBM Corporation, Armonk, NY) unless stated otherwise.

In **study I** the differences between rat strains were analysed with two-tailed Student's t-test (all except microarray results). Statistically significant differences in individual genes between HCR and LCR rats were tested using Student's t-test and *P* values were adjusted with Benjamin-Hochberg algorithm controlling false discovery rate (FDR). Adjusted values of $P < 0.05$ were considered statistically significant. When the differently expressed genes were clustered with DAVID functional annotation tool the statistical significance of clusters was estimated by modified Fisher Exact *P*-Value. Linear univariate analysis of variance was performed using phenotype-defining parameters as dependent variables, rat strain as a fixed factor and mean centroids of the most significant gene subsets (derived from GSEA analyses) as the independent explanatory covariates. The commonly found effect of mass on respiratory values was ac-

counted for in the analysis of covariance (Packard & Boardman 1999). In this analysis a hierarchical method was used (Hendrix, Carter & Scott 1982).

In **study II** two-way ANOVA was used to determine the effect of diet (low-fat diet and high-fat diet), activity (sedentary and active/voluntary running), and their interaction on the measured variables when the normality and equality of variance assumptions were met. In this case, Holm-Bonferroni method was used for post hoc testing. If assumptions were not met, logarithmic transformations were performed. If these parameters still did not meet the assumptions, the Kruskal Wallis Test was used for multiple comparisons and Mann-Whitney U for post-hoc analysis. The significance level was set at $P < 0.05$.

In **study III,** when the normality and equality of variance assumptions were met, ANOVA was used to determine the differences between the time points within groups and the paired t-test with Holm-Bonferroni correction was used for post hoc comparisons. When the assumptions were not met, logarithmic transformations were conducted. If these parameters still did not meet the assumptions, non-parametric Friedman's two way ANOVA by ranks test was used to determine differences between time points within groups. Wilcoxon signed-rank test was used for post hoc analysis. Differences between the groups were determined using the Mann–Whitney U test. The similarity of the measured activity variables and the true values were assessed with Pearson correlation coefficient and Bland–Altman plots (Bland & Altman 1986). LOA was calculated using the formula: mean ± 2 x standard deviation (Bland & Altman 1986). As a measure of repeatability, the average root-mean-square coefficient of variation (CV_{rms}) was calculated from repeated measurements. The significance level was set at $P < 0.05$.

In **study IV,** due to the small sample size and random violations in the normal distribution and homogeneity of variance assumptions, a nonparametric Friedman's two-way ANOVA by ranks test was used to determine differences between time points (PRE, 30′ and 180′) within groups (RE and EE). Wilcoxon matched-pair signed-rank test with Holm–Bonferroni correction was used for post hoc analysis. A Spearman's rank correlation test was used to test whether changes in p38 MAPKThr180/Tyr182 or AMPKαThr172 phosphorylation were associated with exercise-induced gene expression changes. The significance level was set at $P < 0.05$.

5 RESULTS

The main findings of the present series of experiments are presented. For more details the original articles (I-IV) should be consulted.

5.1 Characteristics of inherited running capacity (I)

5.1.1 Physiological characteristics of HCR and LCR rats

Maximal exercise capacity was determined at 11 weeks of age using a standard incremental treadmill running test (Wu et al. 1999) in 12 low capacity runners (LCR) and 12 high capacity runners (HCR) born at 18 generations of selection (all females). The mean distance run at exhaustion was 305 ± 16 m in LCR vs. 1883 ± 45 m in HCR, which corresponded to maximal running times of 20.8 ± 0.8 min and 69.8 ± 1.0 min, respectively. HCR females were 38 g (24%) lighter ($P < 0.001$) than LCR at two months of age and this weight difference was retained at 5 and 8 months of age (Figure 13A). Daily voluntary running distance was ~4-fold greater ($P < 0.001$) in HCR compared to LCR during three weeks spent in the cages with running wheels (Figure 13). HCR spent more time in the running wheel than LCR (2.6-fold, $P < 0.001$), which explained most of the difference in running distance (r=0.96, $P < 0.001$).

5.1.2 Energy uptake and resting metabolic rate

HCR consumed more energy than LCR when the rats had access to running wheels and after the running period ($P < 0.05$). HCR energy intake also tended to be higher before they were given running wheels (7%, $P = 0.13$). From analysis of covariance we found that HCR rats had higher CO_2 production at rest than LCR rats (150.3 ± 5.8 vs. 125.9 ± 6.4 ml/h, $F_{1,17} = 5.848$, $P < 0.05$). This result was evident when the significant effect of body mass ($F_{1,17} = 14.755$, $P < 0.001$)

and HCR/LCR- age interaction effect ($F_{1,17}$ =6.663, $P < 0.05$) on CO_2 production were taken into account.

5.1.3 Glucose balance and blood lipids

Fasting blood glucose and random (no fasting) serum insulin were higher in LCR relative to HCR (Figure 13C), but no significant difference was found between the strains for glucose tolerance (area under the curve analysis). The HOMA index was significantly higher in LCR (21.6 ± 8.3 vs. 10.8 ± 3.9, $P < 0.001$). Serum triglycerides were higher and high density lipoprotein and free fatty acids were lower in LCR compared to HCR (Figure 13D).

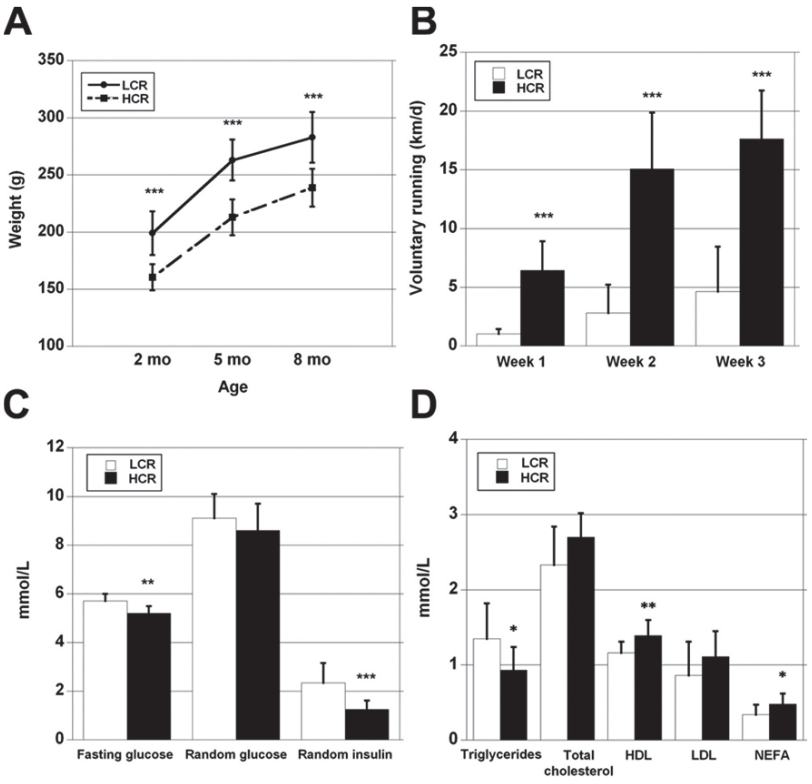

FIGURE 13 (A) LCR rats were heavier (~20%) throughout the study. (B) HCR rats ran ~4 times the distance in a day compared with LCR rats during the 3 week period in cages with running wheels. (C) LCR rats had higher unfed (fasting) blood glucose and serum insulin than HCR rats, but no statistical difference was observed in intraperitoneal glucose tolerance test or random glucose. (D) LCR rats had higher serum triglyceride concentration, and HCR rats, in turn, had higher HDL cholesterol and NEFA. Student's t-test HCR vs. LCR within time points *$P < 0.05$; **$P < 0.01$; ***$P < 0.001$.

5.1.4 Oxygen delivery system

Blood haemoglobin (135.8 ± 7.6 g/L in LCR vs. 135.1 ± 9.7 g/L in HCR) and haematocrit (47.1 ± 1.5 vs. 47.1 ± 1.7) did not differ between the groups. Capillary density (capillaries/mm^2) and capillary-to-fiber (C/F) ratio were significantly greater in soleus ($P < 0.01$) and in mixed gastrocnemius muscle ($P < 0.05$) from HCR. The C/F in fast EDL muscle ($P < 0.05$) was also greater in HCR relative to LCR (Figure 14A).

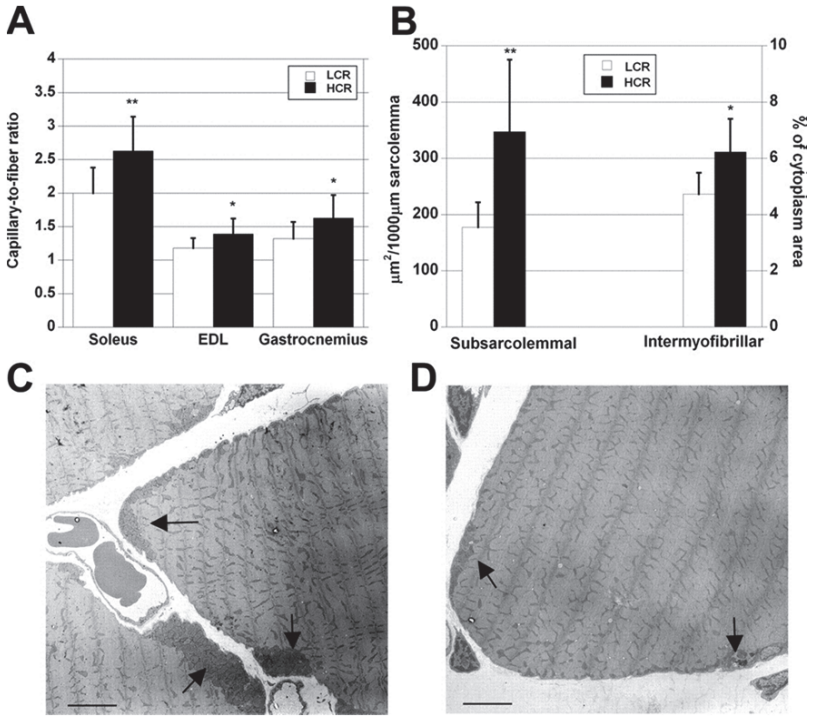

FIGURE 14 (A) Capillary-to-fiber ratio was higher in HCR rats in all studied muscles: slow soleus, fast EDL and mixed gastrocnemius muscles. (B) HCR rats had significantly larger subsarcolemmal and intermyofibrillar mitochondrial area compared with LCR rats. (C) Large mitochondrial stocks were found under the sarcolemma in HCR animals. These stocks were located close to nuclei and blood capillaries (arrows). (D) In LCR rat muscle, subsarcolemmal mitochondrial stocks were usually much smaller than in HCR rats (arrows). Scale bars = 5 µm. Student's t-test HCR vs. LCR within muscle *$P < 0.05$; **$P < 0.01$.

5.1.5 Muscle fiber type, mitochondrial area and lipid droplet content of muscle fibers

No difference between the LCR and HCR was observed in fiber type distribution in the soleus and EDL muscles. The myosin heavy chain composition of HCR analysed by SDS-PAGE showed a more oxidative phenotype in fast fibers than in LCR rats for gastrocnemius muscle, while there were no significant dif-

ferences in EDL and soleus (Table 4). Subsarcolemmal mitochondrial area, which was analysed in soleus, was 96% ($P < 0.01$) larger in HCR rats (Figure 14B), and the largest stocks of mitochondria were localized close to capillaries and around nuclei (Figure 14C,D). Also, intermyofibrillar mitochondrial area was 32% larger in HCR ($P < 0.05$). Only a few intramyocellular lipid droplets were found in either HCR or LCR soleus muscles with EM, and there were no differences between the strains.

TABLE 4 Fiber type and myosin heavy chain composition for the three studied muscles.

	Soleus		EDL		Gastrocnemius	
	LCR	HCR	LCR	HCR	LCR	HCR
Type I fibers (%)	75±9	77±12	3±2	4±2	-	-
Type II fibers (%)	25±9	23±11	97±2	96±2	-	-
MHC I (%)	78±8	84±8	3±2	2±1*	10±4	6±3**
MHC IIa/x (%)	22±8	16±8	24±9	34±16	22±14	42±16**
MHC IIb (%)	0±0	0±0	73±11	64±15	68±13	52±15*

Values are means ± SD. Student's t-test HCR vs. LCR within muscle **$P < 0.01$, *$P < 0.05$. MHC, myosin heavy chain.

5.1.6 Messenger RNA expression analyses

In genome-wide microarray analysis 239 known or predicted genes were differently expressed between HCR and LCR lines (n = 12 HCR + 12 LCR, FDR < 0.05). 126 of the genes were upregulated in HCR versus LCR, and 113 genes down-regulated (data not shown). Functional clustering of the differentially expressed genes according to their GO-annotations with DAVID revealed that many of the genes were related to mitochondria, carboxyl acid metabolism, lipid metabolism, oxido-reductase activity, immune response, and protein metabolism (Table 5).

TABLE 5 GO categories that were overrepresented among the differentially expressed genes between HCRs and LCRs in functional clustering analysis with DAVID.

Category	↑	↓
Mitochondrion**	7	
Carboxyl acid metabolism**	9	
Lipid and lipoprotein metabolism**	7	
Lipid catabolism**		3
Oxido reductase activity**	7	
Immuno response**	8	
Protein metabolism*		16
Attachment of cytoskeletal proteins**		6

Values indicate numbers of genes. ↑ = gene expression higher in HCRs than in LCRs; ↓ = gene expression lower in HCRs than in LCRs. *FDR $P < 0.05$; **FDR $P < 0.01$.

Gene set enrichment analysis (GSEA) revealed eight gene sets enriched in HCR rats (FDR q-value ≤ 0.001). These sets included oxidative phosphorylation, fatty acid metabolism, Krebs cycle, valine, leucine and isoleucine degradation, and PPAR-signalling pathway (Table 6). The two most enriched sets in LCR gastrocnemius muscle (FDR q-value ≤ 0.001) spanned genes expressed in renal cell carcinoma and chronic myeloid leukemia, both sets including genes of various signalling pathways (e.g. MAPK signalling route).

TABLE 6 Gene sets of cellular processes that were enriched among the differentially expressed genes between HCRs and LCRs in GSEA analysis.

Gene set name	Size (*n*)	ES	NES	NOM *P*	FDR q	FWER *P*
Overrepresented in HCR						
HSA00190_oxidative_ phosphorylation	78	0.496	4.823	0.000	0.000	0.000
Oxidative_ phosphorylation	46	0.462	3.492	0.000	0.000	0.000
HSA00071_fatty_acid_ metabolism	36	0.517	3.485	0.000	0.000	0.000
HSA00020_citrate_cycle	22	0.580	3.158	0.000	0.000	0.000
Valine_leucine_and_isoleucine_degradation	29	0.482	3.003	0.000	0.000	0.000
Krebs_tca_cycle	24	0.532	2.910	0.000	0.000	0.000
HSA00280_valine_leucine_and_isoleucine_ degradation	35	0.422	2.821	0.000	0.000	0.000
HSA03320_ppar_signaling_pathway	55	0.329	2.652	0.000	0.001	0.006
Overrepresented in LCR						
HSA05211_renal_cell_ carcinoma	58	-0.322	-2.933	0.000	0.001	0.001
HSA05220_chronic_ myeloid_leukemia	65	-0.291	-2.919	0.000	0.001	0.001

GSEA revealed 8 gene sets enriched in HCR rats and 2 gene sets enriched in LCR rats with FDR q ≤ 0.001. Size, number of genes in the gene set; ES, enrichment score; NES, normalized enrichment score; NOM *P*, nominal *P* value; FDR *q*, false discovery rate *q* value; FWER *P*, familywise error rate *P* value.

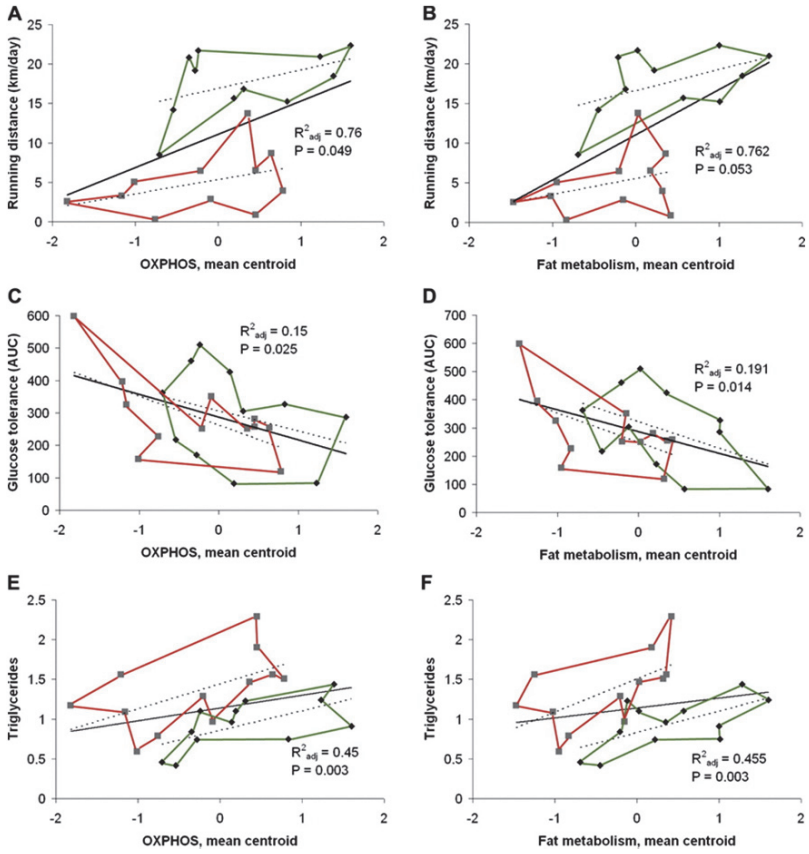

FIGURE 15 Expression of oxidative phosphorylation (A, C, E) and fat metabolism genes (B, D, F) are associated with voluntary running performance (A, B; running distance), glucose tolerance (C, D), and serum triglyceride concentration (E, F). Diamonds indicate HCR values; green lines indicate outer values. Squares indicate LCR values; red lines indicate outer values. Explanatory power and significance are shown.

Univariate analysis of variance showed strong positive relationships between parameters related to voluntary running performance and serum triglycerides and mRNA expression centroids of mitochondrial oxidative phosphorylation and fat metabolism. The centroids of mitochondrial oxidative phosphorylation and fat metabolism correlated negatively with glucose tolerance (Figure 15).

The genes involved in lipid metabolism were more closely examined from the microarray data and nine were chosen for further evaluation with real-time qPCR in three different muscles: soleus, EDL, and gastrocnemius. Seven of the nine genes showed significantly higher expression in the HCR rats for at least one of the three muscles tested (Figure 16).

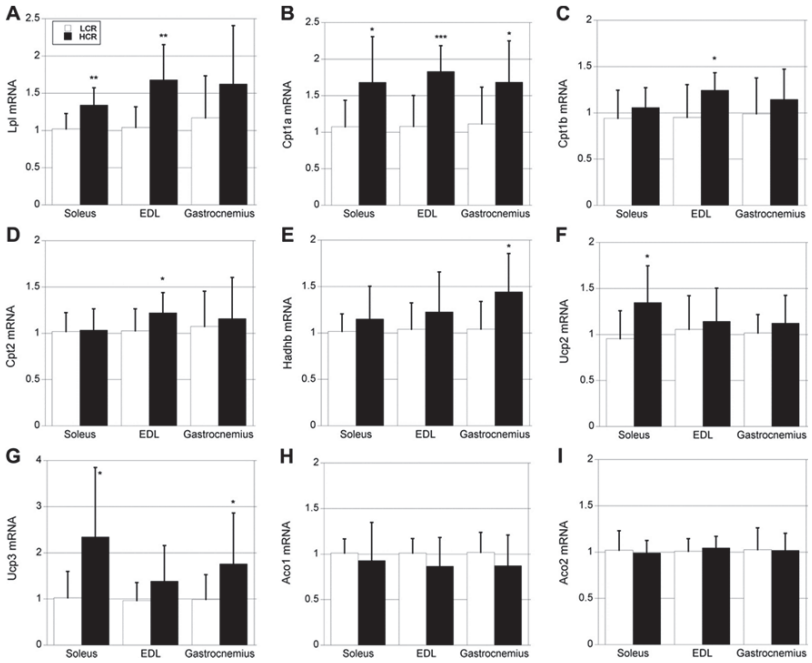

FIGURE 16 Real-time qPCR results from the 3 studied muscles showed that several genes related to lipid oxidation were upregulated in HCR rats compared with LCR rats: Lpl, lipoprotein lipase (A); Cpt1a, carnitine palmitoyl transferase 1a ; (B) Cpt1b, carnitine palmitoyl transferase 1b (C); Cpt2, carnitine palmitoyl transferase 2 (D); Hadhb, hydroxyacyl-CoA dehydrogenase b (E); Ucp2, uncoupling protein 2 (F); Ucp3, uncoupling protein 3 (G); Aco1, Aconitase 1 (H); Aco2, Aconitase 2 (I). Student's t-test HCR vs. LCR within muscle *$P < 0.05$; **$P < 0.01$; ***$P < 0.001$.

5.2 Effects of diet and physical activity on skeletal muscle capillarization (II)

5.2.1 Physiological characteristics

The effects of diet and physical activity on physiological characteristics are presented in Table 7. Energy intake was 15% higher in the mice fed HFD compared to those fed LFD. At the end of the study the HFD fed mice had higher body mass, epididymal fat mass, gastrocnemius muscle mass and quadriceps femoris muscle mass than LFD fed mice (diet effect $P < 0.001$). At the same time point, active mice had lower body mass and higher quadriceps femoris mass (activity effect $P < 0.05$) than sedentary mice. The LFA mice voluntarily ran a significantly longer distance during the study than the HFA mice (428 ± 110 vs. 346 ± 138 km, $P < 0.05$). The running distances of LFA and HFA mice increased during the four first weeks but decreased thereafter until the end of the study.

TABLE 7 Physiological characteristics of mice in study II.

	Sedentary		Active		ANOVA *P*-value		
Basic data	Low-fat diet	High-fat diet	Low-fat diet	High-fat diet	Diet (D)	Activity (A)	D x A
Body mass (beginning)(g)	20.8 ± 1.4	21.0 ± 1.5	20.1 ± 1.4	21.0 ± 1.5	0.758	0.825	0.878
Body mass (g)	32.6 ± 2.9	45.4 ± 5.3***	29.2 ± 1.7**	44.4 ± 3.1***	<0.001	<0.05	0.183
Body mass change (%)#	57 ± 10	116 ± 18***	39 ± 8***	112 ± 20***	<0.001	<0.001	<0.01
Gastrocnemius (mg)	145 ± 13	151 ± 9	141 ± 8	155 ± 7	<0.001	0.936	0.137
Quadriceps femoris (mg)	207 ± 10	221 ± 13**	211 ± 12	228 ± 11***	<0.001	<0.05	0.646
Epididymal fat (mg)#	799 ± 345	1767 ± 383***	424 ± 65***	1925 ± 541**	<0.001	<0.05	<0.05
Energy intake (KJ/day)	57 ± 3	66 ± 4***	60 ± 3**	69 ± 5***	-	-	-

The muscle masses are average values of both hind limbs. Energy intake is expressed as an average energy intake over the whole experiment. Values are means ± SD. *** =P < 0.001 vs. LFS; ** =P < 0.01 vs. LFS; #Logarithmic transformation for normality and comparison; - Normal distribution and equal variance assumptions were not met.

5.2.2 Glucose balance and blood lipids

After 18 weeks, HFD fed mice had higher levels of fasting glucose, fasting insulin and HOMA-IR values (diet effect P < 0.001) than LFD fed mice. Total cholesterol levels were also higher in HFD fed mice (HFS and HFA vs. LFS, P < 0.001). Physical activity did not have a significant effect on fasting glucose, fasting insulin or HOMA-IR values. HFA had lower total cholesterol values than HFS (P < 0.05). Serum triglyceride concentrations were similar in all groups. HFD fed mice had lower free fatty acid levels than LFD fed mice (HFS and HFA vs. LFS, P < 0.001) but there were no significant differences between active and sedentary groups with the same diet. Glucose balance and blood lipid results are presented in Table 8.

TABLE 8 Glucose balance and blood lipids in mice of study II.

	Sedentary		Active		ANOVA *P*-value		
Blood profile	Low-fat diet	High-fat diet	Low-fat diet	High-fat diet	Diet (D)	Activity (A)	D x A
Total cholesterol (mmol/L)	3.0 ± 0.9	4.9 ± 0.5***	2.7 ± 0.4	4.5 ± 0.5***,§	-	-	-
Triglycerides (mmol/L)	0.97 ± 0.23	1.00 ± 0.24	1.05 ± 0.21	0.90 ± 0.13	-	-	-
Free fatty acids (mmol/L)	0.82 ± 0.15	0.49 ± 0.13***	0.92 ± 0.16	0.44 ± 0.12***	-	-	-
Fasting glucose (mmol/L)	8.9 ± 1.1	9.4 ± 1.1	8.4 ± 0.9	10.5 ± 0.7***,§§	<0.001	0.201	<0.01
Fasting insulin (mIU/L)	9.4 ± 5.3	49.5 ± 24.3***	5.9 ± 3.5	47.1 ± 18.0***	<0.001	0.125	0.112
HOMA-IR	3.9 ± 2.4	20.9 ± 10.2***	2.3 ± 1.5	22.1 ± 8.6***	<0.001	0.894	0.451

Values are means ± SD. *** =P < 0.001 vs. LFS; ** =P < 0.01 vs. LFS; * =P < 0.05 vs. LFS; §§ =P < 0.01 vs. HFS; § =P < 0.05 vs. HFS; HOMA-IR, homeostatic model assessment of insulin resistance; #Logarithmic transformation for normality and comparison; - Normal distribution and equal variance assumptions were not met.

5.2.3 Muscle capillarization and fiber cross-sectional area

The sedentary HFD fed mice had higher capillary density (21%) and capillary-to-fiber-ratio (18%) in quadriceps femoris muscles than the sedentary LFD fed mice (Figure 17A-B). The LFA mice had higher capillary density (32%) and capillary-to-fiber ratio (32%) than LFS. There were no significant differences between HFA and HFS in capillary density and capillary-to-fiber-ratio. However, the capillary-to-fiber-ratio was slightly higher in the HFA mice, the difference approaching significance (P=0.08). Diet had no effect on muscle fiber cross sectional area (CSA) but active mice groups had higher CSA than sedentary mice (activity effect $P < 0.05$) (Figure 17C).

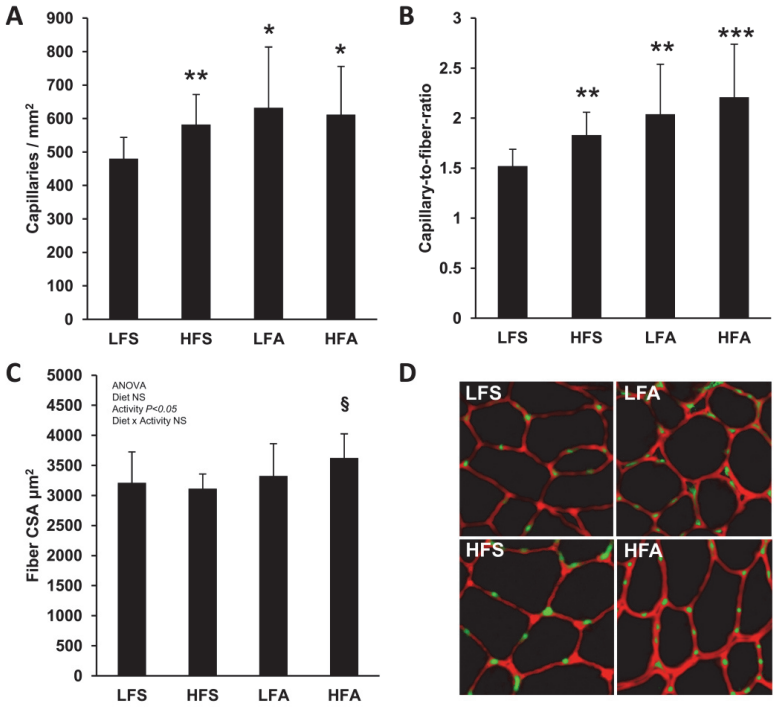

FIGURE 17 (A) HFS, LFA and HFA mice had higher capillary density and (B) capillary-to-fiber-ratio in quadriceps femoris muscles than LFS mice. (C) Fiber cross-sectional area (CSA) was similar with both diets but active mice had higher CSA than sedentary mice. (D) Representative composite images of muscle fibers and capillaries (20 x magnifications). Capillaries (green) were visualized by staining with Isolectin-GS-IB_4 containing fluorescent Alexa Fluor 488 label. This was combined with anti-dystrophin staining with Alexa Fluor 555 secondary antibody to visualize muscle fibers (red). Values are means ± SD. * = $P < 0.05$ vs. LFS, ** = $P < 0.01$ vs. LFS, *** = $P < 0.001$ vs. LFS, § = $P < 0.05$ vs. HFS. Group abbreviations: LFS=low-fat sedentary, HFS=high-fat sedentary, LFA=low-fat active and HFA=high-fat active.

5.2.4 The protein levels of angiogenesis regulating factors and mitochondrial quantity marker Cytochrome C

Both physical activity and HFD increased the levels of VEGF-A (diet effect and activity effect $P < 0.05$ Figure 18A) in the quadriceps femoris muscle. The protein levels of mitochondrial quantity marker Cytochrome C were higher in LFA, HFS and HFA mice compared to LFS mice (Figure 18B), but no difference was observed between HFA and HFS. The protein levels of angiogenesis regulating factors HIF-1α (Figure 18C) and PGC-1α (Figure 18D) were similar in all groups, thus neither physical activity nor diet had long-term effects on these regulators. Active mice had higher levels of ERRα protein in their skeletal muscle compared to sedentary mice (diet effect $P < 0.05$).

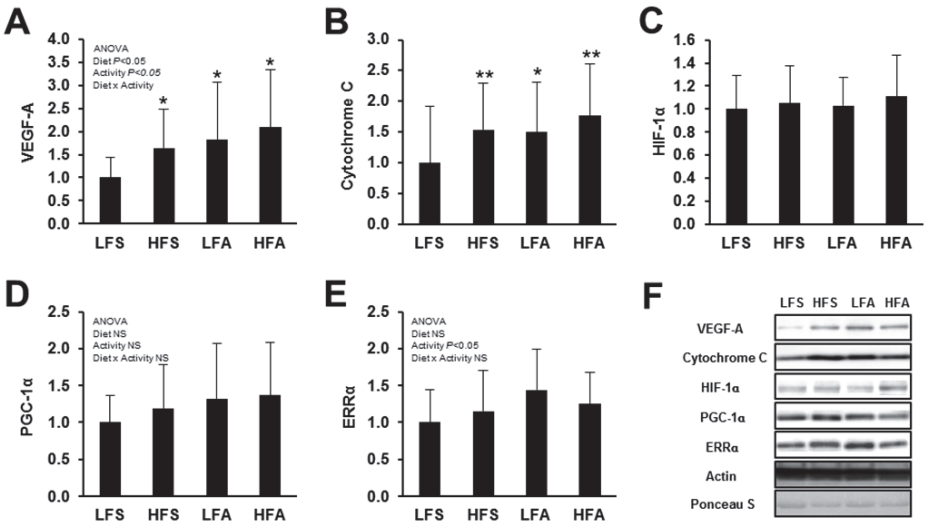

FIGURE 18 (A) HFD and physical activity increased the protein levels of VEGF-A (B) Cytochrome C protein levels were higher in the quadriceps femoris muscles of LFA, HFS and HFA mice compared to LFS mice. Protein levels of (C) HIF-1α and (D) PGC-1α (full length) were similar in all groups. Protein levels of (E) ERRα were higher in active groups compared to sedentary groups. The results are normalized to the mean value of LFS. (F) Representative western blot images. Values are means ± SD. * = $P < 0.05$ vs. LFS, ** = $P < 0.01$ vs. LFS.

5.2.5 The messenger RNA levels of angiogenesis-regulating genes

The mRNA levels of VEGF-A were higher in the muscle capillary samples of the HFS and HFA mice compared to LFS mice (89% and 108%, respectively, Figure 19A), however there were no differences between these groups in muscle fibers. The expression level of VEGF-A mRNA was also found to be higher in the muscle homogenates of HFA compared to LFS. There were no significant differences in the expression levels of VEGF-A between the active and sedentary groups (LFA vs. LFA or HFA vs. HFS) in any sample type. However, in

capillary samples, VEGF-A mRNA expression was slightly higher in LFA compared to LFS, the difference (P=0.053) being very near the limit of statistical significance. The mRNA expression of HIF-1α was upregulated in the muscle capillary samples and muscle homogenates but not in muscle fibers of the HFS mice (Figure 19B). HIF-1α expression levels were not different between the active and corresponding sedentary groups in any sample type. The gene expression of total PGC-1α was higher in the capillary samples of the HFS mice compared to LFS mice, the difference approaching significance (P=0.06). Other differences were not found in total PGC-1α expression between the groups in any sample type (Figure 19C). ERRα gene expression was higher in muscle homogenate samples of HFA compared to LFS and HFS, but no other differences were found between the groups in any sample type (Figure 19D).

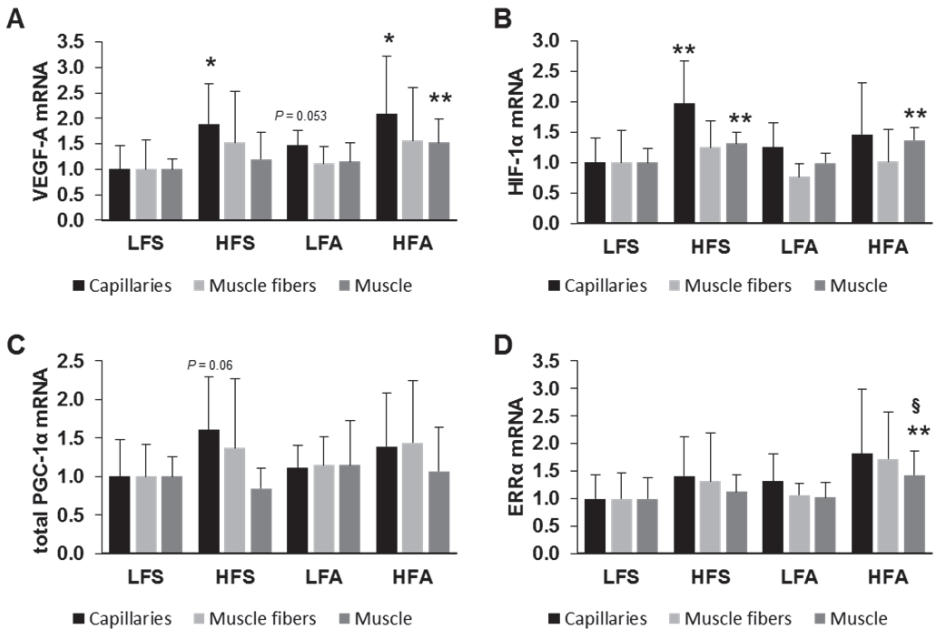

FIGURE 19 (A) The mRNA levels of VEGF-A were higher in capillary samples of HFS and HFA mice compared to LFS mice. (B) HIF-1α was upregulated in the capillaries and muscle homogenates of HFS mice. (C) The gene expression of total PGC-1α was higher in the capillaries of HFS compared to LFS mice, the difference approaching significance (P = 0.06). (d) ERRα gene expression was higher in muscle homogenate samples of HFA compared to LFS and HFS. There were no expression differences between groups in any of the studied genes in the muscle fiber samples. The expressions of the studied genes are normalized to the expression of GAPDH. The results are expressed in relation to the LFS mean. Values are means ± SD. * =P < 0.05 vs. LFS, ** =P < 0.01 vs. LFS, § =P < 0.05 vs. HFS.

5.3 Validity of spontaneous activity measurement system

5.3.1 Validation measurements with calibration devices

The validity of the activity measurement system was tested against calibration devices. The association was very strong between measured activity index values and true values (R^2= 1, $P < 0.01$). The absolute measured activity index values were 9.7% (95% LOA, -28.6–9.4%) smaller than true values. As a measure of repeatability, the average root-mean-square coefficient of variation (CV_{rms}) was calculated from repeated measurements. The CV_{rms} of activity index analysis in the validation measurement was 2.6%.

There was a very strong association between the measured activity time and the true time (R^2= 1, $P < 0.01$). The measured activity time values were similar to true values. The mean difference was +0.9% (95% LOA, -1.2–3.0%) and the CV_{rms} of the measurement was 0.52%.

A very strong association was also found between measured distance and true distance (R^2= 1, $P < 0.01$). The measured distances were similar to true distances. The distances analysed from the force plate data were 0.7% (95% LOA, -4.6–6.0%) higher than true distances. The CV_{rms} of distance measurement was 2.81%.

5.3.2 Mouse experiment

The activity measurement system was tested in situ by measuring spontaneous activities of two mice groups: control (n=4) and running group (n=8). The physical activity variables were measured first at baseline, when both mice groups were living in normal cages without running wheels. After baseline measurements, the running group mice were given running wheels in their cage and they were allowed to run ad libitum 24h/day for the next four weeks. Control mice continued living in a normal cage without running wheels. The physical activity of all control and running mice was measured once a week for 48 hours. After four weeks, the running wheels were taken away from the cages and after living one week without running wheels, the POST- activity measurements were performed for all animals similarly as in previous weeks. The activity results are presented in Figure 20 as relative changes compared to baseline values.

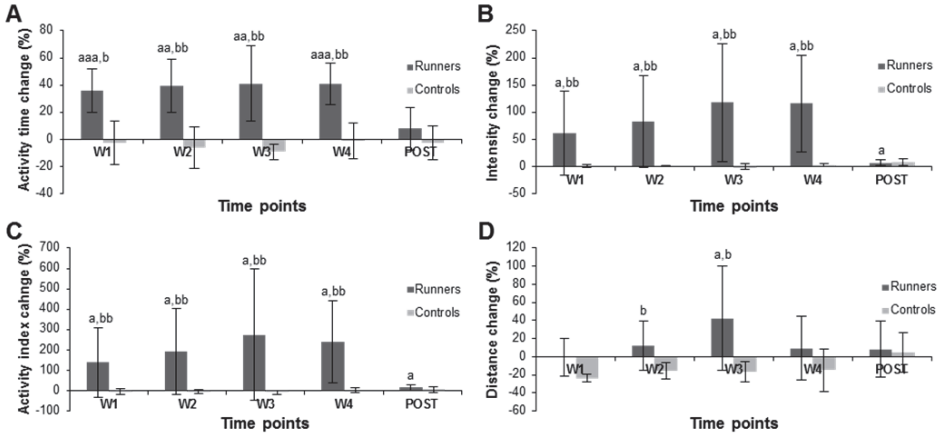

FIGURE 20 (A) Activity time changes (%). (B) Intensity changes (%). (C) Activity index changes (%). (D) Distance changes (%). W1 to W4 are time points in weeks after baseline measurement, and the time point POST is one week after removing the running wheel. Results are mean percentage changes compared to baseline values ± SE. Running group n=8, Control group n=4. a $P < 0.05$ vs. baseline, aa $P < 0.01$ vs. baseline, aaa $P < 0.001$ vs. baseline, b $P < 0.05$ vs. control, bb $P < 0.01$ vs. control, bbb $P < 0.001$ vs. control.

On average, the mice in the running group ran 1634 ± 1952 meters per day. The running distances increased from week 1 and peaked at week 3. The body mass of the mice decreased by 6.8 ± 3.6% ($P < 0.01$) during 4 weeks of running. The running wheels increased activity time by 39 ± 19% ($P < 0.01$), intensity by 94 ± 90% ($P < 0.05$) and activity index by 211 ± 227% ($P < 0.05$) (Figure 20A-C). The running wheel-induced changes were similar between different time points. However, as was the case with running distances, activity index and intensity values peaked after 3 weeks of running. The running wheels did not have a clear effect on distance values (Figure 20D). Compared to the baseline values, distances were increased only at the 3 week time point (42 ± 49%, $P < 0.05$), when the running distances were at their highest level. Activity index (R^2=0.982, $P < 0.01$), activity time (R^2=0.618, $P < 0.01$), intensity (R^2=0.920, $P < 0.01$) and distance (R^2= 0.405, $P < 0.01$) were significantly associated with running distance (Figure 21A-D).

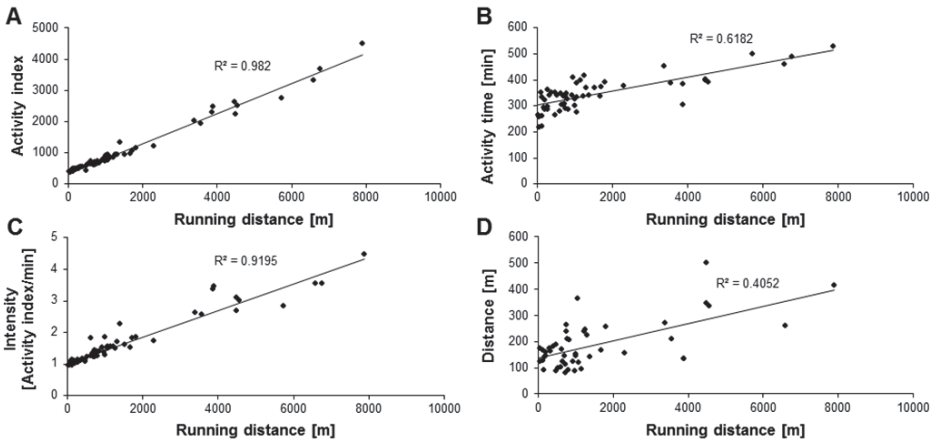

FIGURE 21 The relationship of activity index (A), activity time (B), intensity (C) and distance (D) to running distance.

5.4 The gene expression responses of PGC-1 isoforms and their target genes after a single bout of endurance and resistance exercise

5.4.1 Exercise-induced systemic responses

Resistance exercise (RE) led to a decrease of 45 ± 16% ($P < 0.01$) in MVC and 17 ± 24% (NS, $P = 0.07$) in CMJ from pre- to post-exercise. Blood lactate increased to 11.1 ± 3.0 mmol/L ($P < 0.01$) immediately after RE. During the loading in endurance exercise (EE), averaged treadmill speed was 6.2 ± 0.4 km/h and the slope 4.1 ± 0.8 degrees, blood lactate was 4.2 ± 1.0 mmol/L, and HR was 83 ± 8% of HR_{max}. Immediately after EE, MVC was 9 ± 14% (NS, P=0.06) and CMJ 7 ± 6% ($P < 0.05$) lower than before the exercise, and blood lactate was 2.4 ± 1.5 mmol/L ($P < 0.01$).

5.4.2 Gene expression responses of PGC1 transcript variants after RE and EE

The expression of PGC-1α exon 1a-derived transcripts increased by 1.7-fold ($P < 0.05$, Figure 22A) 30 min after EE. After RE no significant response was detected. The expression of PGC-1α exon 1b-derived transcripts was significantly increased in response to both RE and EE (Figure 22B) while the peak changes were detected 180 min after exercise. At this time point the average gene expression change was 170-fold ($P < 0.05$) after EE and 997-fold ($P < 0.01$) after RE. The expression of PGC-1α exon 1b'-derived transcripts were low in the present basal conditions. In the RE group, the transcripts were detected in 6 PRE samples from 11 and in EE group in 3 PRE samples from 8. However, after RE and EE the expression of PGC-1α exon 1b'-derived transcripts was substantially in-

creased (Figure 22C). When PRE values below the detection limit were replaced with the detection limit values, the average change was 67-fold 180 min after RE ($P < 0.01$) and 9-fold 180 min after EE ($P < 0.05$). The expression of truncated PGC-1α transcripts (total NT-PGC-1α) (Figure 22D) was increased 180 min after RE (5-fold, $P < 0.01$) and 30 min after EE (1.7-fold, $P < 0.01$). The expression of total PGC1α (all truncated and nontruncated splice variants together) (Figure 22E) was increased 180 min after RE (4-fold, $P < 0.01$) and 30 min after EE (1.8-fold, $P < 0.05$). PGC1β had no significant gene expression response to either of the exercises (Figure 22F). Relative concentration values of RNA:cDNA hybrids are presented in Figure 22G.

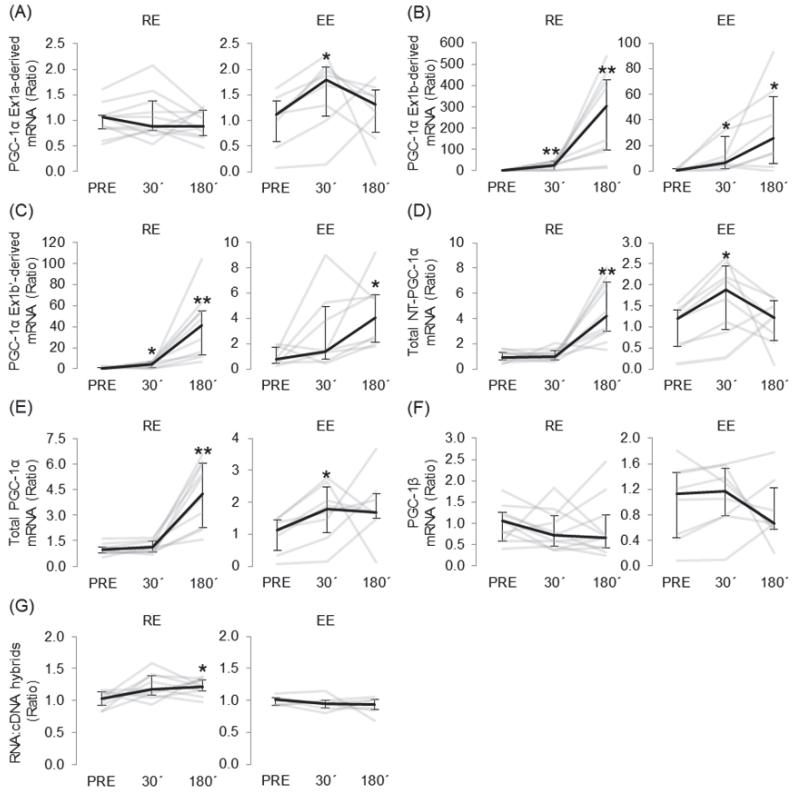

FIGURE 22 The expression profiles of PGC-1α exon 1a-derived transcripts (A), PGC-1α exon 1b-derived transcripts (B), PGC-1α exon 1b′-derived transcripts (C), Total NT-PGC-1α (D), Total PGC-1α (E) and PGC1β (F) 30 min (30´) and 180 min (180´) after resistance exercise (RE, n=11) and endurance exercise (EE, n=8). The gene expression data of each sample are normalised to the corresponding relative concentration value of RNA:cDNA hybrids (G). The gene expression changes are presented in relation to PRE average. Black lines represent median responses to exercise and grey lines individual responses. Error bars represent interquartile range. * Wilcoxon matched pairs signed-rank test with Holm-Bonferroni correction $P < 0.05$ vs. PRE, ** $P < 0.01$ vs. PRE.

5.4.3 Gene expression responses of PGC-1α-regulated genes after RE and EE

The gene expression of mitochondrial marker cytochrome c was increased 30 min after EE (1.7-fold, $P < 0.05$, Figure 23A), but there were no responses to RE. However, the gene expression of angiogenesis regulator *VEGF-A* was increased after both EE (3-fold, $P < 0.05$) and RE (2-fold, $P < 0.05$). EE-induced response was significant already 30 min after exercise, but RE-induced response did not appear until 180 min after exercise (Figure 23B). RE decreased (2.5-fold, $P < 0.05$) the gene expression of myostatin, the known inhibitor of muscle growth, without a response to EE (Figure 23C).

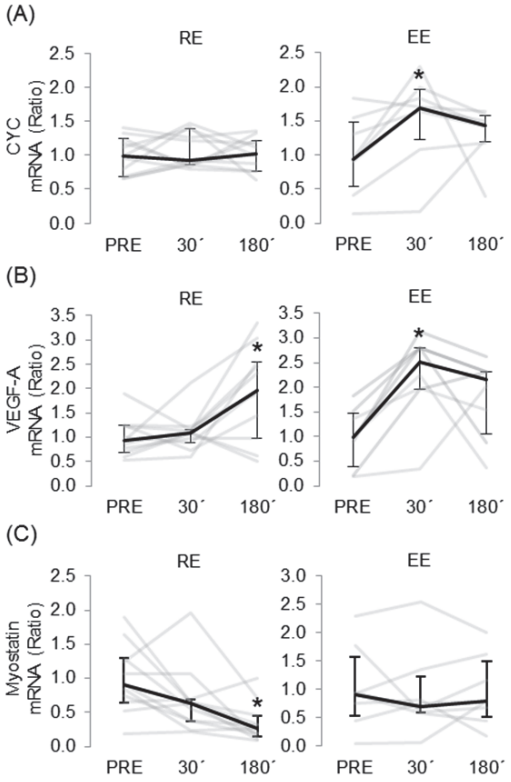

FIGURE 23 Gene expression changes of known PGC-1α target genes Cytochrome C (A, CYC), VEGF-A (B) and Myostatin (C) 30 min (30´) and 180 min (180´) after resistance exercise (RE, n=11) and endurance exercise (EE, n=8). The gene expression changes are presented in relation to PRE average. Black lines represent median responses to exercise and grey lines individual responses. Error bars represent interquartile range. * Wilcoxon matched pairs signed-rank test with Holm-Bonferroni correction $P < 0.05$ vs. PRE, ** $P < 0.01$ vs. PRE.

5.4.4 The level of PGC-1α proteins, p-p38 MAPK and p-AMPKα, and their associations with studied gene expression changes

The protein level of full length nontruncated PGC-1α was increased 180 min after RE (2.3-fold, $P < 0.05$, Figure 24A) with no changes after EE (n=7). The level of the active phosphorylated form of p38 MAPK$^{Thr180/Tyr182}$ was increased by 9-fold ($P < 0.05$, Figure 24B) 30 min after RE, but not after 180 min or EE. The level of p-AMPKα^{Thr172} was increased by 4-fold 30 min after RE (Figure 24C), but not after 180 min. There was also a trend ($P = 0.07$) towards increased levels of p-AMPKα^{Thr172} 30 min after EE. Representative immunoblot images of one individual are presented in Figure 24D.

There were no strong associations between exercise-induced changes in p-p38 MAPK$^{Thr180/Tyr182}$ or p-AMPKα^{Thr172} levels and gene expression responses of PGC-1 isoforms, PGC-1β and myostatin in either of the exercise groups. However, the level change of p-AMPKα^{Thr172} (ratio 30′/PRE) was associated with the corresponding changes in VEGF-A (r_s=.821, $P < 0.05$) and CYC (r_s = .750, P = 0.052) 30 min after EE. Similar associations were also found after EE when the time points were pooled and analysed together (VEGF-A: r_s = .608, $P < 0.05$; CYC: r_s = .601, $P < 0.05$).

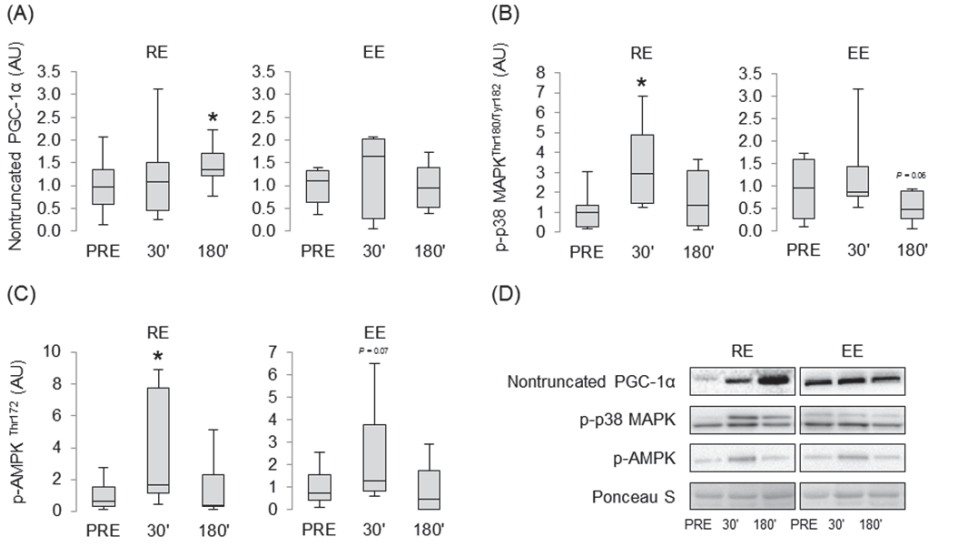

FIGURE 24 The effect of endurance exercise (EE, n=7) and resistance exercise (RE, n=9) on levels of nontruncated PGC-1α proteins (A), p-p38-MAPK (B) and p-AMPK (C) 30 min (30′) and 180 min (180′) after exercise. The results are presented in relation to PRE average and the box plots show minimum-maximum values, interquartile ranges and medians. * Wilcoxon matched pairs signed-rank test with Holm-Bonferroni correction $P < 0.05$ vs. PRE. Representative immunoblot images of one individual (D).

6 DISCUSSION

The main findings of the present dissertation are as follows:

1) HCRs were lighter and had lower blood glucose, insulin, and triglycerides compared to LCRs. They also had higher resting metabolic rate, voluntary activity, serum high density lipoproteins, as well as higher capillarization and mitochondrial area in their skeletal muscles. In addition, HCRs had higher expression of genes related to oxidative phosphorylation, fatty acid metabolism, Krebs cycle, valine, leucine and isoleucine degradation, and PPAR-signalling pathway in their skeletal muscles. It was also found that the expression of genes related to oxidative phosphorylation and lipid metabolism was significantly linked to voluntary running performance and whole-body glucose balance. (I)

2) HFD induced capillarization in murine skeletal muscle without an additive effect of physical activity. As an indication of activated angiogenesis we also found an increased level of angiogenic factor VEGF-A protein in muscle tissue. Because HFD did not change the protein-levels of HIF-1α or PGC-1α, the protein level results do not support the involvement of these proteins in HFD-induced angiogenesis. However, the mRNA expression of HIF-1α and VEGF-A were increased in endothelial cells after HFD. (II)

3) Calibration measurements and actual long-term measurements of mouse movements showed that the developed activity measurement system is valid for the quantification of spontaneous physical activity of mice housed in cages with or without running wheels. The activity index and activity time were the most valid measures for these conditions. The mouse experiment showed that wheel running triples the mean total activity of mice. The main part of this effect is explained by increases in the intensity of activity and activity time. (III)

4) The alternative promoter originated transcripts (PGC-1α exon 1b and 1b′ derived transcripts) were significantly upregulated after both EE and RE, whereas the proximal promoter originated PGC-1α exon 1a derived transcripts were less inducible and were upregulated only after EE. Truncated PGC-1α transcripts (total NT-PGC-1α) were upregulated after both EE and RE. EE upregulated the gene expression of angiogenesis mediator VEGF-A and mitochondrial marker CYC, while RE upregulated VEGF-A expression and downregulated the expression of myostatin, the inhibitor of muscle hypertrophy. (IV)

6.1 Characteristics of inherited running capacity in skeletal muscle

Numerous studies have shown that high aerobic exercise capacity decreases the risk of cardiovascular diseases, type 2 diabetes and premature death (Blair et al. 1989; Blair et al. 1996; Kokkinos et al. 2008; Myers et al. 2002; Gulati et al. 2003; Kodama et al. 2009; Carnethon et al. 2009). These conclusions were based on cohort studies that cannot separate the effects of inherited and acquired (by exercise) high aerobic capacity. The rat strains developed by Koch et al. contrasting in inherited aerobic running capacity (HCR, high running capacity; LCR, low running capacity) provide a useful model to study inherited capacity without confounding environmental factors (Koch & Britton 2001). Wisloff et al. showed with these rat strains that low inherited aerobic capacity scored highly on cardiovascular risk factors that constitute metabolic syndrome (Wisloff et al. 2005). Furthermore, recent studies indicated that LCR rats have a significantly shorter lifespan (Koch et al. 2011). These results are clearly in line with foregoing human studies, and show that at least inherited aerobic capacity seems to have a significant influence on health and life span.

One of the aims of the current thesis was to investigate the differences in skeletal muscle characteristics between LCR and HCR rats. These rat strains differed significantly in their running capacity (distance run at exhaustion was 305 ± 16 m in LCR vs. 1883 ± 45 m in HCR). Thus, we hypothesised that the rat strains would also differ in their skeletal muscle fiber type distribution. ATPase based fiber type analysis revealed that there were no differences in fiber type distribution in soleus (slow oxidative) and EDL (fast glycolytic) muscles between rat strains. However, the myosin heavy chain composition analysed by SDS-PAGE showed that HCR had less MHCIIb (typical for fast glycolytic fibers) and more MHCIIa/x (typical for fast oxidative fibers) myosin than LCR rats in gastrocnemius muscle, while there were no significant differences in EDL and soleus. This is consistent with the fact that fiber type transformations are generally transitions from one fast fiber subclass to another (Schiaffino & Reggiani

2011). However, we cannot exclude the possibility that this difference in myosin type distribution between rat strains was caused by different levels of physical activity.

When mitochondrial content was analysed in soleus muscles, it was found that the subsarcolemmal mitochondrial area was significantly larger in HCR rats, and the largest stocks of mitochondria were localized close to capillaries. Moreover, intermyofibrillar mitochondrial area was 32% larger in HCR. Rivas et al. studied mitochondrial content in skeletal muscle of HCR-LCR-rats from generations 20 and 22 (Rivas et al. 2011). In their study mitochondrial content was not significantly different between rat strains in soleus muscle, but in EDL muscle mitochondrial content was ~70% higher in HCR rats. Because oxygen delivery is a major limiting factor of maximal aerobic capacity (Bassett & Howley 2000) and mitochondrial content is tightly coupled with capillarization (O'Hagan et al. 2009), it was hypothesised that capillarization should also be different between rat strains. As expected, HCR rats had higher capillarization in skeletal muscles. This was evident in all studied muscles (soleus, EDL and gastrocnemius). Recently, Beighley et al. studied arteriolar branching structures of LCR and HCR rats, but they did not find any differences in these upstream blood vessel structures (Beighley et al. 2013). A high amount of mitochondria, high capillary density and the observed short distance between capillaries and mitochondria allow efficient oxygen delivery and aerobic energy production, which may at least partly explain the big difference in maximal running capacity between HCR and LCR.

The microarray results showed clearly that a large variety of genes related to aerobic capacity were upregulated in HCR compared to LCR. This suggests that inherited high skeletal muscle oxidative capacity is to a great extent regulated at the transcriptional level. Interestingly, the results also indicated that several genes coding proteins of PPAR signalling and MAPK signalling pathways were regulated at mRNA level. PPAR and MAPK signalling pathways are known regulators of mitochondrial biogenesis, angiogenesis and fatty acid oxidation (Olesen, Kiilerich & Pilegaard 2010). Furthermore, higher expression of the gene set of valine, leucine and isoleucine degradation in HCRs suggests that HCRs have a higher need for proteins involved in catabolism of branched-chain amino acids. It has been hypothesised that increased branched-chain amino acid catabolism is an essential part of increased fatty acid oxidation and better metabolic health (Kainulainen, Hulmi & Kujala 2013).

6.2 Inherited aerobic capacity and risk factors of metabolic diseases

Previously it was demonstrated that LCR rats have higher levels of metabolic and cardiovascular risk factors than HCR rats (Wisloff et al. 2005). In the present study (I) we aimed to confirm these findings and investigate the gene-

phenotype relationships that connect aerobic exercise capacity with metabolic disease risk factors. We hypothesised that LCR rats have higher levels of risk factors for complex metabolic diseases in comparison to HCR rats. In addition, we expected to find differences in mRNA expression of genes linked to aerobic capacity that can explain the higher risk of metabolic syndrome in LCR rats.

Significantly higher daily voluntary running distances (~4-fold) and longer times spent in the running wheel (2.6-fold) indicated that HCR rats were physically more active. At two months of age the LCR rats were significantly heavier than HCR, and remained about 20-25% heavier throughout the study. In line with the results of Wisloff et al. (Wisloff et al. 2005), LCR rats had higher blood glucose, serum insulin and triglyceride concentrations, and lower HDL cholesterol, which are all risk factors for metabolic syndrome. In contrast, HCR rats had significantly higher serum free fatty acid concentration, which may reflect enhanced lipolysis from adipose tissue and increased usage of fatty acids for energy (Lessard et al. 2009). Consistent with this result, it has been demonstrated that HCRs have enhanced capacity for hepatic and skeletal muscle oxidation of lipids relative to LCRs (Rivas et al. 2011; Thyfault et al. 2009). It has been hypothesised that accumulation of lipids is part of the development of insulin resistance in skeletal muscles (Manco, Calvani & Mingrone 2004; Savage, Petersen & Shulman 2007). Although we found differences in whole-body insulin sensitivity between rats, this could not be explained by lipid accumulation differences because only a few intramyocellular lipid droplets were found in either HCR or LCR skeletal muscles with EM, and there were no differences between the strains.

Because HCR rats were leaner and physically more active than LCR rats, the data is consistent with previous findings proposing that these traits are associated with inherited aerobic capacity. The association between inherited aerobic capacity and physical activity has been reported earlier in both humans and rodents (Koch & Britton 2001; Novak et al. 2009). Furthermore, it has been shown that an individual's level of daily physical activity is a biologically regulated heritable trait that tends to be associated with leanness (Levine et al. 2005; Novak et al. 2009). To determine whether inherited aerobic capacity is associated with resting energy expenditure (EE), CO_2 production was measured at rest. We found that HCR rats had higher CO_2 production at rest than LCR rats when the significant effect of body mass was taken into account. The lower CO2 production of LCR rats indicates lower resting EE that could partly account for the higher body weight and higher body fat in LCRs relative to HCRs. However, Gavini et al. have recently shown that nonresting EE is probably a more important factor in remaining lean (Gavini et al. 2014). They found that HCR had heightened nonresting EE, but not resting EE, compared with female LCR. They also found that HCR had higher muscle heat dissipation during activity, explaining their low economy of activity and high activity EE. The differences between the results of the present study and those of Gavini et al. (Gavini et al. 2014) may be influenced by differences in EE measurements. Gavini et al. (Gavini et al. 2014) used significantly longer acclimatization time (24h vs. 1h)

and measurement time (24h vs. 3 × 20 min) compared to the present study, and they measured both O_2 uptake and CO_2 production, which allows more accurate estimation of EE. Nonexercise activity thermogenesis (NEAT) accounts for the majority of nonresting EE, and the ability to increase NEAT in the face of additional caloric intake is a key trait distinguishing people who resist gaining fat (Levine, Eberhardt & Jensen 1999). Interestingly, Novak et al. have shown that HCR rats are resistant to the sizeable increases in body mass and fat mass induced by a high-fat diet (Novak et al. 2010). In their study, HCRs were consistently more active than LCRs, and they had lower fuel economy of activity, regardless of diet. They also showed that HCRs were more sensitive to neuropeptides (orexin-A) regulating PA and NEAT. Thus, high inherited aerobic capacity seems to be linked to efficient energy dissipation and resistance to fat gain in an obesogenic environment.

In order to compare pheno- and genotypes, the most significant gene clusters obtained from the GSEA analysis were correlated to physiological and biochemical parameters. The analyses revealed that the expression of oxidative phosphorylation and fat metabolism genes was positively correlated with voluntary running performance (running distance). This suggests that higher mRNA expression of oxidative phosphorylation and lipid metabolism genes could result in higher aerobic capacity and fatty acid oxidation capacity in skeletal muscle, which would allow higher aerobic running capacity. The most interesting finding was that the expression of oxidative phosphorylation and fat metabolism genes correlated negatively with the glucose tolerance test results (AUCs). Because there was an inverse relationship between AUCs and glucose tolerance, the results of the present study indicate that the mRNA expression of oxidative phosphorylation and lipid metabolism related genes in skeletal muscle are significantly linked to whole-body glucose balance. These results support the hypothesis that small mRNA expression differences in oxidative phosphorylation and lipid metabolism related genes account at least partially for the differences in exercise capacity and disease risk phenotypes.

6.3 High-fat diet-induced adaptation in the capillarization of skeletal muscle

Skeletal muscles can adapt to several environmental factors such as different types of exercise and diet. A number of studies have shown that high-fat diet (HFD) increases the amount of mitochondrial enzymes (Hancock et al. 2008; Miller, Bryce & Conlee 1984; Nemeth et al. 1992; Simi et al. 1991; Garcia-Roves et al. 2007), mitochondrial biogenesis and fatty acid oxidation capacity in the skeletal muscle of mice and rats (Hancock et al. 2008; Garcia-Roves et al. 2007; Turner et al. 2007). These results were supported by our finding (study II) that HFD increased the levels of mitochondrial quantity marker protein cytochrome-c in the quadriceps femoris muscle. Because mitochondrial biogenesis normally

occurs in response to increased cellular ATP demand, HFD-induced mitochondrial biogenesis could be a consequence of insufficient capacity to oxidize fatty acids. We hypothesized that in addition to mitochondrial biogenesis, HFD should also stimulate angiogenesis in order to match oxygen supply with increased oxygen demand. We found that in sedentary mice HFD for 19 weeks induced significant increases in capillary density and capillary-to-fiber-ratio in the quadriceps femoris muscle compared to LFD-fed sedentary mice. Because both the capillary-to-fiber ratio and capillary density were increased, we interpret this to mean that HFD can improve capillarization in murine muscle via induction of angiogenesis. As expected, physically active LFD fed mice (LFA) had higher capillary density and capillary-to-fiber ratio compared to the respective sedentary animals. The magnitude of the effect of increased physical activity was similar to the effect of HFD. In contrast to LFD, no difference in muscle capillary density was observed in the HFD-fed animals regardless of whether they were sedentary or active. However, the capillary-to-fiber-ratio was slightly higher in the HFA mice, the difference approaching significance ($P = 0.08$). We speculate that the lack of additive effect of voluntary running and HFD on capillary density may be partly explained by the detected muscle hypertrophy in HFA mice and the lower amount of running in HFA compared to LFA.

The enhancing effect of voluntary running on capillary density of murine skeletal muscle has been demonstrated previously (Waters et al. 2004; Chinsomboon et al. 2009). However, to our knowledge the present study (II) was the first to report that HFD per se increases capillarization in skeletal muscle. At the time of the study, Roudier et al. had reported that 8 weeks on HFD resulted in a higher capillary density and capillary-to-fiber ratio in the plantaris muscle of endurance trained rats (Roudier et al. 2009). In sedentary rats, a significant difference was not found in capillarization. Li et al. reported that HFD impairs angiogenesis in murine skeletal muscle after experimental ischemia (Li et al. 2007). Furthermore, as in our study, they found that HFD increased VEGF-A levels in the healthy control limb; however, changes in capillarization were not detected. There are certain important differences in the experimental set-up between the studies that may explain the discrepancies in the results. The duration of the study by Li et al. was shorter (12wk vs. 19wk) and the fat content of the HFD was lower (45% vs. 60%) (Li et al. 2007). Furthermore, the surgically induced ischemia in the other hind limb may have had confusing effects on the control limb via e.g. decreased spontaneous activity or increased loading of the control limb. Although long-term HFD seems to have a positive effect on capillarization in murine skeletal muscle, it has been shown that HFD induces adverse effects in rodents. For example, the majority of HFD fed rodents become obese and insulin resistant and endothelial function is impaired in their blood vessels (Costa et al. 2011; Burcelin et al. 2002).

Water et al. have shown that voluntary running stimulates angiogenesis preferentially in a subpopulation of type IIb + IId/x fibers before the switch towards type IIa fibers (Waters et al. 2004). This phenomenon is logical because the fast fibers have the highest need to improve their oxidative capacity and

oxygen delivery. This may also be the case with HFD-induced mitochondrial biogenesis and angiogenesis. Normally, fast fibers produce energy primarily by using glucose as a substrate. When fast muscles are forced to rely more on fatty acid oxidation, they need a greater capacity to oxidize fat. Thus far, no studies have shown that HFD induces mitochondrial biogenesis or angiogenesis in human muscles. The phenomenon may be easier to detect in rodent studies because the content of fast glycolytic type muscle fibers in skeletal muscles is higher in rodents than in humans. For example, in the human vastus lateralis muscle (part of MQF), 26% of muscle fibers are fast glycolytic fibers (Staron et al. 2000), whereas in mouse vastus lateralis muscle, almost all the muscle fibers are fast glycolytic fibers (Hämäläinen & Pette 1993).

In order to reveal the signalling pathways used in HFD-induced angiogenesis, we measured the protein levels of VEGF-A, the key angiogenesis promoting factor, and the levels of HIF-1α, PGC-1α (full length) and ERRα, which are important signalling proteins known to regulate VEGF-A expression and angiogenesis in skeletal muscles. The protein levels of VEGF-A were higher in the muscle homogenates of HFS, LFA and HFA mice compared to LFS; however, voluntary running did not increase VEGF levels in the HFD-fed mice. Since the protein levels of HIF-1α, PGC-1α (full length) and ERRα showed no differences between the experimental groups, the protein results did not provide clear support for the activation of either the HIF-1 or PGC-1α pathway in HFD-induced angiogenesis.

Since muscle tissue consists of several cell types that are not directly involved in angiogenesis, we measured the mRNA levels of VEGF-A, HIF-1α, total PGC-1α and ERRα in the total skeletal muscle homogenate, and also separately in the muscle fiber and capillary samples obtained by the LCM method. The mRNA levels of VEGF-A were higher in the capillary samples of the HFS and HFA mice compared to LFS mice; however, no such differences were seen in muscle fibers. This suggests that HFD induces VEGF-A expression preferentially in the endothelial cells of capillaries. This response seems to be different from the exercise-induced response, since recent studies have shown that in response to exercise, the majority of VEGF-A present within skeletal muscle is thought to originate from skeletal myocytes rather than endothelial cells (Delavar et al. 2014).

The mRNA expression of HIF-1α was upregulated in the muscle homogenate and in the capillaries but not in the muscle fibers of the HFS mice. The mRNA expression of HIF-1α is not stimulated significantly by hypoxia (Huang et al. 1996). However, Milkiewicz et al. have reported that upregulation of HIF-1α mRNA plays a central role in stretch-induced angiogenesis in skeletal muscle (Milkiewicz et al. 2007; Milkiewicz & Haas 2005). Thus, HFD-induced angiogenesis may at least partly occur via the same mechanisms involved in stretch-induced angiogenesis.

6.4 Effect of high-fat diet and physical activity on metabolic disease risk factors

As expected based on earlier studies (Burcelin et al. 2002; Turner et al. 2007), HFD increased the epididymal fat mass and body mass of the mice. In addition, after the intervention, the HFD fed mice had higher levels of total serum cholesterol and they were insulin-resistant (high fasting insulin levels, glucose levels and HOMA-IR). Stimulated physical activity decreased body mass but did not have an effect on fasting insulin levels, glucose levels or HOMA-IR. It may be that the volume of stimulated physical activity was not enough to counteract the effect of HFD. However, it is generally known that increased physical activity per se without restriction of energy intake has only mild effects on body mass and weight gain (Thomas et al. 2012). Statistically significant effects of voluntary running on body mass and glucose balance have been demonstrated earlier in mice after 6 weeks of HFD (Bradley et al. 2008).

6.5 Effect of voluntary running on total spontaneous activity of mice

Voluntary running is a common exercise model for studying the effects of physical activity with rats and mice. Voluntarily running animals live in cages where they have free access to running wheels. It is generally thought that the benefit of the voluntary running model is the higher volume of exercise and the lower psychological stress compared to forced exercise models. To determine the effects of physical activity on the studied variables in many types of experiments, it is important to have a method for the quantification of total activity of both sedentary and voluntarily running animals. There are a variety of methods available to analyse physical activity and behaviour, such as video tracking (Dielenberg, Halasz & Day 2006; Pan, Lee & Lim 1996; Rantalainen et al. 2011), infrared photo-beam systems (Teicher et al. 1996; Beninger, Cooper & Mazurski 1985), force-plate actometers (Biesiadecki et al. 1999; Chiesa, Araujo & Diez-Noguera 2006; Fowler et al. 2001) and touch-pad transducers (Kao et al. 1995). However, there is a lack of validated methods that are capable of measuring total physical activity from cages with and without running wheels. For this purpose we developed and validated a ground reaction force measurement system that measures four different variables from force data: activity index (total activity), activity time, mean intensity of the activity and distance. The system was validated in calibration measurements and in situ by measuring the activity of mice with and without running wheels.

Activity index was originally developed for spontaneous activity measurements of rats (Biesiadecki et al. 1999). In the present study, activity index analysis was modified for measuring activity of mice with the developed sys-

tem. Mass correction was added to the analysis to remove the effect of body mass on the results. In addition, the resolution of the analysis was enhanced with background subtraction. High resolution is crucial when the activities of small animals like mice are measured.

The calibration measurements showed that activity index and activity time were associated very strongly with the true values and the precision was adequate, indicating that these variables and their derivative (mean intensity of the activity) are valid measures. Furthermore, the calibration measurements indicated that distance analysis was accurate and precise. However, during analysis of the mouse experiment, we observed that water evaporation caused significant drift in distances leading to overestimated results during long measurements (>10 h). To test the system in practice we performed experiments to determine the effect of voluntary running on total activity of mice. The results showed that running wheels nearly doubled the intensity of activity (94 ± 90%) and also increased significantly the time of activity (39 ± 19%). These changes resulted in over 200% increase in total activity. The strong associations between the measured activity variables and running distance confirmed that running clearly affects the physical activity of mice. Running seems to boost total activity, especially by increasing the intensity of physical activity. The strong associations also confirm that activity time, activity index and activity intensity analyses are reliable in actual measurement conditions, and that these variables can be used in the quantification of physical activity of mice with or without running wheels. The distance analysis was not sensitive to wheel running, thus its use is limited to cages without running wheels.

Because the developed activity measurement system was not available when study II was performed, we were not able to report comparable physical activity values in sedentary and active groups. However, the data from study III showed that voluntary running increased the total activity of all mice, even when the running distances were low and the total activity was strongly associated with running distance (R^2=0.95, $P < 0.001$). Using the equation derived from the association data and the running distances of study II we estimated that LFA mice were about 100% and HFA at least 60% more active than sedentary mice at the end of the study.

6.6 Acute gene expression responses of PGC1 isoforms after endurance and resistance exercise

Skeletal muscle has an outstanding capability to adapt to a variety of external stimuli that explains, in part, the marked differences observed in physical performance (e.g. endurance and strength) and health profiles between individuals (Hawley et al. 2014). However, the early signalling events that drive exercise mode-specific adaptations are not well known. Recent studies have shown that PGC- 1α, a well-known mediator of endurance exercise adaptations, has several

distinct isoforms (Ruas et al. 2012; Zhang et al. 2009). These studies also suggested that the isoforms may differ in their function and responses to different types of exercise. To investigate the role of PGC- 1 isoforms in the muscle adaptation mechanism, we aimed to investigate the acute gene expression responses of different PGC-1 isoforms after a single bout of high-load resistance exercise (leg press protocol) or moderate intensity endurance exercise (uphill walking on a treadmill) in human skeletal muscle. At the time when study IV was started, only a few studies had reported acute gene expression responses of different PGC-1α isoforms in human skeletal muscle (Norrbom et al. 2011; Ydfors et al. 2013; Ruas et al. 2012), and these studies did not report clearly the design or the specificity of the RT-PCR primers used in the detection of these isoforms. Thus, we thought it was important to confirm the earlier findings after different types of exercise and with well-tested and defined primers.

The current results together with other studies (Norrbom et al. 2011; Ydfors et al. 2013; Gidlund et al. 2015; Lundberg et al. 2014) showed clearly that the expression of alternative promoter driven PGC-1α transcripts (exon 1b and 1b'-derived) is strongly induced after different types of resistance exercise (RE) and endurance exercise (EE), whereas transcripts originating from proximal promoter (PGC-1α exon 1a-derived) are much less inducible. Rodent studies have shown that alternative promoter-originated PGC-1α isoforms, which were also induced in the present study, promote angiogenesis (Chinsomboon et al. 2009), mitochondrial biogenesis and improve fatty acid oxidation capacity in skeletal muscles (Miura et al. 2008). Despite different exercise modes and protocols, both RE and EE increased the expression of truncated PGC-1α transcripts (Total NT-PGC-1α) similarly to earlier studies (Ydfors et al. 2013; Gidlund et al. 2015; Popov et al. 2014). Interestingly, it has been shown recently that hypoxia specifically induces truncated forms of PGC-1α (NT-PGC-1α and PGC-1α4), which induces VEGF expression and angiogenesis, while having only a small effect on mitochondrial genes (Thom et al. 2014). In this study neither RE nor EE modulated the expression of PGC-1β thus supporting the assumption that PGC-1β is not transcriptionally regulated after exercise (Meirhaeghe et al. 2003).

In study IV we also determined how RE and EE affect the expression of a selection of known PGC-1α target genes related to mitochondrial biogenesis, angiogenesis, and muscle hypertrophy. According to conventional dogma, chronic EE (low intensity-high volume loading) favours skeletal muscle adaptations (e.g. mitochondrial biogenesis, angiogenesis and improved β-oxidation) enhancing oxidative capacity with a modest effect on muscle size (Holloszy & Booth 1976). Conversely, RE (high intensity-low volume loading) increases protein accretion promoting muscle hypertrophy and force (Hawley et al. 2014). The observed increased gene expression of mitochondrial marker cytochrome c by EE but not RE suggests that mitochondrial adaptation was induced preferentially by EE. In contrast, gene expression changes typical of angiogenic responses seemed to be stimulated by both EE and RE because both exercise types increased the mRNA expression of pro-angiogenic factor VEGF-A. As expected, RE decreased the gene expression of myostatin, the known target of PGC-1α4

(Ruas et al. 2012) and an inhibitor of muscle growth, but EE did not have any effect. The down-regulation of myostatin may be part of a hypertrophic response induced by RE (Hulmi et al. 2007). However, the importance of the role of myostatin in the hypertrophic response to RE in humans is still unclear and needs further experimental evidence.

In order to check whether the activation changes of known signalling molecules regulating PGC-1α expression were associated with expression changes of specific isoforms of PGC-1, the levels of p-p38 MAPK and p-AMPKα were measured. The levels of p-p38 MAPK were increased after RE and levels of p-AMPKα after both RE and EE. However, the phosphorylation changes of these signalling molecules were not associated with the gene expression responses of PGC-1 isoforms. This result is not fully in line with the study of Norrbom et al., which indicated that AMPK is a major regulator of PGC-1α transcripts from the proximal promoter, but the expression of transcripts from an alternative promoter is regulated by β-adrenergic signalling in combination with AMPK (Norrbom et al. 2011). Based on the findings of Norrbom et al. (2011) we expected to find an association between responses of AMPKα and PGC-1α exon 1a-derived mRNA. A recent study by Popov et al. indicated that exercise-induced gene expression responses of proximal promoter originated PGC-1α transcripts are independent of AMPK activation (Popov et al. 2015). Furthermore, their study proposed that the exercise-induced gene expression responses of alternative promoter originated transcripts are dependent on cAMP response element-binding protein activation.

6.7 Strengths and limitations

Rat strains with high and low inherited aerobic capacity are an excellent model for studying characteristics of inherited aerobic capacity and pathogenesis of metabolic diseases. The idea is that in this model functional alleles at multiple interacting loci that affect intrinsic aerobic capacity have been enriched or fixed differentially between LCR and HCR. Compared to inbred strains, in which essentially all loci have been taken to fixation, outbred selected lines maintain genetic complexity (Koch, Britton & Wisloff 2012). The model is also superior compared to models where individual genes or pathways are manipulated, because the current conception is that biological function resides within highly interconnected modules of molecular networks (Jeong et al. 2000). With this animal model the effects of both genetic and environmental factors could be controlled, which is rather hard in human studies. The rat model that was used consisted of HCR and LCR strains but there was no unselected strain to represent rats with normal aerobic capacity. This limitation somewhat interferes with the interpretation of results. Furthermore, because the rat strains diverge significantly in levels of physical activity, it is hard to distinguish the direct effects of genes from the secondary effects of physical activity differences. With this model we were able to comprehensively characterise the main structural and

molecular differences that explain disparity of skeletal muscle oxidative capacity between rat strains. However, the present study did not include functional measurements like VO_{2max} test, mitochondrial respiration measurements or endothelial function. Furthermore, the focus was primarily on skeletal muscle, although it is clear that cardiac function is a very important limiting factor for whole-body aerobic capacity. However, these traits have been investigated comprehensively by others (Johnsen et al. 2013; Hussain et al. 2001; Rivas et al. 2011; Wisloff et al. 2005). Since almost all human genes known to be associated with disease have orthologs in the rat genome, rats are considered a highly applicable model system for questions regarding gene expression and human diseases (Gibbs et al. 2004). However, all of the findings also need to be confirmed with human subjects.

The experimental setup of study II allowed us to determine simultaneously the effects of diet and physical activity on skeletal muscle capillarization. To our knowledge, the present study was the first to report that HFD per se increases capillarization in skeletal muscle. With a voluntary running model it was possible to study the effects of physical activity without disturbing stress effects, which is a common problem with forced exercise protocols such as treadmill running (Yanagita et al. 2007). The experimental setup of study II was primarily designed to detect long-term adaptation induced by HFD and voluntary running. Thus, it is probable that our experimental set-up did not allow us to detect some important acute HFD- or voluntary running-induced changes in the protein and mRNA levels of the studied angiogenesis regulators. The measurements were performed in an adapted state after the intervention had lasted 19 weeks, at a time when the mice had also fasted and were passive. Because mice are active and eat appreciably more during night time, this might have been a more favourable moment to measure the acute responses of the angiogenesis-regulating factors. In addition to muscle homogenate that contains many cell types that are not involved in angiogenesis, we were also able to measure the expressions of angiogenesis regulators from extracted muscle fiber and capillary samples. However, we cannot be sure that the collected capillary samples were 100% pure from other cell types. To eliminate the risk of accumulation of other cells, a very small (7.5 µm) spot size of the laser beam was used and only blood vessels smaller than 10 µm, i.e. capillaries, were captured. However, we cannot exclude the possibility that periendothelial cells such as pericytes and fibroblasts, which remain in close proximity to the microvascular endothelial cells, could be accumulated unintentionally. Nevertheless, endothelial cells were dominant in the collected cell population, because in a cross section of skeletal muscle only 10% of capillaries are accompanied by adjacent pericyte or fibroblast nuclei (Egginton et al. 2001).

The strength of the developed physical activity measurement system is that sensitive force plates can detect almost all movements of mice, including stationary movements (e.g. eating, drinking and grooming). In addition, it is the first system to be developed and validated specifically for experiments that include voluntary running cages. With the system it is possible to measure com-

parable total physical activity levels of mice from both voluntary running and sedentary animals. Since the force plates are so sensitive, efficient data filtering and background subtraction procedures are needed to enable adequate resolution. The disadvantage of data filtering is that it may lead to loss of some real activity signals. We were able to conduct dynamic validation measurements that allowed the variable specific optimization of data filtering and background subtraction procedures. This is crucial because physical activity-induced dynamic force changes are much more challenging to measure compared to stationary situations. Since man-made calibration devices can never perfectly mimic real animal movements, and since individual animals differ in their behaviour, it is probable that filtering is not always optimal and a small proportion of movements are not recorded.

Because two separate exercise groups were used in study IV, the experimental set-up did not allow direct comparison of gene expression responses between RE and EE. Study IV included strenuous walking endurance exercise, and it should be noted that a different type of endurance exercise might induce different cellular signalling responses in the thigh muscles. The primer sets used in the current study did not separate all the possible truncated and nontruncated splice variants, which may somewhat limit the interpretation of results. Since only three time points were used to measure the acute responses of mRNA and protein molecules, it is probable that we could not detect the peak levels of all studied variables. Furthermore, study IV measured only acute exercise responses without physiological outcome variables of long-term training effects, which could be connected to acute exercise responses.

6.8 Future directions

Based on the findings of study I and previous literature, high inherited aerobic capacity is linked to high physical activity, efficient oxygen delivery and use, and high nonexercise activity thermogenesis. These traits seem to enable efficient dissipation of energy that protects from the adverse effects of an obesogenic environment. The big question for future studies is whether or not it is possible to develop effective exercise or pharmaceutical therapies that could help people to get this HCR-like protective phenotype if they don't have the genotype in question.

In study II, it was found that HFD increased capillarization of mixed type skeletal muscle. In future studies, the effects of HFD on capillarization should be studied separately in different types of muscle fibers. Further studies are also needed to confirm the exact mechanisms, especially in the acute phase of high-fat exposure. It is also important to determine whether diet-induced adaptation in skeletal muscle capillarity also occurs in humans and, if so, whether this adaptation is relevant for normal muscle function and health.

The results of study IV, combined with those of previous studies, comprehensively show the responses of different PGC-1α isoforms to different types of

exercise. In the future, mechanistical studies are required that demonstrate the specific roles of each PGC-1α isoform in exercise-induced skeletal muscle adaptation.

7 MAIN FINDINGS AND CONLUSIONS

The main findings and conclusions of the present thesis are:

1) The analysis of risk factors of complex metabolic diseases revealed that rats with high inherited aerobic capacity (HCR) were lighter and had lower blood glucose, insulin, and triglyceride levels compared to rats with low inherited aerobic capacity (HCR). HCRs also had higher resting metabolic rate, voluntary activity, serum high density lipoproteins, and higher capillarization and mitochondrial area in their skeletal muscles. Bioinformatic analysis of skeletal muscle gene expression data revealed that HCRs had higher expression of genes related to oxidative phosphorylation, fatty acid metabolism, Krebs cycle, valine, leucine and isoleucine degradation, and PPAR-signalling pathway. Furthermore, the analysis showed that the expression of oxidative phosphorylation and lipid metabolism related genes in skeletal muscle is significantly linked to voluntary running performance and whole-body glucose balance. The results support the significance of aerobic metabolism in the development of metabolic diseases. (I)

2) A high-fat diet induced capillarization in murine skeletal muscle without an additive effect of physical activity. As an indication of activated angiogenesis, we also found an increased level of angiogenic factor VEGF-A protein in muscle tissue. Because HFD did not change the protein-levels of HIF-1α and PGC-1α, the protein level results do not support the involvement of these proteins in HFD-induced angiogenesis. However, when gene expression was measured in capillary endothelial cells and muscle fibers using a novel laser capture microdissection technique, it was found that the mRNA expression of HIF-1α and VEGF-A were increased in endothelial cells after HFD. Since a similar response has been induced earlier by experimental stretch stress, the same or a similar mechanism may be activated in HFD-induced angiogenesis. (II)

3) Calibration measurements and actual long-term measurements of mouse movements showed that the developed activity measurement system is valid for the quantification of spontaneous physical activity of mice housed in cages with or without running wheels. The activity index and activity time are the most valid measures for these conditions. The distance analysis is acceptable when the maximum measuring time is 24 hours and there is no running wheel in the cage. The mouse experiment showed that wheel running triples the mean total activity of mice. The main part of this effect is explained by increases in the intensity of activity and the activity time. The developed method causes minimal disturbance to the experimental animals and can therefore be considered well-suited to estimating physical activity in various research paradigms. (III)

4) The comprehensive assay of PGC-1 mRNA expression responses in human skeletal muscle showed specific response profiles after RE and EE. The study confirmed that the alternative promoter originated transcripts (PGC-1α exon 1b and 1b′ derived transcripts) are vastly upregulated after both EE and RE, whereas the proximal promoter originated PGC-1α exon 1a derived transcripts are less inducible and were upregulated only after EE. Truncated PGC-1α transcripts were upregulated after both EE and RE, and thus no clear exercise type specificity was observed in the responses of these transcripts. The expression changes of marker genes suggested that EE induced responses typical of angiogenesis and mitochondrial biogenesis, while RE induced responses typical of angiogenesis and muscle hypertrophy. Our results improve the understanding of exercise type-specific early signalling events and support the idea that gene expression responses of PGC-1α isoforms may have an important role in exercise-induced muscle adaptations. However, future studies are still required to verify the roles of different PGC-1α isoforms in the mechanisms of muscle adaptation. (IV)

YHTEENVETO (FINNISH SUMMARY)

Lihaksen hapenottokyky: perimän, rasvaisen ruokavalion ja fyysisen aktiivisuuden vaikutukset

Elimistön hapenottokyky on erittäin tärkeää ihmisen terveydelle ja toimintakyvylle. Hapenottokyky kertoo elimistön kyvystä tuottaa tarvitsemaansa energiaa solujen mitokondrioissa hapellisten energiantuottoreittien avulla. Elimistön hapenottokykyyn voivat vaikuttaa keuhkojen diffuusiokapasiteetti, sydämen maksimaalinen minuuttitilavuus, veren hapenkuljetuskyky sekä luurankolihasten ominaisuudet. Nykytiedon mukaan lihasten vähäinen mitokondrioiden määrä, heikentynyt mitokondrioiden toiminta ja matala rasvojen hapetuskapasiteetti ovat yhteydessä metabolisen oireyhtymän ja tyypin 2 diabeteksen kehittymiseen. Perimä vaikuttaa merkittävästi lihasten hapenottokykyyn, mutta myös liikunnan määrällä ja ruokavaliolla on siihen merkittävä vaikutus.

Tämän väitöskirjan päätarkoituksena oli kuvata miten perimä, rasvainen ruokavalio ja fyysinen aktiivisuus vaikuttavat raajalihaksen hapenottokykyyn vaikuttaviin rakenteellisiin osatekijöihin. Osatöiden tavoitteena oli 1) kuvata miten perinnöllisesti korkean ja matalan hapenottokyvyn omaavat rotat eroavat toisistaan lihaksiensa ominaisuuksien suhteen, sekä selvittää voisiko lihasten geenien ilmenemisprofiilit osaltaan selittää hapenottokyvyn ja metabolisen oireyhtymän riskitekijöiden välistä yhteyttä; 2) tutkia rasvaisen ruokavalion ja vapaaehtoisella juoksulla lisätyn fyysisen aktiivisuuden vaikutuksia hiirten lihasten kapillarisaatioon; 3) kehittää spontaanin fyysisen aktiivisuuden mittausmenetelmä, jota voidaan käyttää sekä juoksupyörällä aktivoitujen (vapaaehtoinen juoksuharjoittelu) että juoksupyörättömien vähemmän liikkuvien hiirten mittaamiseen; 4) tutkia ihmisen lihaksen adaptaatiomekanismeja mittaamalla eri PGC-1 isoformien akuutteja geenien ilmenemisvasteita yksittäisen kestävyys- ja voimaharjoituksen jälkeen.

Perinnöllisesti matalan hapenottokyvyn omaavilla rotilla (LCR-rotat) oli enemmän metabolisen oireyhtymän riskitekijöitä. Perinnöllisesti korkean hapenottokyvyn omaavat rotat (HCR-rotat) olivat fyysisesti aktiivisempia, niillä oli nopeampi lepoaineenvaihdunta ja niillä oli tiheämpi kapillarisaatio ja suurempi mitokondrioiden määrä raajalihaksissa. Tämän lisäksi HCR-rottien lihaksissa oli hapellisiin energiantuottoreitteihin ja haaraketjuisten aminohappojen hajotukseen liittyvien geenien lähetti-RNA-tason ilmeneminen suurempaa kuin LCR-rottien raajalihaksissa. Analyysit osoittivat myös, että oksidatiiviseen fosforylaatioon ja rasvametaboliaan liittyvien geenien ilmenemisen määrä oli yhteydessä juoksusuorituskykyyn sekä glukoositasapainoon.

Rasvainen ruokavalio ja vapaaehtoinen juoksu juoksupyörässä lisäsivät molemmat erikseen hiirten lihasten kapillarisaatiota. Lisätty fyysinen aktiivisuus ei kuitenkaan vaikuttanut rasvaista ruokavaliota syöneiden hiirten lihasten kapillarisaatioon. Kun tutkittiin rasvaisen ruokavalion vaikutuksen mahdollista mekanismia, havaittiin että rasvaista ruokavaliota syöneiden hiirten lihaksissa oli lisääntynyt pitoisuus VEGF-A proteiinia, joka indusoi angiogeneesiä eli

kapillaariverisuonten uudismuodostusta. Havaittiin myös, että rasvaista ruokavaliota syöneillä hiirillä oli kapillaarien endoteelisoluissa suurempi pitoisuus VEGF-A:n ja sitä säätelevän HIF-1α:n lähetti-RNA:ta.

Kalibrointimittaukset sekä varsinaiset testimittaukset hiirillä osoittivat, että kehitetty aktiivisuusmittausjärjestelmä on tarkka ja luotettava ja sitä voidaan näin käyttää sekä tavallisissa häkeissä että juoksupyörällä varustetuissa häkeissä elävien hiirten fyysisen aktiivisuuden mittaamiseen. Tutkimus osoitti myös sen, että juoksupyörien lisääminen hiirten häkkeihin kasvattaa niiden fyysisen aktiivisuuden noin kolminkertaiseksi.

Tutkittaessa harjoittelun aiheuttamia akuutteja PGC-1α isoformien lähetti-RNA-tason vasteita ihmisen raajalihaksessa, havaittiin, että vaihtoehtoisen promoottorialueen säätelemien isoformien (PGC-1α eksoni 1b ja eksoni 1b′ lähtöiset) geenien ilmeneminen kasvoi hyvin merkittävästi sekä kestävyys- (KH) että voimaharjoittelun (VH) jälkeen. Proksimaalisen promoottorialueen ohjaamien PGC-1α isoformien geenien ilmenemisen muutos harjoittelun jälkeen oli selvästi vähäisempi, ja merkittävä muutos havaittiin vain KH:n jälkeen. Typistyneiden NT-PGC-1α-isoformien geenien ilmeneminen lisääntyi merkittävästi niin KH:n kuin VH:nkin jälkeen eli näiden isoformien vasteissa ei havaittu harjoitusmuotospesifisyyttä. Kun tutkittiin harjoittelun aiheuttamia geenien ilmenemismuutoksia PGC-1α:n säätelyn alaisissa geeneissä, havaittiin, että KH lisäsi angiogeneesin aktivaattorin VEGF-A:n sekä mitokondrioiden määrään yhteydessä olevan CYC:n ilmenemistä. VH:n havaittiin lisäävän VEGF-A:n ilmenemistä sekä laskevan lihasten kasvua rajoittavan myostatiinin ilmenemistä.

Yhteenvetona voidaan sanoa, että perimältään erilaisen koko kehon hapenottokyvyn omaavat rotat erosivat toisistaan merkittävästi myös lihaksien hapenottokykyyn liittyviltä ominaisuuksiltaan, mikä osaltaan saattaa selittää kyseisten rottakantojen erot kestävyyssuorituskyvyssä sekä glukoositasapainon ylläpidossa. Lisäksi tutkimus osoitti ensi kertaa, että rasvainen ruokavalio lisää juoksuharjoittelun tavoin hiirten lihasten kapillarisaatiota, joka saattaa olla yhteydessä angiogeneesiä säätelevien HIF-1α:n ja VEGF-A:n lisääntyneeseen ilmenemiseen kapillaarisuonten endoteelisoluissa. Tutkimuksen tulokset tukivat myös sitä käsitystä, että PGC-1α:n eri isoformeilla voi olla merkittävä rooli harjoitustyyppikohtaisissa lihasadaptaatioissa. Tutkimuksen tulokset lisäävät ymmärrystämme lihaksen oksidatiiviseen kapasiteettiin vaikuttavista tekijöistä, mikä saattaa auttaa ymmärtämään myös niiden sairauksien kehittymistä, jotka liittyvät matalaan lihasten oksidatiiviseen kapasiteettiin ja vähäiseen liikunnan määrään. Vaaditaan kuitenkin vielä jatkotutkimuksia osoittamaan eläinkokeissa havaitut ilmiöt myös ihmisessä sekä mekanistisia tutkimuksia syyseuraussuhteiden selventämiseksi.

REFERENCES

Ahtiainen, J. P., Pakarinen, A., Alen, M., Kraemer, W. J. & Häkkinen, K. 2003. Muscle hypertrophy, hormonal adaptations and strength development during strength training in strength-trained and untrained men. European Journal of Applied Physiology 89 (6), 555-563.

Akimoto, T., Pohnert, S. C., Li, P., Zhang, M., Gumbs, C., Rosenberg, P. B., Williams, R. S. & Yan, Z. 2005. Exercise stimulates Pgc-1alpha transcription in skeletal muscle through activation of the p38 MAPK pathway. The Journal of Biological Chemistry 280 (20), 19587-19593.

Alvehus, M., Boman, N., Söderlund, K., Svensson, M. B. & Buren, J. 2014. Metabolic adaptations in skeletal muscle, adipose tissue, and whole-body oxidative capacity in response to resistance training. European Journal of Applied Physiology 114 (7), 1463-1471.

Andersen, J. L. & Aagaard, P. 2000. Myosin heavy chain IIX overshoot in human skeletal muscle. Muscle & Nerve 23 (7), 1095-1104.

Andersen, P. & Henriksson, J. 1977. Capillary supply of the quadriceps femoris muscle of man: adaptive response to exercise. The Journal of Physiology 270 (3), 677-690.

Augustin, H. G., Koh, G. Y., Thurston, G. & Alitalo, K. 2009. Control of vascular morphogenesis and homeostasis through the angiopoietin-Tie system. Nature Reviews. Molecular Cell Biology 10 (3), 165-177.

Baar, K., Wende, A. R., Jones, T. E., Marison, M., Nolte, L. A., Chen, M., Kelly, D. P. & Holloszy, J. O. 2002. Adaptations of skeletal muscle to exercise: rapid increase in the transcriptional coactivator PGC-1. FASEB Journal 16 (14), 1879-1886.

Barlow, C. E., LaMonte, M. J., Fitzgerald, S. J., Kampert, J. B., Perrin, J. L. & Blair, S. N. 2006. Cardiorespiratory fitness is an independent predictor of hypertension incidence among initially normotensive healthy women. American Journal of Epidemiology 163 (2), 142-150.

Bassett, D. R.,Jr & Howley, E. T. 2000. Limiting factors for maximum oxygen uptake and determinants of endurance performance. Medicine and Science in Sports and Exercise 32 (1), 70-84.

Beighley, P. E., Zamir, M., Wentz, R. J., Koch, L. G., Britton, S. L. & Ritman, E. L. 2013. Vascularity of myocardium and gastrocnemius muscle in rats selectively bred for endurance running capacity. Physiological Genomics 45 (3), 119-125.

Beninger, R. J., Cooper, T. A. & Mazurski, E. J. 1985. Automating the measurement of locomotor activity. Neurobehavioral Toxicology and Teratology 7 (1), 79-85.

Bergeron, R., Ren, J. M., Cadman, K. S., Moore, I. K., Perret, P., Pypaert, M., Young, L. H., Semenkovich, C. F. & Shulman, G. I. 2001. Chronic activation of AMP kinase results in NRF-1 activation and mitochondrial biogenesis. American Journal of Physiology - Endocrinology and Metabolism 281 (6), E1340-6.

Biesiadecki, B. J., Brand, P. H., Koch, L. G. & Britton, S. L. 1999. A gravimetric method for the measurement of total spontaneous activity in rats. Proceedings of the Society for Experimental Biology and Medicine. 222 (1), 65-69.

Blair, S. N., Kampert, J. B., Kohl, H. W.,3rd, Barlow, C. E., Macera, C. A., Paffenbarger, R. S.,Jr & Gibbons, L. W. 1996. Influences of cardiorespiratory fitness and other precursors on cardiovascular disease and all-cause mortality in men and women. Journal of American Medical Association 276 (3), 205-210.

Blair, S. N., Kohl, H. W.,3rd, Paffenbarger, R. S.,Jr, Clark, D. G., Cooper, K. H. & Gibbons, L. W. 1989. Physical fitness and all-cause mortality. A prospective study of healthy men and women. Journal of American Medical Association 262 (17), 2395-2401.

Bland, J. M. & Altman, D. G. 1986. Statistical methods for assessing agreement between two methods of clinical measurement. Lancet 1 (8476), 307-310.

Bodine, S. C., Stitt, T. N., Gonzalez, M., Kline, W. O., Stover, G. L., Bauerlein, R., Zlotchenko, E., Scrimgeour, A., Lawrence, J. C., Glass, D. J. & Yancopoulos, G. D. 2001. Akt/mTOR pathway is a crucial regulator of skeletal muscle hypertrophy and can prevent muscle atrophy in vivo. Nature Cell Biology 3 (11), 1014-1019.

Bolster, D. R., Crozier, S. J., Kimball, S. R. & Jefferson, L. S. 2002. AMP-activated protein kinase suppresses protein synthesis in rat skeletal muscle through down-regulated mammalian target of rapamycin (mTOR) signaling. The Journal of Biological Chemistry 277 (27), 23977-23980.

Booth, F. W., Gordon, S. E., Carlson, C. J. & Hamilton, M. T. 2000. Waging war on modern chronic diseases: primary prevention through exercise biology. Journal of Applied Physiology 88 (2), 774-787.

Bouchard, C., An, P., Rice, T., Skinner, J. S., Wilmore, J. H., Gagnon, J., Perusse, L., Leon, A. S. & Rao, D. C. 1999. Familial aggregation of VO(2max) response to exercise training: results from the HERITAGE Family Study. Journal of Applied Physiology 87 (3), 1003-1008.

Bouchard, C., Daw, E. W., Rice, T., Perusse, L., Gagnon, J., Province, M. A., Leon, A. S., Rao, D. C., Skinner, J. S. & Wilmore, J. H. 1998. Familial resemblance for VO2max in the sedentary state: the HERITAGE family study. Medicine and Science in Sports and Exercise 30 (2), 252-258.

Boyadjiev, N. 1996. Increase of aerobic capacity by submaximal training and high-fat diets. Folia Medica 38 (1), 49-59.

Bradley, R. L., Jeon, J. Y., Liu, F. F. & Maratos-Flier, E. 2008. Voluntary exercise improves insulin sensitivity and adipose tissue inflammation in diet-induced obese mice. American Journal of Physiology.Endocrinology and Metabolism 295 (3), E586-94.

Brew, K. & Nagase, H. 2010. The tissue inhibitors of metalloproteinases (TIMPs): an ancient family with structural and functional diversity. Biochimica Et Biophysica Acta 1803 (1), 55-71.

Brinkworth, G. D., Noakes, M., Clifton, P. M. & Buckley, J. D. 2009. Effects of a low carbohydrate weight loss diet on exercise capacity and tolerance in obese subjects. Obesity 17 (10), 1916-1923.

Brodal, P., Ingjer, F. & Hermansen, L. 1977. Capillary supply of skeletal muscle fibers in untrained and endurance-trained men. The American Journal of Physiology 232 (6), H705-12.

Brooke, M. H. & Kaiser, K. K. 1970. Three "myosin adenosine triphosphatase" systems: the nature of their pH lability and sulfhydryl dependence. The Journal of Histochemistry and Cytochemistry 18 (9), 670-672.

Buick, F. J., Gledhill, N., Froese, A. B., Spriet, L. & Meyers, E. C. 1980. Effect of induced erythrocythemia on aerobic work capacity. Journal of Applied Physiology: Respiratory, Environmental and Exercise Physiology 48 (4), 636-642.

Burcelin, R., Crivelli, V., Dacosta, A., Roy-Tirelli, A. & Thorens, B. 2002. Heterogeneous metabolic adaptation of C57BL/6J mice to high-fat diet. American Journal of Physiology - Endocrinology and Metabolism 282 (4), E834-42.

Burgomaster, K. A., Howarth, K. R., Phillips, S. M., Rakobowchuk, M., Macdonald, M. J., McGee, S. L. & Gibala, M. J. 2008. Similar metabolic adaptations during exercise after low volume sprint interval and traditional endurance training in humans. The Journal of Physiology 586 (1), 151-160.

Burke, L. M. & Hawley, J. A. 2002. Effects of short-term fat adaptation on metabolism and performance of prolonged exercise. Medicine and Science in Sports and Exercise 34 (9), 1492-1498.

Carling, D. & Hardie, D. G. 1989. The substrate and sequence specificity of the AMP-activated protein kinase. Phosphorylation of glycogen synthase and phosphorylase kinase. Biochimica Et Biophysica Acta 1012 (1), 81-86.

Carnethon, M. R., Sternfeld, B., Schreiner, P. J., Jacobs, D. R.,Jr, Lewis, C. E., Liu, K. & Sidney, S. 2009. Association of 20-year changes in cardiorespiratory fitness with incident type 2 diabetes: the coronary artery risk development in young adults (CARDIA) fitness study. Diabetes Care 32 (7), 1284-1288.

Chang, J. S., Huypens, P., Zhang, Y., Black, C., Kralli, A. & Gettys, T. W. 2010. Regulation of NT-PGC-1alpha subcellular localization and function by protein kinase A-dependent modulation of nuclear export by CRM1. The Journal of Biological Chemistry 285 (23), 18039-18050.

Chaurasia, B. & Summers, S. A. 2015. Ceramides - Lipotoxic Inducers of Metabolic Disorders. Trends in Endocrinology and Metabolism 26 (10), 538-550.

Chiesa, J. J., Araujo, J. F. & Diez-Noguera, A. 2006. Method for studying behavioural activity patterns during long-term recordings using a force-plate actometer. Journal of Neuroscience Methods 158 (1), 157-168.

Chilibeck, P. D., Syrotuik, D. G. & Bell, G. J. 1999. The effect of strength training on estimates of mitochondrial density and distribution throughout muscle fibres. European Journal of Applied Physiology and Occupational Physiology 80 (6), 604-609.

Chinsomboon, J., Ruas, J., Gupta, R. K., Thom, R., Shoag, J., Rowe, G. C., Sawada, N., Raghuram, S. & Arany, Z. 2009. The transcriptional coactivator

PGC-1alpha mediates exercise-induced angiogenesis in skeletal muscle. Proceedings of the National Academy of Sciences of the United States of America 106 (50), 21401-21406.

Costa, R. R., Villela, N. R., Souza, M. G., Boa, B. C., Cyrino, F. Z., Silva, S. V., Lisboa, P. C., Moura, E. G., Barja-Fidalgo, T. C. & Bouskela, E. 2011. High fat diet induces central obesity, insulin resistance and microvascular dysfunction in hamsters. Microvascular Research 82 (3), 416-422.

Crunkhorn, S., Dearie, F., Mantzoros, C., Gami, H., da Silva, W. S., Espinoza, D., Faucette, R., Barry, K., Bianco, A. C. & Patti, M. E. 2007. Peroxisome proliferator activator receptor gamma coactivator-1 expression is reduced in obesity: potential pathogenic role of saturated fatty acids and p38 mitogen-activated protein kinase activation. The Journal of Biological Chemistry 282 (21), 15439-15450.

Daniels, J. & Oldridge, N. 1970. The effects of alternate exposure to altitude and sea level on world-class middle-distance runners. Medicine and Science in Sports 2 (3), 107-112.

Dashti, H. M., Mathew, T. C., Hussein, T., Asfar, S. K., Behbahani, A., Khoursheed, M. A., Al-Sayer, H. M., Bo-Abbas, Y. Y. & Al-Zaid, N. S. 2004. Long-term effects of a ketogenic diet in obese patients. Experimental and Clinical Cardiology 9 (3), 200-205.

Delavar, H., Nogueira, L., Wagner, P. D., Hogan, M. C., Metzger, D. & Breen, E. C. 2014. Skeletal myofiber VEGF is essential for the exercise training response in adult mice. American Journal of Physiology - Regulatory, Integrative and Comparative Physiology 306 (8), R586-95.

Dempsey, J. A., Hanson, P. G. & Henderson, K. S. 1984. Exercise-induced arterial hypoxaemia in healthy human subjects at sea level. The Journal of Physiology 355, 161-175.

Dennis, G.,Jr, Sherman, B. T., Hosack, D. A., Yang, J., Gao, W., Lane, H. C. & Lempicki, R. A. 2003. DAVID: Database for Annotation, Visualization, and Integrated Discovery. Genome Biology 4 (5), P3.

Dielenberg, R. A., Halasz, P. & Day, T. A. 2006. A method for tracking rats in a complex and completely dark environment using computerized video analysis. Journal of Neuroscience Methods 158 (2), 279-286.

Dolmetsch, R. E., Lewis, R. S., Goodnow, C. C. & Healy, J. I. 1997. Differential activation of transcription factors induced by Ca2+ response amplitude and duration. Nature 386 (6627), 855-858.

Dominy, J. E.,Jr, Lee, Y., Gerhart-Hines, Z. & Puigserver, P. 2010. Nutrient-dependent regulation of PGC-1alpha's acetylation state and metabolic function through the enzymatic activities of Sirt1/GCN5. Biochimica Et Biophysica Acta 1804 (8), 1676-1683.

Dube, J. J., Amati, F., Stefanovic-Racic, M., Toledo, F. G., Sauers, S. E. & Goodpaster, B. H. 2008. Exercise-induced alterations in intramyocellular lipids and insulin resistance: the athlete's paradox revisited. American Journal of Physiology - Endocrinology and Metabolism 294 (5), E882-8.

Egan, B. & Zierath, J. R. 2013. Exercise metabolism and the molecular regulation of skeletal muscle adaptation. Cell Metabolism 17 (2), 162-184.

Egginton, S. 2009. Invited review: activity-induced angiogenesis. Pflugers Archiv: European Journal of Physiology 457 (5), 963-977.

Egginton, S., Hudlicka, O., Brown, M. D., Walter, H., Weiss, J. B. & Bate, A. 1998. Capillary growth in relation to blood flow and performance in overloaded rat skeletal muscle. Journal of Applied Physiology 85 (6), 2025-2032.

Egginton, S., Zhou, A. L., Brown, M. D. & Hudlicka, O. 2001. Unorthodox angiogenesis in skeletal muscle. Cardiovascular Research 49 (3), 634-646.

Ekblom, B., Astrand, P. O., Saltin, B., Stenberg, J. & Wallstrom, B. 1968. Effect of training on circulatory response to exercise. Journal of Applied Physiology 24 (4), 518-528.

Erlenbusch, M., Haub, M., Munoz, K., MacConnie, S. & Stillwell, B. 2005. Effect of high-fat or high-carbohydrate diets on endurance exercise: a meta-analysis. International Journal of Sport Nutrition and Exercise Metabolism 15 (1), 1-14.

Faye, C., Moreau, C., Chautard, E., Jetne, R., Fukai, N., Ruggiero, F., Humphries, M. J., Olsen, B. R. & Ricard-Blum, S. 2009. Molecular interplay between endostatin, integrins, and heparan sulfate. The Journal of Biological Chemistry 284 (33), 22029-22040.

Fluck, M., Carson, J. A., Gordon, S. E., Ziemiecki, A. & Booth, F. W. 1999. Focal adhesion proteins FAK and paxillin increase in hypertrophied skeletal muscle. The American Journal of Physiology 277 (1 Pt 1), C152-62.

Fluck, M. & Hoppeler, H. 2003. Molecular basis of skeletal muscle plasticity--from gene to form and function. Reviews of Physiology, Biochemistry and Pharmacology 146, 159-216.

Folland, J. P., Irish, C. S., Roberts, J. C., Tarr, J. E. & Jones, D. A. 2002. Fatigue is not a necessary stimulus for strength gains during resistance training. British Journal of Sports Medicine 36 (5), 370.

Forsythe, J. A., Jiang, B. H., Iyer, N. V., Agani, F., Leung, S. W., Koos, R. D. & Semenza, G. L. 1996. Activation of vascular endothelial growth factor gene transcription by hypoxia-inducible factor 1. Molecular and Cellular Biology 16 (9), 4604-4613.

Foster, G. D., Wyatt, H. R., Hill, J. O., McGuckin, B. G., Brill, C., Mohammed, B. S., Szapary, P. O., Rader, D. J., Edman, J. S. & Klein, S. 2003. A randomized trial of a low-carbohydrate diet for obesity. The New England Journal of Medicine 348 (21), 2082-2090.

Fowler, S. C., Birkestrand, B. R., Chen, R., Moss, S. J., Vorontsova, E., Wang, G. & Zarcone, T. J. 2001. A force-plate actometer for quantitating rodent behaviors: illustrative data on locomotion, rotation, spatial patterning, stereotypies, and tremor. Journal of Neuroscience Methods 107 (1-2), 107-124.

Friedewald, W. T., Levy, R. I. & Fredrickson, D. S. 1972. Estimation of the concentration of low-density lipoprotein cholesterol in plasma, without use of the preparative ultracentrifuge. Clinical Chemistry 18 (6), 499-502.

Garcia-Roves, P., Huss, J. M., Han, D. H., Hancock, C. R., Iglesias-Gutierrez, E., Chen, M. & Holloszy, J. O. 2007. Raising plasma fatty acid concentration induces increased biogenesis of mitochondria in skeletal muscle. Proceedings of the National Academy of Sciences of the United States of America 104 (25), 10709-10713.

Gautier, L., Cope, L., Bolstad, B. M. & Irizarry, R. A. 2004. affy-analysis of Affymetrix GeneChip data at the probe level. Bioinformatics 20 (3), 307-315.

Gavin, T. P., Robinson, C. B., Yeager, R. C., England, J. A., Nifong, L. W. & Hickner, R. C. 2004. Angiogenic growth factor response to acute systemic exercise in human skeletal muscle. Journal of Applied Physiology 96 (1), 19-24.

Gavini, C. K., Mukherjee, S., Shukla, C., Britton, S. L., Koch, L. G., Shi, H. & Novak, C. M. 2014. Leanness and heightened nonresting energy expenditure: role of skeletal muscle activity thermogenesis. American Journal of Physiology.Endocrinology and Metabolism 306 (6), E635-47.

Gerhart-Hines, Z., Rodgers, J. T., Bare, O., Lerin, C., Kim, S. H., Mostoslavsky, R., Alt, F. W., Wu, Z. & Puigserver, P. 2007. Metabolic control of muscle mitochondrial function and fatty acid oxidation through SIRT1/PGC-1alpha. The EMBO Journal 26 (7), 1913-1923.

Gibala, M. 2009. Molecular responses to high-intensity interval exercise. Applied Physiology, Nutrition, and Metabolism 34 (3), 428-432.

Gibbs, R. A., Weinstock, G. M., Metzker, M. L., Muzny, D. M., Södergren, E. J., Scherer, S., Scott, G., Steffen, D., Worley, K. C., Burch, P. E., Okwuonu, G., Hines, S., Lewis, L., DeRamo, C., Delgado, O., Dugan-Rocha, S., Miner, G., Morgan, M., Hawes, A., Gill, R., Celera, Holt, R. A., Adams, M. D., Amanatides, P. G., Baden-Tillson, H., Barnstead, M., Chin, S., Evans, C. A., Ferriera, S., Fosler, C., Glodek, A., Gu, Z., Jennings, D., Kraft, C. L., Nguyen, T., Pfannkoch, C. M., Sitter, C., Sutton, G. G., Venter, J. C., Woodage, T., Smith, D., Lee, H. M., Gustafson, E., Cahill, P., Kana, A., Doucette-Stamm, L., Weinstock, K., Fechtel, K., Weiss, R. B., Dunn, D. M., Green, E. D., Blakesley, R. W., Bouffard, G. G., De Jong, P. J., Osoegawa, K., Zhu, B., Marra, M., Schein, J., Bosdet, I., Fjell, C., Jones, S., Krzywinski, M., Mathewson, C., Siddiqui, A., Wye, N., McPherson, J., Zhao, S., Fraser, C. M., Shetty, J., Shatsman, S., Geer, K., Chen, Y., Abramzon, S., Nierman, W. C., Havlak, P. H., Chen, R., Durbin, K. J., Egan, A., Ren, Y., Song, X. Z., Li, B., Liu, Y., Qin, X., Cawley, S., Worley, K. C., Cooney, A. J., D'Souza, L. M., Martin, K., Wu, J. Q., Gonzalez-Garay, M. L., Jackson, A. R., Kalafus, K. J., McLeod, M. P., Milosavljevic, A., Virk, D., Volkov, A., Wheeler, D. A., Zhang, Z., Bailey, J. A., Eichler, E. E., Tuzun, E., Birney, E., Mongin, E., Ureta-Vidal, A., Woodwark, C., Zdobnov, E., Bork, P., Suyama, M., Torrents, D., Alexandersson, M., Trask, B. J., Young, J. M., Huang, H., Wang, H., Xing, H., Daniels, S., Gietzen, D., Schmidt, J., Stevens, K., Vitt, U., Wingrove, J., Camara, F., Mar Alba, M., Abril, J. F., Guigo, R., Smit, A., Dubchak, I., Rubin, E. M., Couronne, O., Poliakov, A., Hubner, N., Ganten, D.,

Goesele, C., Hummel, O., Kreitler, T., Lee, Y. A., Monti, J., Schulz, H., Zimdahl, H., Himmelbauer, H., Lehrach, H., Jacob, H. J., Bromberg, S., Gullings-Handley, J., Jensen-Seaman, M. I., Kwitek, A. E., Lazar, J., Pasko, D., Tonellato, P. J., Twigger, S., Ponting, C. P., Duarte, J. M., Rice, S., Goodstadt, L., Beatson, S. A., Emes, R. D., Winter, E. E., Webber, C., Brandt, P., Nyakatura, G., Adetobi, M., Chiaromonte, F., Elnitski, L., Eswara, P., Hardison, R. C., Hou, M., Kolbe, D., Makova, K., Miller, W., Nekrutenko, A., Riemer, C., Schwartz, S., Taylor, J., Yang, S., Zhang, Y., Lindpaintner, K., Andrews, T. D., Caccamo, M., Clamp, M., Clarke, L., Curwen, V., Durbin, R., Eyras, E., Searle, S. M., Cooper, G. M., Batzoglou, S., Brudno, M., Sidow, A., Stone, E. A., Venter, J. C., Payseur, B. A., Bourque, G., Lopez-Otin, C., Puente, X. S., Chakrabarti, K., Chatterji, S., Dewey, C., Pachter, L., Bray, N., Yap, V. B., Caspi, A., Tesler, G., Pevzner, P. A., Haussler, D., Roskin, K. M., Baertsch, R., Clawson, H., Furey, T. S., Hinrichs, A. S., Karolchik, D., Kent, W. J., Rosenbloom, K. R., Trumbower, H., Weirauch, M., Cooper, D. N., Stenson, P. D., Ma, B., Brent, M., Arumugam, M., Shteynberg, D., Copley, R. R., Taylor, M. S., Riethman, H., Mudunuri, U., Peterson, J., Guyer, M., Felsenfeld, A., Old, S., Mockrin, S., Collins, F. & Rat Genome Sequencing Project Consortium 2004. Genome sequence of the Brown Norway rat yields insights into mammalian evolution. Nature 428 (6982), 493-521.

Gidlund, E. K., Ydfors, M., Appel, S., Rundqvist, H., Sundberg, C. J. & Norrbom, J. 2015. Rapidly elevated levels of PGC-1alpha-b protein in human skeletal muscle after exercise: exploring regulatory factors in a randomized controlled trial. Journal of Applied Physiology 119 (4), 374-384.

Green, H., Goreham, C., Ouyang, J., Ball-Burnett, M. & Ranney, D. 1999. Regulation of fiber size, oxidative potential, and capillarization in human muscle by resistance exercise. The American Journal of Physiology 276 (2 Pt 2), R591-6.

Gulati, M., Pandey, D. K., Arnsdorf, M. F., Lauderdale, D. S., Thisted, R. A., Wicklund, R. H., Al-Hani, A. J. & Black, H. R. 2003. Exercise capacity and the risk of death in women: the St James Women Take Heart Project. Circulation 108 (13), 1554-1559.

Gustafsson, T., Puntschart, A., Kaijser, L., Jansson, E. & Sundberg, C. J. 1999. Exercise-induced expression of angiogenesis-related transcription and growth factors in human skeletal muscle. The American Journal of Physiology 276 (2 Pt 2), H679-85.

Gustafsson, T., Rundqvist, H., Norrbom, J., Rullman, E., Jansson, E. & Sundberg, C. J. 2007. The influence of physical training on the angiopoietin and VEGF-A systems in human skeletal muscle. Journal of Applied Physiology 103 (3), 1012-1020.

Haas, T. L., Milkiewicz, M., Davis, S. J., Zhou, A. L., Egginton, S., Brown, M. D., Madri, J. A. & Hudlicka, O. 2000. Matrix metalloproteinase activity is required for activity-induced angiogenesis in rat skeletal muscle. American Journal of Physiology - Heart and Circulatory Physiology 279 (4), H1540-7.

Haas, T. L. & Nwadozi, E. 2015. Regulation of skeletal muscle capillary growth in exercise and disease. Applied Physiology, Nutrition, and Metabolism 40 (12), 1221-1232.

Häkkinen, K., Pakarinen, A., Kraemer, W. J., Häkkinen, A., Valkeinen, H. & Alen, M. 2001. Selective muscle hypertrophy, changes in EMG and force, and serum hormones during strength training in older women. Journal of Applied Physiology 91 (2), 569-580.

Hallal, P. C., Andersen, L. B., Bull, F. C., Guthold, R., Haskell, W., Ekelund, U. & Lancet Physical Activity Series Working Group 2012. Global physical activity levels: surveillance progress, pitfalls, and prospects. Lancet 380 (9838), 247-257.

Hämäläinen, N. & Pette, D. 1993. The histochemical profiles of fast fiber types IIB, IID, and IIA in skeletal muscles of mouse, rat, and rabbit. The Journal of Histochemistry and Cytochemistry 41 (5), 733-743.

Hancock, C. R., Han, D. H., Chen, M., Terada, S., Yasuda, T., Wright, D. C. & Holloszy, J. O. 2008. High-fat diets cause insulin resistance despite an increase in muscle mitochondria. Proceedings of the National Academy of Sciences of the United States of America 105 (22), 7815-7820.

Hardie, D. G., Salt, I. P., Hawley, S. A. & Davies, S. P. 1999. AMP-activated protein kinase: an ultrasensitive system for monitoring cellular energy charge. The Biochemical Journal 338 (Pt 3), 717-722.

Harridge, S. D., Bottinelli, R., Canepari, M., Pellegrino, M. A., Reggiani, C., Esbjornsson, M. & Saltin, B. 1996. Whole-muscle and single-fibre contractile properties and myosin heavy chain isoforms in humans. Pflugers Archiv: European Journal of Physiology 432 (5), 913-920.

Hawley, J. A., Hargreaves, M., Joyner, M. J. & Zierath, J. R. 2014. Integrative biology of exercise. Cell 159 (4), 738-749.

Helge, J. W. 2002. Long-term fat diet adaptation effects on performance, training capacity, and fat utilization. Medicine and Science in Sports and Exercise 34 (9), 1499-1504.

Hellsten, Y. & Hoier, B. 2014. Capillary growth in human skeletal muscle: physiological factors and the balance between pro-angiogenic and angiostatic factors. Biochemical Society Transactions 42 (6), 1616-1622.

Hendrix, L. J., Carter, M. W. & Scott, D. T. 1982. Covariance analyses with heterogeneity of slopes in fixed models. Biometrics 38 (3), 641-650.

Hill, M. & Goldspink, G. 2003. Expression and splicing of the insulin-like growth factor gene in rodent muscle is associated with muscle satellite (stem) cell activation following local tissue damage. The Journal of Physiology 549 (Pt 2), 409-418.

Hoier, B., Nordsborg, N., Andersen, S., Jensen, L., Nybo, L., Bangsbo, J. & Hellsten, Y. 2012. Pro- and anti-angiogenic factors in human skeletal muscle in response to acute exercise and training. The Journal of Physiology 590 (Pt 3), 595-606.

Hoier, B., Olsen, K., Nyberg, M., Bangsbo, J. & Hellsten, Y. 2010a. Contraction-induced secretion of VEGF from skeletal muscle cells is mediated by

adenosine. American Journal of Physiology - Heart and Circulatory Physiology 299 (3), H857-62.

Hoier, B., Prats, C., Qvortrup, K., Pilegaard, H., Bangsbo, J. & Hellsten, Y. 2013. Subcellular localization and mechanism of secretion of vascular endothelial growth factor in human skeletal muscle. FASEB Journal 27 (9), 3496-3504.

Hoier, B., Rufener, N., Bojsen-Moller, J., Bangsbo, J. & Hellsten, Y. 2010b. The effect of passive movement training on angiogenic factors and capillary growth in human skeletal muscle. The Journal of Physiology 588 (Pt 19), 3833-3845.

Holloszy, J. O. 1973. Biochemical adaptations to exercise: aerobic metabolism. Exercise and Sport Sciences Reviews 1, 45-71.

Holloszy, J. O. & Booth, F. W. 1976. Biochemical adaptations to endurance exercise in muscle. Annual Review of Physiology 38, 273-291.

Holloszy, J. O. & Coyle, E. F. 1984. Adaptations of skeletal muscle to endurance exercise and their metabolic consequences. Journal of Applied Physiology: Respiratory, Environmental and Exercise Physiology 56 (4), 831-838.

Hood, D. A., Irrcher, I., Ljubicic, V. & Joseph, A. M. 2006. Coordination of metabolic plasticity in skeletal muscle. The Journal of Experimental Biology 209 (Pt 12), 2265-2275.

Hook, S. S. & Means, A. R. 2001. Ca(2+)/CaM-dependent kinases: from activation to function. Annual Review of Pharmacology and Toxicology 41, 471-505.

Hoydal, M. A., Wisloff, U., Kemi, O. J., Britton, S. L., Koch, L. G., Smith, G. L. & Ellingsen, O. 2007. Nitric oxide synthase type-1 modulates cardiomyocyte contractility and calcium handling: association with low intrinsic aerobic capacity. European Journal of Cardiovascular Prevention and Rehabilitation 14 (2), 319-325.

Huang da, W., Sherman, B. T. & Lempicki, R. A. 2009. Systematic and integrative analysis of large gene lists using DAVID bioinformatics resources. Nature Protocols 4 (1), 44-57.

Huang, L. E., Arany, Z., Livingston, D. M. & Bunn, H. F. 1996. Activation of hypoxia-inducible transcription factor depends primarily upon redox-sensitive stabilization of its alpha subunit. The Journal of Biological Chemistry 271 (50), 32253-32259.

Hubal, M. J., Gordish-Dressman, H., Thompson, P. D., Price, T. B., Hoffman, E. P., Angelopoulos, T. J., Gordon, P. M., Moyna, N. M., Pescatello, L. S., Visich, P. S., Zoeller, R. F., Seip, R. L. & Clarkson, P. M. 2005. Variability in muscle size and strength gain after unilateral resistance training. Medicine and Science in Sports and Exercise 37 (6), 964-972.

Hulmi, J. J., Ahtiainen, J. P., Kaasalainen, T., Pöllänen, E., Häkkinen, K., Alen, M., Selänne, H., Kovanen, V. & Mero, A. A. 2007. Postexercise myostatin and activin IIb mRNA levels: effects of strength training. Medicine and Science in Sports and Exercise 39 (2), 289-297.

Hulmi, J. J., Walker, S., Ahtiainen, J. P., Nyman, K., Kraemer, W. J. & Häkkinen, K. 2012. Molecular signaling in muscle is affected by the specificity of resistance exercise protocol. Scandinavian Journal of Medicine & Science in Sports 22 (2), 240-248.

Hulver, M. W., Berggren, J. R., Cortright, R. N., Dudek, R. W., Thompson, R. P., Pories, W. J., MacDonald, K. G., Cline, G. W., Shulman, G. I., Dohm, G. L. & Houmard, J. A. 2003. Skeletal muscle lipid metabolism with obesity. American Journal of Physiology.Endocrinology and Metabolism 284 (4), E741-7.

Hussain, S. O., Barbato, J. C., Koch, L. G., Metting, P. J. & Britton, S. L. 2001. Cardiac function in rats selectively bred for low- and high-capacity running. American Journal of Physiology - Regulatory, Integrative and Comparative Physiology 281 (6), R1787-91.

Ingjer, F. 1979. Effects of endurance training on muscle fibre ATP-ase activity, capillary supply and mitochondrial content in man. The Journal of Physiology 294, 419-432.

Jager, S., Handschin, C., St-Pierre, J. & Spiegelman, B. M. 2007. AMP-activated protein kinase (AMPK) action in skeletal muscle via direct phosphorylation of PGC-1alpha. Proceedings of the National Academy of Sciences of the United States of America 104 (29), 12017-12022.

Jensen, L., Schjerling, P. & Hellsten, Y. 2004. Regulation of VEGF and bFGF mRNA expression and other proliferative compounds in skeletal muscle cells. Angiogenesis 7 (3), 255-267.

Jeong, H., Tombor, B., Albert, R., Oltvai, Z. N. & Barabasi, A. L. 2000. The large-scale organization of metabolic networks. Nature 407 (6804), 651-654.

Johnsen, A. B., Rolim, N. P., Stolen, T., Alves, M., Sousa, M. M., Slupphaug, G., Britton, S. L., Koch, L. G., Smith, G. L., Wisloff, U. & Hoydal, M. A. 2013. Atrial myocyte function and Ca2+ handling is associated with inborn aerobic capacity. PloS ONE 8 (10), e76568.

Kahn, B. B., Alquier, T., Carling, D. & Hardie, D. G. 2005. AMP-activated protein kinase: ancient energy gauge provides clues to modern understanding of metabolism. Cell Metabolism 1 (1), 15-25.

Kainulainen, H., Hulmi, J. J. & Kujala, U. M. 2013. Potential role of branched-chain amino acid catabolism in regulating fat oxidation. Exercise and Sport Sciences Reviews 41 (4), 194-200.

Kalliokoski, K. K., Oikonen, V., Takala, T. O., Sipilä, H., Knuuti, J. & Nuutila, P. 2001. Enhanced oxygen extraction and reduced flow heterogeneity in exercising muscle in endurance-trained men. American Journal of Physiology - Endocrinology and Metabolism 280 (6), E1015-21.

Kampert, J. B., Blair, S. N., Barlow, C. E. & Kohl, H. W.,3rd 1996. Physical activity, physical fitness, and all-cause and cancer mortality: a prospective study of men and women. Annals of Epidemiology 6 (5), 452-457.

Kao, S. D., Shaw, F. Z., Young, M. S. & Jan, G. J. 1995. A new automated method for detection and recording of animal moving path. Journal of Neuroscience Methods 63 (1-2), 205-209.

Keeler, L. K., Finkelstein, L. H., Miller, W. & Fernhall, B. 2001. Early-phase adaptations of traditional-speed vs. superslow resistance training on strength and aerobic capacity in sedentary individuals. Journal of Strength and Conditioning Research 15 (3), 309-314.

Kelley, D. E., Goodpaster, B., Wing, R. R. & Simoneau, J. A. 1999. Skeletal muscle fatty acid metabolism in association with insulin resistance, obesity, and weight loss. The American Journal of Physiology 277 (6 Pt 1), E1130-41.

Kelly, D. P. & Scarpulla, R. C. 2004. Transcriptional regulatory circuits controlling mitochondrial biogenesis and function. Genes & Development 18 (4), 357-368.

Kim, J. S., Petrella, J. K., Cross, J. M. & Bamman, M. M. 2007. Load-mediated downregulation of myostatin mRNA is not sufficient to promote myofiber hypertrophy in humans: a cluster analysis. Journal of Applied Physiology 103 (5), 1488-1495.

Kim, J. Y., Hickner, R. C., Cortright, R. L., Dohm, G. L. & Houmard, J. A. 2000. Lipid oxidation is reduced in obese human skeletal muscle. American Journal of Physiology - Endocrinology and Metabolism 279 (5), E1039-44.

Klausen, K., Andersen, L. B. & Pelle, I. 1981. Adaptive changes in work capacity, skeletal muscle capillarization and enzyme levels during training and detraining. Acta Physiologica Scandinavica 113 (1), 9-16.

Klossner, S., Durieux, A. C., Freyssenet, D. & Flueck, M. 2009. Mechano-transduction to muscle protein synthesis is modulated by FAK. European Journal of Applied Physiology 106 (3), 389-398.

Koch, L. G. & Britton, S. L. 2001. Artificial selection for intrinsic aerobic endurance running capacity in rats. Physiological Genomics 5 (1), 45-52.

Koch, L. G., Britton, S. L. & Wisloff, U. 2012. A rat model system to study complex disease risks, fitness, aging, and longevity. Trends in Cardiovascular Medicine 22 (2), 29-34.

Koch, L. G., Kemi, O. J., Qi, N., Leng, S. X., Bijma, P., Gilligan, L. J., Wilkinson, J. E., Wisloff, H., Hoydal, M. A., Rolim, N., Abadir, P. M., van Grevenhof, E. M., Smith, G. L., Burant, C. F., Ellingsen, O., Britton, S. L. & Wisloff, U. 2011. Intrinsic aerobic capacity sets a divide for aging and longevity. Circulation Research 109 (10), 1162-1172.

Koch, S. & Claesson-Welsh, L. 2012. Signal transduction by vascular endothelial growth factor receptors. Cold Spring Harbor Perspectives in Medicine 2 (7), a006502.

Kodama, S., Saito, K., Tanaka, S., Maki, M., Yachi, Y., Asumi, M., Sugawara, A., Totsuka, K., Shimano, H., Ohashi, Y., Yamada, N. & Sone, H. 2009. Cardiorespiratory fitness as a quantitative predictor of all-cause mortality and cardiovascular events in healthy men and women: a meta-analysis. Journal of American Medical Association 301 (19), 2024-2035.

Kokkinos, P., Myers, J., Kokkinos, J. P., Pittaras, A., Narayan, P., Manolis, A., Karasik, P., Greenberg, M., Papademetriou, V. & Singh, S. 2008. Exercise

capacity and mortality in black and white men. Circulation 117 (5), 614-622.

Koressaar, T. & Remm, M. 2007. Enhancements and modifications of primer design program Primer3. Bioinformatics 23 (10), 1289-1291.

Kosek, D. J., Kim, J. S., Petrella, J. K., Cross, J. M. & Bamman, M. M. 2006. Efficacy of 3 days/wk resistance training on myofiber hypertrophy and myogenic mechanisms in young vs. older adults. Journal of Applied Physiology 101 (2), 531-544.

Koves, T. R., Li, P., An, J., Akimoto, T., Slentz, D., Ilkayeva, O., Dohm, G. L., Yan, Z., Newgard, C. B. & Muoio, D. M. 2005. Peroxisome proliferator-activated receptor-gamma co-activator 1alpha-mediated metabolic remodeling of skeletal myocytes mimics exercise training and reverses lipid-induced mitochondrial inefficiency. The Journal of Biological Chemistry 280 (39), 33588-33598.

Lagouge, M., Argmann, C., Gerhart-Hines, Z., Meziane, H., Lerin, C., Daussin, F., Messadeq, N., Milne, J., Lambert, P., Elliott, P., Geny, B., Laakso, M., Puigserver, P. & Auwerx, J. 2006. Resveratrol improves mitochondrial function and protects against metabolic disease by activating SIRT1 and PGC-1alpha. Cell 127 (6), 1109-1122.

Larsson, L., Biral, D., Campione, M. & Schiaffino, S. 1993. An age-related type IIB to IIX myosin heavy chain switching in rat skeletal muscle. Acta Physiologica Scandinavica 147 (2), 227-234.

Larsson, L., Muller, U., Li, X. & Schiaffino, S. 1995. Thyroid hormone regulation of myosin heavy chain isoform composition in young and old rats, with special reference to IIX myosin. Acta Physiologica Scandinavica 153 (2), 109-116.

Lerin, C., Rodgers, J. T., Kalume, D. E., Kim, S. H., Pandey, A. & Puigserver, P. 2006. GCN5 acetyltransferase complex controls glucose metabolism through transcriptional repression of PGC-1alpha. Cell Metabolism 3 (6), 429-438.

Lessard, S. J., Rivas, D. A., Chen, Z. P., van Denderen, B. J., Watt, M. J., Koch, L. G., Britton, S. L., Kemp, B. E. & Hawley, J. A. 2009. Impaired skeletal muscle beta-adrenergic activation and lipolysis are associated with whole-body insulin resistance in rats bred for low intrinsic exercise capacity. Endocrinology 150 (11), 4883-4891.

Levine, J. A., Eberhardt, N. L. & Jensen, M. D. 1999. Role of nonexercise activity thermogenesis in resistance to fat gain in humans. Science 283 (5399), 212-214.

Levine, J. A., Lanningham-Foster, L. M., McCrady, S. K., Krizan, A. C., Olson, L. R., Kane, P. H., Jensen, M. D. & Clark, M. M. 2005. Interindividual variation in posture allocation: possible role in human obesity. Science 307 (5709), 584-586.

Lexell, J., Taylor, C. C. & Sjöström, M. 1988. What is the cause of the ageing atrophy? Total number, size and proportion of different fiber types studied

in whole vastus lateralis muscle from 15- to 83-year-old men. Journal of the Neurological Sciences 84 (2-3), 275-294.

Li, Y., Hazarika, S., Xie, D., Pippen, A. M., Kontos, C. D. & Annex, B. H. 2007. In mice with type 2 diabetes, a vascular endothelial growth factor (VEGF)-activating transcription factor modulates VEGF signaling and induces therapeutic angiogenesis after hindlimb ischemia. Diabetes 56 (3), 656-665.

Lin, J., Handschin, C. & Spiegelman, B. M. 2005. Metabolic control through the PGC-1 family of transcription coactivators. Cell Metabolism 1 (6), 361-370.

Lin, J., Wu, H., Tarr, P. T., Zhang, C. Y., Wu, Z., Boss, O., Michael, L. F., Puigserver, P., Isotani, E., Olson, E. N., Lowell, B. B., Bassel-Duby, R. & Spiegelman, B. M. 2002. Transcriptional co-activator PGC-1 alpha drives the formation of slow-twitch muscle fibres. Nature 418 (6899), 797-801.

Liu, Y., Randall, W. R. & Schneider, M. F. 2005. Activity-dependent and -independent nuclear fluxes of HDAC4 mediated by different kinases in adult skeletal muscle. The Journal of Cell Biology 168 (6), 887-897.

Lundberg, T. R., Fernandez-Gonzalo, R., Norrbom, J., Fischer, H., Tesch, P. A. & Gustafsson, T. 2014. Truncated splice variant PGC-1alpha4 is not associated with exercise-induced human muscle hypertrophy. Acta Physiologica 212 (2), 142-151.

Lundby, C. & Montero, D. 2015. CrossTalk opposing view: Diffusion limitation of O2 from microvessels into muscle does not contribute to the limitation of VO2 max. The Journal of Physiology 593 (17), 3759-3761.

Lundby, C., Nordsborg, N., Kusuhara, K., Kristensen, K. M., Neufer, P. D. & Pilegaard, H. 2005. Gene expression in human skeletal muscle: alternative normalization method and effect of repeated biopsies. European Journal of Applied Physiology 95 (4), 351-360.

Luthi, J. M., Howald, H., Claassen, H., Rosler, K., Vock, P. & Hoppeler, H. 1986. Structural changes in skeletal muscle tissue with heavy-resistance exercise. International Journal of Sports Medicine 7 (3), 123-127.

MacDougall, J. D., Sale, D. G., Moroz, J. R., Elder, G. C., Sutton, J. R. & Howald, H. 1979. Mitochondrial volume density in human skeletal muscle following heavy resistance training. Medicine and Science in Sports 11 (2), 164-166.

Malek, M. H. & Olfert, I. M. 2009. Global deletion of thrombospondin-1 increases cardiac and skeletal muscle capillarity and exercise capacity in mice. Experimental Physiology 94 (6), 749-760.

Manco, M., Calvani, M. & Mingrone, G. 2004. Effects of dietary fatty acids on insulin sensitivity and secretion. Diabetes, Obesity & Metabolism 6 (6), 402-413.

Matthews, D. R., Hosker, J. P., Rudenski, A. S., Naylor, B. A., Treacher, D. F. & Turner, R. C. 1985. Homeostasis model assessment: insulin resistance and beta-cell function from fasting plasma glucose and insulin concentrations in man. Diabetologia 28 (7), 412-419.

Maxwell, P. H., Wiesener, M. S., Chang, G. W., Clifford, S. C., Vaux, E. C., Cockman, M. E., Wykoff, C. C., Pugh, C. W., Maher, E. R. & Ratcliffe, P. J.

1999. The tumour suppressor protein VHL targets hypoxia-inducible factors for oxygen-dependent proteolysis. Nature 399 (6733), 271-275.

McArdle, W. D., Katch, F. I. & Katch, V. L. 2014. Exercise Physiology: Nutrition, Energy, and Human Performance. (Eighth edition edition) Netherlands: Wolters Kluwer.

McCall, G. E., Byrnes, W. C., Dickinson, A., Pattany, P. M. & Fleck, S. J. 1996. Muscle fiber hypertrophy, hyperplasia, and capillary density in college men after resistance training. Journal of Applied Physiology 81 (5), 2004-2012.

McGee, S. L., Fairlie, E., Garnham, A. P. & Hargreaves, M. 2009. Exercise-induced histone modifications in human skeletal muscle. The Journal of Physiology 587 (Pt 24), 5951-5958.

Meirhaeghe, A., Crowley, V., Lenaghan, C., Lelliott, C., Green, K., Stewart, A., Hart, K., Schinner, S., Sethi, J. K., Yeo, G., Brand, M. D., Cortright, R. N., O'Rahilly, S., Montague, C. & Vidal-Puig, A. J. 2003. Characterization of the human, mouse and rat PGC1 beta (peroxisome-proliferator-activated receptor-gamma co-activator 1 beta) gene in vitro and in vivo. The Biochemical Journal 373 (Pt 1), 155-165.

Merrill, G. F., Kurth, E. J., Hardie, D. G. & Winder, W. W. 1997. AICA riboside increases AMP-activated protein kinase, fatty acid oxidation, and glucose uptake in rat muscle. The American Journal of Physiology 273 (6 Pt 1), E1107-12.

Milkiewicz, M., Doyle, J. L., Fudalewski, T., Ispanovic, E., Aghasi, M. & Haas, T. L. 2007. HIF-1alpha and HIF-2alpha play a central role in stretch-induced but not shear-stress-induced angiogenesis in rat skeletal muscle. The Journal of Physiology 583 (Pt 2), 753-766.

Milkiewicz, M. & Haas, T. L. 2005. Effect of mechanical stretch on HIF-1{alpha} and MMP-2 expression in capillaries isolated from overloaded skeletal muscles: laser capture microdissection study. American Journal of Physiology - Heart and Circulatory Physiology 289 (3), H1315-20.

Milkiewicz, M., Uchida, C., Gee, E., Fudalewski, T. & Haas, T. L. 2008. Shear stress-induced Ets-1 modulates protease inhibitor expression in microvascular endothelial cells. Journal of Cellular Physiology 217 (2), 502-510.

Miller, W. C., Bryce, G. R. & Conlee, R. K. 1984. Adaptations to a high-fat diet that increase exercise endurance in male rats. Journal of Applied Physiology: Respiratory, Environmental and Exercise Physiology 56 (1), 78-83.

Miura, S., Kai, Y., Kamei, Y. & Ezaki, O. 2008. Isoform-specific increases in murine skeletal muscle peroxisome proliferator-activated receptor-gamma coactivator-1alpha (PGC-1alpha) mRNA in response to beta2-adrenergic receptor activation and exercise. Endocrinology 149 (9), 4527-4533.

Morbidelli, L., Chang, C. H., Douglas, J. G., Granger, H. J., Ledda, F. & Ziche, M. 1996. Nitric oxide mediates mitogenic effect of VEGF on coronary venular endothelium. The American Journal of Physiology 270 (1 Pt 2), H411-5.

Myers, J., Prakash, M., Froelicher, V., Do, D., Partington, S. & Atwood, J. E. 2002. Exercise capacity and mortality among men referred for exercise testing. The New England Journal of Medicine 346 (11), 793-801.

Nemeth, P. M., Rosser, B. W., Choksi, R. M., Norris, B. J. & Baker, K. M. 1992. Metabolic response to a high-fat diet in neonatal and adult rat muscle. The American Journal of Physiology 262 (2 Pt 1), C282-6.

Norrbom, J., Sallstedt, E. K., Fischer, H., Sundberg, C. J., Rundqvist, H. & Gustafsson, T. 2011. Alternative splice variant PGC-1alpha-b is strongly induced by exercise in human skeletal muscle. American Journal of Physiology - Endocrinology and Metabolism 301 (6), E1092-8.

Novak, C. M., Escande, C., Burghardt, P. R., Zhang, M., Barbosa, M. T., Chini, E. N., Britton, S. L., Koch, L. G., Akil, H. & Levine, J. A. 2010. Spontaneous activity, economy of activity, and resistance to diet-induced obesity in rats bred for high intrinsic aerobic capacity. Hormones and Behavior 58 (3), 355-367.

Novak, C. M., Escande, C., Gerber, S. M., Chini, E. N., Zhang, M., Britton, S. L., Koch, L. G. & Levine, J. A. 2009. Endurance capacity, not body size, determines physical activity levels: role of skeletal muscle PEPCK. PloS ONE 4 (6), e5869.

O'Hagan, K. A., Cocchiglia, S., Zhdanov, A. V., Tambuwala, M. M., Cummins, E. P., Monfared, M., Agbor, T. A., Garvey, J. F., Papkovsky, D. B., Taylor, C. T. & Allan, B. B. 2009. PGC-1alpha is coupled to HIF-1alpha-dependent gene expression by increasing mitochondrial oxygen consumption in skeletal muscle cells. Proceedings of the National Academy of Sciences of the United States of America 106 (7), 2188-2193.

Olesen, J., Kiilerich, K. & Pilegaard, H. 2010. PGC-1alpha-mediated adaptations in skeletal muscle. Pflugers Archiv: European Journal of Physiology 460 (1), 153-162.

Olfert, I. M., Breen, E. C., Gavin, T. P. & Wagner, P. D. 2006. Temporal thrombospondin-1 mRNA response in skeletal muscle exposed to acute and chronic exercise. Growth Factors 24 (4), 253-259.

Olfert, I. M., Howlett, R. A., Tang, K., Dalton, N. D., Gu, Y., Peterson, K. L., Wagner, P. D. & Breen, E. C. 2009. Muscle-specific VEGF deficiency greatly reduces exercise endurance in mice. The Journal of Physiology 587 (Pt 8), 1755-1767.

O'Neil, T. K., Duffy, L. R., Frey, J. W. & Hornberger, T. A. 2009. The role of phosphoinositide 3-kinase and phosphatidic acid in the regulation of mammalian target of rapamycin following eccentric contractions. The Journal of Physiology 587 (Pt 14), 3691-3701.

O'Reilly, M. S., Boehm, T., Shing, Y., Fukai, N., Vasios, G., Lane, W. S., Flynn, E., Birkhead, J. R., Olsen, B. R. & Folkman, J. 1997. Endostatin: an endogenous inhibitor of angiogenesis and tumor growth. Cell 88 (2), 277-285.

Packard, G. C. & Boardman, T. J. 1999. The use of percentages and size specific indices to normalize physiological data for variation in body size: Wasted

time, wasted effort? Comparative Biochemistry and Physiology 122 (1), 37-37-44.

Pan, W. H., Lee, C. R. & Lim, L. H. 1996. A new video path analyzer to monitor travel distance, rearing, and stereotypic movement of rats. Journal of Neuroscience Methods 70 (1), 39-43.

Perry, C. G., Lally, J., Holloway, G. P., Heigenhauser, G. J., Bonen, A. & Spriet, L. L. 2010. Repeated transient mRNA bursts precede increases in transcriptional and mitochondrial proteins during training in human skeletal muscle. The Journal of Physiology 588 (Pt 23), 4795-4810.

Petersen, A. C., McKenna, M. J., Medved, I., Murphy, K. T., Brown, M. J., Della Gatta, P. & Cameron-Smith, D. 2012. Infusion with the antioxidant N-acetylcysteine attenuates early adaptive responses to exercise in human skeletal muscle. Acta Physiologica 204 (3), 382-392.

Petersen, K. F., Dufour, S., Befroy, D., Garcia, R. & Shulman, G. I. 2004. Impaired mitochondrial activity in the insulin-resistant offspring of patients with type 2 diabetes. The New England Journal of Medicine 350 (7), 664-671.

Phillips, S. M. 2014. A brief review of critical processes in exercise-induced muscular hypertrophy. Sports Medicine 44 Suppl 1, S71-7.

Philp, A., Hamilton, D. L. & Baar, K. 2011. Signals mediating skeletal muscle remodeling by resistance exercise: PI3-kinase independent activation of mTORC1. Journal of Applied Physiology 110 (2), 561-568.

Pilegaard, H., Saltin, B. & Neufer, P. D. 2003. Exercise induces transient transcriptional activation of the PGC-1alpha gene in human skeletal muscle. The Journal of Physiology 546 (Pt 3), 851-858.

Ponticos, M., Lu, Q. L., Morgan, J. E., Hardie, D. G., Partridge, T. A. & Carling, D. 1998. Dual regulation of the AMP-activated protein kinase provides a novel mechanism for the control of creatine kinase in skeletal muscle. The EMBO Journal 17 (6), 1688-1699.

Popov, D. V., Bachinin, A. V., Lysenko, E. A., Miller, T. F. & Vinogradova, O. L. 2014. Exercise-induced expression of peroxisome proliferator-activated receptor gamma coactivator-1alpha isoforms in skeletal muscle of endurance-trained males. The Journal of Physiological Sciences 64 (5), 317-323.

Popov, D. V., Lysenko, E. A., Vepkhvadze, T. F., Kurochkina, N. S., Maknovskii, P. A. & Vinogradova, O. L. 2015. Promoter-specific regulation of PPARGC1A gene expression in human skeletal muscle. Journal of Molecular Endocrinology 55 (2), 159-168.

Porter, C., Reidy, P. T., Bhattarai, N., Sidossis, L. S. & Rasmussen, B. B. 2015. Resistance Exercise Training Alters Mitochondrial Function in Human Skeletal Muscle. Medicine and Science in Sports and Exercise 47 (9), 1922-31.

Powers, S. K., Duarte, J., Kavazis, A. N. & Talbert, E. E. 2010. Reactive oxygen species are signalling molecules for skeletal muscle adaptation. Experimental Physiology 95 (1), 1-9.

Powers, S. K., Lawler, J., Dempsey, J. A., Dodd, S. & Landry, G. 1989. Effects of incomplete pulmonary gas exchange on VO2 max. Journal of Applied Physiology 66 (6), 2491-2495.

Puigserver, P., Rhee, J., Lin, J., Wu, Z., Yoon, J. C., Zhang, C. Y., Krauss, S., Mootha, V. K., Lowell, B. B. & Spiegelman, B. M. 2001. Cytokine stimulation of energy expenditure through p38 MAP kinase activation of PPARgamma coactivator-1. Molecular Cell 8 (5), 971-982.

Puigserver, P., Wu, Z., Park, C. W., Graves, R., Wright, M. & Spiegelman, B. M. 1998. A cold-inducible coactivator of nuclear receptors linked to adaptive thermogenesis. Cell 92 (6), 829-839.

Raney, M. A. & Turcotte, L. P. 2008. Evidence for the involvement of CaMKII and AMPK in Ca2+-dependent signaling pathways regulating FA uptake and oxidation in contracting rodent muscle. Journal of Applied Physiology 104 (5), 1366-1373.

Rantalainen, T., Silvennoinen, M., Kainulainen, H. & Sievänen, H. 2011. Vertical ground reaction force measurements and video measurements provide comparable estimates of distance moved by mice during artificial light and dark periods. Journal of Neuroscience Methods 197 (1), 104-108.

Rivas, D. A., Lessard, S. J., Saito, M., Friedhuber, A. M., Koch, L. G., Britton, S. L., Yaspelkis, B. B.,3rd & Hawley, J. A. 2011. Low intrinsic running capacity is associated with reduced skeletal muscle substrate oxidation and lower mitochondrial content in white skeletal muscle. American Journal of Physiology - Regulatory, Integrative and Comparative Physiology 300 (4), R835-43.

Rodgers, J. T., Lerin, C., Gerhart-Hines, Z. & Puigserver, P. 2008. Metabolic adaptations through the PGC-1 alpha and SIRT1 pathways. FEBS Letters 582 (1), 46-53.

Romijn, J. A., Coyle, E. F., Sidossis, L. S., Gastaldelli, A., Horowitz, J. F., Endert, E. & Wolfe, R. R. 1993. Regulation of endogenous fat and carbohydrate metabolism in relation to exercise intensity and duration. The American Journal of Physiology 265 (3 Pt 1), E380-91.

Rooney, K. J., Herbert, R. D. & Balnave, R. J. 1994. Fatigue contributes to the strength training stimulus. Medicine and Science in Sports and Exercise 26 (9), 1160-1164.

Rooyackers, J. M., Dekhuijzen, P. N., Van Herwaarden, C. L. & Folgering, H. T. 1997. Training with supplemental oxygen in patients with COPD and hypoxaemia at peak exercise. The European Respiratory Journal 10 (6), 1278-1284.

Rose, A. J., Kiens, B. & Richter, E. A. 2006. Ca2+-calmodulin-dependent protein kinase expression and signalling in skeletal muscle during exercise. The Journal of Physiology 574 (Pt 3), 889-903.

Roudier, E., Chapados, N., Decary, S., Gineste, C., Le Bel, C., Lavoie, J. M., Bergeron, R. & Birot, O. 2009. Angiomotin p80/p130 ratio: a new indicator of exercise-induced angiogenic activity in skeletal muscles from obese and non-obese rats? The Journal of Physiology 587 (Pt 16), 4105-4119.

Ruas, J. L., White, J. P., Rao, R. R., Kleiner, S., Brannan, K. T., Harrison, B. C., Greene, N. P., Wu, J., Estall, J. L., Irving, B. A., Lanza, I. R., Rasbach, K. A., Okutsu, M., Nair, K. S., Yan, Z., Leinwand, L. A. & Spiegelman, B. M. 2012. A PGC-1alpha isoform induced by resistance training regulates skeletal muscle hypertrophy. Cell 151 (6), 1319-1331.

Saltin, B. 1985. Hemodynamic adaptations to exercise. The American Journal of Cardiology 55 (10), 42D-47D.

Saltin, B., Henriksson, J., Nygaard, E., Andersen, P. & Jansson, E. 1977. Fiber types and metabolic potentials of skeletal muscles in sedentary man and endurance runners. Annals of the New York Academy of Sciences 301, 3-29.

Savage, D. B., Petersen, K. F. & Shulman, G. I. 2007. Disordered lipid metabolism and the pathogenesis of insulin resistance. Physiological Reviews 87 (2), 507-520.

Schiaffino, S. & Reggiani, C. 2011. Fiber types in mammalian skeletal muscles. Physiological Reviews 91 (4), 1447-1531.

Schiaffino, S. & Reggiani, C. 1996. Molecular diversity of myofibrillar proteins: gene regulation and functional significance. Physiological Reviews 76 (2), 371-423.

Schoenfeld, B. J. 2010. The mechanisms of muscle hypertrophy and their application to resistance training. Journal of Strength and Conditioning Research 24 (10), 2857-2872.

Schott, J., McCully, K. & Rutherford, O. M. 1995. The role of metabolites in strength training. II. Short versus long isometric contractions. European Journal of Applied Physiology and Occupational Physiology 71 (4), 337-341.

Schwer, B. & Verdin, E. 2008. Conserved metabolic regulatory functions of sirtuins. Cell Metabolism 7 (2), 104-112.

Semenza, G. L. 2001. HIF-1, O(2), and the 3 PHDs: how animal cells signal hypoxia to the nucleus. Cell 107 (1), 1-3.

Shen, T., Liu, Y. & Schneider, M. F. 2012. Localization and regulation of the N terminal splice variant of PGC-1alpha in adult skeletal muscle fibers. Journal of Biomedicine & Biotechnology 2012, 989263.

Short, K. R., Bigelow, M. L., Kahl, J., Singh, R., Coenen-Schimke, J., Raghavakaimal, S. & Nair, K. S. 2005. Decline in skeletal muscle mitochondrial function with aging in humans. Proceedings of the National Academy of Sciences of the United States of America 102 (15), 5618-5623.

Sillanpää, E., Häkkinen, A., Nyman, K., Mattila, M., Cheng, S., Karavirta, L., Laaksonen, D. E., Huuhka, N., Kraemer, W. J. & Häkkinen, K. 2008. Body composition and fitness during strength and/or endurance training in older men. Medicine and Science in Sports and Exercise 40 (5), 950-958.

Sillanpää, E., Laaksonen, D. E., Häkkinen, A., Karavirta, L., Jensen, B., Kraemer, W. J., Nyman, K. & Häkkinen, K. 2009. Body composition, fitness, and metabolic health during strength and endurance training and their combi-

nation in middle-aged and older women. European Journal of Applied Physiology 106 (2), 285-296.

Simi, B., Sempore, B., Mayet, M. H. & Favier, R. J. 1991. Additive effects of training and high-fat diet on energy metabolism during exercise. Journal of Applied Physiology 71 (1), 197-203.

Simoneau, J. A. & Bouchard, C. 1995. Genetic determinism of fiber type proportion in human skeletal muscle. FASEB Journal 9 (11), 1091-1095.

Simoneau, J. A. & Bouchard, C. 1989. Human variation in skeletal muscle fiber-type proportion and enzyme activities. The American Journal of Physiology 257 (4 Pt 1), E567-72.

Simoneau, J. A. & Kelley, D. E. 1997. Altered glycolytic and oxidative capacities of skeletal muscle contribute to insulin resistance in NIDDM. Journal of Applied Physiology 83 (1), 166-171.

Slopack, D., Roudier, E., Liu, S. T., Nwadozi, E., Birot, O. & Haas, T. L. 2014. Forkhead BoxO transcription factors restrain exercise-induced angiogenesis. The Journal of Physiology 592 (Pt 18), 4069-4082.

Smith, R. C. & Rutherford, O. M. 1995. The role of metabolites in strength training. I. A comparison of eccentric and concentric contractions. European Journal of Applied Physiology and Occupational Physiology 71 (4), 332-336.

Sparks, L. M., Xie, H., Koza, R. A., Mynatt, R., Hulver, M. W., Bray, G. A. & Smith, S. R. 2005. A high-fat diet coordinately downregulates genes required for mitochondrial oxidative phosphorylation in skeletal muscle. Diabetes 54 (7), 1926-1933.

Staron, R. S., Hagerman, F. C., Hikida, R. S., Murray, T. F., Hostler, D. P., Crill, M. T., Ragg, K. E. & Toma, K. 2000. Fiber type composition of the vastus lateralis muscle of young men and women. The Journal of Histochemistry and Cytochemistry 48 (5), 623-629.

Subramanian, A., Tamayo, P., Mootha, V. K., Mukherjee, S., Ebert, B. L., Gillette, M. A., Paulovich, A., Pomeroy, S. L., Golub, T. R., Lander, E. S. & Mesirov, J. P. 2005. Gene set enrichment analysis: a knowledge-based approach for interpreting genome-wide expression profiles. Proceedings of the National Academy of Sciences of the United States of America 102 (43), 15545-15550.

Suga, T., Okita, K., Morita, N., Yokota, T., Hirabayashi, K., Horiuchi, M., Takada, S., Takahashi, T., Omokawa, M., Kinugawa, S. & Tsutsui, H. 2009. Intramuscular metabolism during low-intensity resistance exercise with blood flow restriction. Journal of Applied Physiology 106 (4), 1119-1124.

Tang, K., Breen, E. C., Gerber, H. P., Ferrara, N. M. & Wagner, P. D. 2004. Capillary regression in vascular endothelial growth factor-deficient skeletal muscle. Physiological Genomics 18 (1), 63-69.

Teicher, M. H., Andersen, S. L., Wallace, P., Klein, D. A. & Hostetter, J. 1996. Development of an affordable hi-resolution activity monitor system for laboratory animals. Pharmacology, Biochemistry, and Behavior 54 (2), 479-483.

Terada, N., Patel, H. R., Takase, K., Kohno, K., Nairn, A. C. & Gelfand, E. W. 1994. Rapamycin selectively inhibits translation of mRNAs encoding elongation factors and ribosomal proteins. Proceedings of the National Academy of Sciences of the United States of America 91 (24), 11477-11481.

Tesch, P. A., Colliander, E. B. & Kaiser, P. 1986. Muscle metabolism during intense, heavy-resistance exercise. European Journal of Applied Physiology and Occupational Physiology 55 (4), 362-366.

Tesch, P. A., Komi, P. V. & Häkkinen, K. 1987. Enzymatic adaptations consequent to long-term strength training. International Journal of Sports Medicine 8 Suppl 1, 66-69.

Tesch, P. A., Thorsson, A. & Colliander, E. B. 1990. Effects of eccentric and concentric resistance training on skeletal muscle substrates, enzyme activities and capillary supply. Acta Physiologica Scandinavica 140 (4), 575-580.

Teyssier, C., Ma, H., Emter, R., Kralli, A. & Stallcup, M. R. 2005. Activation of nuclear receptor coactivator PGC-1alpha by arginine methylation. Genes & Development 19 (12), 1466-1473.

Thom, R., Rowe, G. C., Jang, C., Safdar, A. & Arany, Z. 2014. Hypoxic induction of vascular endothelial growth factor (VEGF) and angiogenesis in muscle by truncated peroxisome proliferator-activated receptor gamma coactivator (PGC)-1alpha. The Journal of Biological Chemistry 289 (13), 8810-8817.

Thomas, D. M., Bouchard, C., Church, T., Slentz, C., Kraus, W. E., Redman, L. M., Martin, C. K., Silva, A. M., Vossen, M., Westerterp, K. & Heymsfield, S. B. 2012. Why do individuals not lose more weight from an exercise intervention at a defined dose? An energy balance analysis. Obesity Reviews 13 (10), 835-847.

Thyfault, J. P., Rector, R. S., Uptergrove, G. M., Borengasser, S. J., Morris, E. M., Wei, Y., Laye, M. J., Burant, C. F., Qi, N. R., Ridenhour, S. E., Koch, L. G., Britton, S. L. & Ibdah, J. A. 2009. Rats selectively bred for low aerobic capacity have reduced hepatic mitochondrial oxidative capacity and susceptibility to hepatic steatosis and injury. The Journal of Physiology 587 (Pt 8), 1805-1816.

Toigo, M. & Boutellier, U. 2006. New fundamental resistance exercise determinants of molecular and cellular muscle adaptations. European Journal of Applied Physiology 97 (6), 643-663.

Toledo, F. G., Menshikova, E. V., Ritov, V. B., Azuma, K., Radikova, Z., DeLany, J. & Kelley, D. E. 2007. Effects of physical activity and weight loss on skeletal muscle mitochondria and relationship with glucose control in type 2 diabetes. Diabetes 56 (8), 2142-2147.

Turinsky, J., O'Sullivan, D. M. & Bayly, B. P. 1990. 1,2-Diacylglycerol and ceramide levels in insulin-resistant tissues of the rat in vivo. The Journal of Biological Chemistry 265 (28), 16880-16885.

Turner, N., Bruce, C. R., Beale, S. M., Hoehn, K. L., So, T., Rolph, M. S. & Cooney, G. J. 2007. Excess lipid availability increases mitochondrial fatty acid oxidative capacity in muscle: evidence against a role for reduced fatty

acid oxidation in lipid-induced insulin resistance in rodents. Diabetes 56 (8), 2085-2092.

Uchida, C. & Haas, T. L. 2014. Endothelial cell TIMP-1 is upregulated by shear stress via Sp-1 and the TGFbeta1 signaling pathways. Biochemistry and Cell Biology 92 (1), 77-83.

Uchida, C., Nwadozi, E., Hasanee, A., Olenich, S., Olfert, I. M. & Haas, T. L. 2015. Muscle-derived vascular endothelial growth factor regulates microvascular remodelling in response to increased shear stress in mice. Acta Physiologica 214 (3), 349-360.

Untergasser, A., Cutcutache, I., Koressaar, T., Ye, J., Faircloth, B. C., Remm, M. & Rozen, S. G. 2012. Primer3-new capabilities and interfaces. Nucleic Acids Research 40 (15), e115.

van Loon, L. J., Greenhaff, P. L., Constantin-Teodosiu, D., Saris, W. H. & Wagenmakers, A. J. 2001. The effects of increasing exercise intensity on muscle fuel utilisation in humans. The Journal of Physiology 536 (Pt 1), 295-304.

Vierck, J., O'Reilly, B., Hossner, K., Antonio, J., Byrne, K., Bucci, L. & Dodson, M. 2000. Satellite cell regulation following myotrauma caused by resistance exercise. Cell Biology International 24 (5), 263-272.

Wagner, P. D. 2015. CrossTalk proposal: Diffusion limitation of O2 from microvessels into muscle does contribute to the limitation of VO2 max. The Journal of Physiology 593 (17), 3757-3758.

Wagner, P. D. 1992. Gas exchange and peripheral diffusion limitation. Medicine and Science in Sports and Exercise 24 (1), 54-58.

Walberg, J. L., Ruiz, V. K., Tarlton, S. L., Hinkle, D. E. & Thye, F. W. 1988. Exercise capacity and nitrogen loss during a high or low carbohydrate diet. Medicine and Science in Sports and Exercise 20 (1), 34-43.

Wallberg, A. E., Yamamura, S., Malik, S., Spiegelman, B. M. & Roeder, R. G. 2003. Coordination of p300-mediated chromatin remodeling and TRAP/mediator function through coactivator PGC-1alpha. Molecular Cell 12 (5), 1137-1149.

Waters, R. E., Rotevatn, S., Li, P., Annex, B. H. & Yan, Z. 2004. Voluntary running induces fiber type-specific angiogenesis in mouse skeletal muscle. American Journal of Physiology. Cell Physiology 287 (5), C1342-8.

Wen, X., Wu, J., Chang, J. S., Zhang, P., Wang, J., Zhang, Y., Gettys, T. W. & Zhang, Y. 2014. Effect of exercise intensity on isoform-specific expressions of NT-PGC-1 alpha mRNA in mouse skeletal muscle. BioMed Research International 2014, 402175.

Whitham, M., Chan, M. H., Pal, M., Matthews, V. B., Prelovsek, O., Lunke, S., El-Osta, A., Broenneke, H., Alber, J., Bruning, J. C., Wunderlich, F. T., Lancaster, G. I. & Febbraio, M. A. 2012. Contraction-induced interleukin-6 gene transcription in skeletal muscle is regulated by c-Jun terminal kinase/activator protein-1. The Journal of Biological Chemistry 287 (14), 10771-10779.

Wilkinson, S. B., Phillips, S. M., Atherton, P. J., Patel, R., Yarasheski, K. E., Tarnopolsky, M. A. & Rennie, M. J. 2008. Differential effects of resistance and endurance exercise in the fed state on signalling molecule phosphorylation and protein synthesis in human muscle. The Journal of Physiology 586 (Pt 15), 3701-3717.

Wisloff, U., Najjar, S. M., Ellingsen, O., Haram, P. M., Swoap, S., Al-Share, Q., Fernstrom, M., Rezaei, K., Lee, S. J., Koch, L. G. & Britton, S. L. 2005. Cardiovascular risk factors emerge after artificial selection for low aerobic capacity. Science 307 (5708), 418-420.

Wright, D. C., Hucker, K. A., Holloszy, J. O. & Han, D. H. 2004. Ca2+ and AMPK both mediate stimulation of glucose transport by muscle contractions. Diabetes 53 (2), 330-335.

Wu, Z., Puigserver, P., Andersson, U., Zhang, C., Adelmant, G., Mootha, V., Troy, A., Cinti, S., Lowell, B., Scarpulla, R. C. & Spiegelman, B. M. 1999. Mechanisms controlling mitochondrial biogenesis and respiration through the thermogenic coactivator PGC-1. Cell 98 (1), 115-124.

Wycherley, T. P., Buckley, J. D., Noakes, M., Clifton, P. M. & Brinkworth, G. D. 2014. Long-term effects of a very low-carbohydrate weight loss diet on exercise capacity and tolerance in overweight and obese adults. Journal of the American College of Nutrition 33 (4), 267-273.

Yanagita, S., Amemiya, S., Suzuki, S. & Kita, I. 2007. Effects of spontaneous and forced running on activation of hypothalamic corticotropin-releasing hormone neurons in rats. Life Sciences 80 (4), 356-363.

Ydfors, M., Fischer, H., Mascher, H., Blomstrand, E., Norrbom, J. & Gustafsson, T. 2013. The truncated splice variants, NT-PGC-1alpha and PGC-1alpha4, increase with both endurance and resistance exercise in human skeletal muscle. Physiological Reports 1 (6), e00140.

Yeo, W. K., Carey, A. L., Burke, L., Spriet, L. L. & Hawley, J. A. 2011. Fat adaptation in well-trained athletes: effects on cell metabolism. Applied Physiology, Nutrition, and Metabolism 36 (1), 12-22.

Yu, C., Chen, Y., Cline, G. W., Zhang, D., Zong, H., Wang, Y., Bergeron, R., Kim, J. K., Cushman, S. W., Cooney, G. J., Atcheson, B., White, M. F., Kraegen, E. W. & Shulman, G. I. 2002. Mechanism by which fatty acids inhibit insulin activation of insulin receptor substrate-1 (IRS-1)-associated phosphatidylinositol 3-kinase activity in muscle. The Journal of Biological Chemistry 277 (52), 50230-50236.

Zajac, A., Poprzecki, S., Maszczyk, A., Czuba, M., Michalczyk, M. & Zydek, G. 2014. The effects of a ketogenic diet on exercise metabolism and physical performance in off-road cyclists. Nutrients 6 (7), 2493-2508.

Zhang, Y., Huypens, P., Adamson, A. W., Chang, J. S., Henagan, T. M., Boudreau, A., Lenard, N. R., Burk, D., Klein, J., Perwitz, N., Shin, J., Fasshauer, M., Kralli, A. & Gettys, T. W. 2009. Alternative mRNA splicing produces a novel biologically active short isoform of PGC-1alpha. The Journal of Biological Chemistry 284 (47), 32813-32826.

Ziada, A., Hudlicka, O. & Tyler, K. R. 1989. The effect of long-term administration of alpha 1-blocker prazosin on capillary density in cardiac and skeletal muscle. Pflugers Archiv : European Journal of Physiology 415 (3), 355-360.

ORIGINAL PAPERS

I

GENE EXPRESSION CENTROIDS THAT LINK WITH LOW INTRINSIC AEROBIC EXERCISE CAPACITY AND COMPLEX DISEASE RISK

by

Kivelä R, Silvennoinen M, Lehti M, Rinnankoski-Tuikka R, Purhonen T, Ketola T, Pullinen K, Vuento M, Mutanen N, Sartor MA, Reunanen H, Koch LG, Britton SL, Kainulainen H. 2010.

The FASEB Journal 24(11), 4565-74.

II

HIGH-FAT FEEDING INDUCES ANGIOGENESIS IN SKELETAL MUSCLE AND ACTIVATES ANGIOGENIC PATHWAYS IN CAPILLARIES

by

Silvennoinen M*, Rinnankoski-Tuikka R*, Vuento M, Hulmi JJ, Torvinen S, Lehti M, Kivelä R, Kainulainen H. 2013.

Angiogenesis 16(2), 297-307.

* These authors contributed equally to the article

III

VALIDATION OF A METHOD TO MEASURE TOTAL SPONTANEOUS PHYSICAL ACTIVITY OF SEDENTARY AND VOLUNTARY RUNNING MICE

by

Silvennoinen M, Rantalainen T, Kainulainen H. 2014

Journal of Neuroscience Methods 235, 51-58.

Journal of Neuroscience Methods 235 (2014) 51–58

Contents lists available at ScienceDirect

Journal of Neuroscience Methods

journal homepage: www.elsevier.com/locate/jneumeth

Computational Neuroscience

Validation of a method to measure total spontaneous physical activity of sedentary and voluntary running mice

M. Silvennoinen[a,*], T. Rantalainen[b,c], H. Kainulainen[a]

[a] Neuromuscular Research Center, Department of Biology of Physical Activity, University of Jyväskylä, Finland
[b] Department of Health Sciences, University of Jyväskylä, Finland
[c] Centre for Physical Activity and Nutrition Research, School of Exercise and Nutrition Sciences, Deakin University, Melbourne, Australia

HIGHLIGHTS

- Novel method for measuring spontaneous activity of mice was developed.
- The system is valid for measuring activity of mice with or without a running wheel.
- Running wheels triple the total spontaneous activity of mice.
- Running wheels increase both the intensity and time of activity.

ARTICLE INFO

Article history:
Received 26 February 2014
Received in revised form 19 June 2014
Accepted 20 June 2014
Available online 28 June 2014

Keywords:
Force plate
Activity index
Activity time
Intensity
Distance
Behavior

ABSTRACT

Background: Running wheels are commonly used to stimulate physical activity of mice. To control the effects of physical activity on study results, it is important to measure the total activity (all movements) of both sedentary and running wheel stimulated mice.
New method: Because there was a lack of a validated system, we built a force-plate based system specifically for this purpose. The validity of the system and its variables (activity index, activity time and distance) were tested in calibration measurements and in situ by measuring the activity of eight mice both with and without running wheels. Four mice served as sedentary controls. Activity index adds changes in vertical reaction forces induced by moving mice. The system records simultaneously all the activity, thus the wheel running is not distinguished from other activity.
Results: There were very strong associations between measured activity variables and their true values ($R^2 = 1$, $p < 0.01$). The mean differences to true values were: activity index −9.7% (95% limits of agreement (LOA), −28.7 to 9.4%), activity time +0.9% (LOA, −1.3 to 3.0%) and distance +0.7% (LOA, −4.7 to 6.1%). The running wheels increased activity index 211 ± 40% (mean ± SE), activity time 39 ± 3% and activity intensity 94 ± 16%. Activity index ($R^2 = 0.982$, $p < 0.01$), activity time ($R^2 = 0.618$, $p < 0.01$) and intensity ($R^2 = 0.920$, $p < 0.01$) were positively associated with running distance.
Comparison with existing methods: To our knowledge, this is the first method properly validated for this purpose.
Conclusions: The system is valid for the quantitation of total physical activity of mice housed in cages with or without running wheels.

1. Introduction

Mice are commonly used as experimental animals in many types of scientific experiments. Physical activity is nowadays considered as an important background factor that may have a significant effect on study results and their interpretation (Martin et al., 2010). Mice are naturally active animals. However, in ordinary laboratory conditions they have only few stimuli for physical activity. Because mice like wheel running (Meijer and Robbers, 2014), running wheels are often used to stimulate physical activity of experimental

Abbreviations: LOA, limits of agreement; CV_{rms}, the average root-mean-square coefficient of variation.

* Corresponding author at: University of Jyväskylä, P.O. Box 35, 40014 Jyväskylä, Finland. Tel.: +358 40 733 8864; fax: +358 14 260 2071.
E-mail addresses: mika.silvennoinen@sport.jyu.fi, mmjsilvennoinen@gmail.com (M. Silvennoinen).

http://dx.doi.org/10.1016/j.jneumeth.2014.06.027
0165-0270/

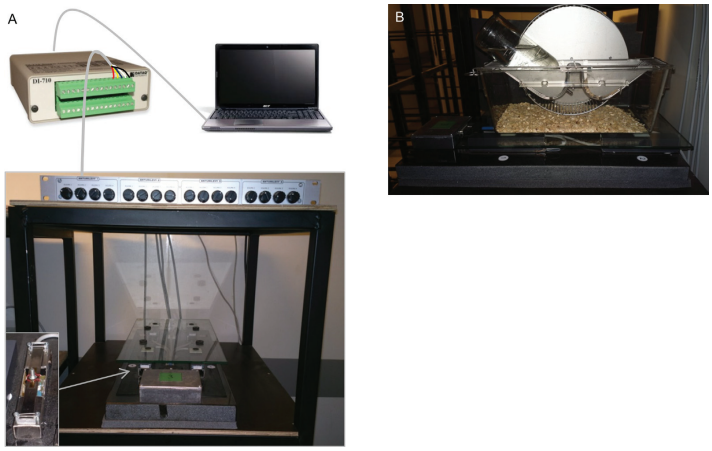

Fig. 1. (A) The main components of the activity measurement system: rack, cellular plastic sheet cushioning, granite base, strain gauge based sensors (enlarged picture in the lower left corner), sensor amplifier, glass plate with rubber ring adapters, controller unit, A/D converter and computer. (B) Side view of the plate with a cage.

mice. Depending on the strain, age and sex, mice run on average 2–10 km/day (Lightfoot et al., 2004) and up to 20.5 km/day when specifically bred for voluntary running (Eisenmann et al., 2009). There are also large inter-individual differences in running distances and the physiological responses to wheel running (Rinnankoski-Tuikka et al., 2012; Coletti et al., 2013; Ma et al., 2010). In typical voluntary running studies that include sedentary groups without running wheels e.g. (Silvennoinen et al., 2013), the running distances are presented as a measure of physical activity for running groups, but there are no comparable measures for physical activity of sedentary groups. Even if all the mice had running wheels, the running distances do not provide an accurate measure of total physical activity, because the wheel running is only one part of the daily activity and the measurement instrument (running wheel system) is reinforcing the measured behavior (de Visser et al., 2005). Thus, to be able to measure total physical activities, special activity measurement systems are needed. There is a variety of methods available to analyze physical activities and behavior, such as video tracking (Dielenberg et al., 2006; Pan et al., 1996; Rantalainen et al., 2011; Brodkin et al., 2014), infrared photo-beam systems (Teicher et al., 1996; Beninger et al., 1985), force-plate actometers (Biesiadecki et al., 1999; Chiesa et al., 2006; Fowler et al., 2001) and touch-pad transducers (Kao et al., 1995), but there is a lack of validated methods that are capable of measuring total physical activity (horizontal and vertical movements) from both cages with and without running wheels. Consequently, the aim of present study was to develop and validate such a system.

2. Materials and methods

2.1. Force-plate system

For the home cage activity analysis, a ground reaction force measurement system was developed in our laboratory. The plates were located on their own shelves (damping rubber sheets between the legs and ground) to avoid cross talk between the plates. To minimize the vibration from the surroundings, cellular plastic sheets (thickness15 mm) were placed between the shelf and the base of the force plate. Granite plate (thickness 35 mm, width 255 mm, length 580 mm, weight 14.3 kg) was used as a stabilizing base on top of which the four force sensors were attached in a rectangular formation (Fig. 1.). The core of the force sensor is the bridge formed by stainless steel sheet fixed from both of its ends. There are two strain gauges (1-LY41-6/700 (HBM, Darmstadt, Germany) attached on both the lower and upper surface of the sheet. The strain gauges are connected so that the classical Wheatstone bridge is formed. The output voltage from the sensor is directly related to the vertical force bending the strain gauges. The forces are mediated by a pin (diameter 4 mm) that is attached on the top of the steel bridge in the middle of two strain gauges. The pins of the four sensors form a rectangle (width 120 mm and length 280 mm) and a glass plate (thickness 5 mm, width 250 mm, length 450 mm) lies on top of them. Horizontal movement of the glass plate is prevented by rubber ring adapters that are attached underneath the glass plate. Similar rubber rings, on the other side of the glass, fix the cage in place on top of the glass. The force plates can measure ground reaction forces from all cage typesregardless of the equipment inside the cage. In the present study, the model of the cage was1284L Eurostandard Type II L (365 mm × 207 mm × 140 mm, Tecniplast, Italy). The output voltages from the sensors were preamplified (AD620, Analog Devices, Norwood, MA, USA) before data collection. The amplifications were adjusted to 0.077 kg/V in each sensor. After amplification, the signals pass through the controller unit that has the capability to zero all sensors. A 14 bit A/D converter (DI-710, DATAQ Instruments, Akron, Ohio, USA) was used for digitizing the data at a sampling rate of 80 Hz. The converter was operated and the data stored with WinDaq/Lite (DATAQ Instruments, Akron, Ohio, USA) data acquisition software. A measurement range of ±192.5 g was used, while the digitization precision was <0.02 g. The force data was turned into activity variables using Java-based analysis software that was programmed in house. The source code can be downloaded from following link: https://github.com/tjrantal/indeksi2011 and it is free to use.

2.2. Activity index

Activity index was originally developed by Biesiadecki et al. (1999) for using laboratory balance as an activity measurement

device. It was developed and tested for measuring the activity of rats. The activity index is simple to calculate and it is insensitive to evaporation-induced mass changes. We modified the analysis of activity index for our system that was developed for measuring mice. The most significant modifications are the body mass correction of the index value and the background subtraction. In detail, the measured force values were summed from four sensors. The sum signal was then smoothed by a 2nd order 10 Hz zerolag low pass Butterworth filter. The filtering cut-off was selected based on pilot experimentation. After filtering, the activity index was calculated as follows: The absolute values of the differences between consecutive force values were calculated. The mean of the absolute values were calculated from every second (from 80 values per second). To obtain a single value for total spontaneous activity, the 1-s means were summed for the total measurement time and the sum was divided by the body mass (kg) of the measured mice. The lowest activity index value for a 5 min interval was analyzed from the data (background activity) and then this value was scaled to the whole measurement time to produce an estimate of the contribution of inactivity to the index (including measurement noise, and forces caused by an inactive animal, e.g. breathing, heart beat). The contribution of background activity was then subtracted from the activity index to produce the index reported in the present paper.

2.3. Activity time

The activity time calculation was based on identifying and summing the active seconds from the activity index data. Each second when the activity index value was higher than 3 times the level of background activity was classified as an active second.

2.4. Intensity of the activity

The intensity of the activity was calculated by summing the final activity indexes from active seconds and dividing the sum by activity time.

2.5. Horizontal distance

Before the determination of instantaneous position and distance calculations, the raw data from all individual force sensors was smoothed by a 2nd order 0.75 Hz zerolag low pass Butterworth filter. The filtering cut-off was selected based on pilot experimentation. The coordinates of the instantaneous position of the animal (or water in validation measurement) were calculated as:

$$x = \frac{f2+f3}{f1+f2+f3+f4} \times \text{Distance between} f1 \text{ and } f2 \quad (1)$$

$$y = \frac{f3+f4}{f1+f2+f3+f4} \times \text{Distance between} f1 \text{ and } f4 \quad (2)$$

where $f1,\ldots,f4$ is the instantaneous force readings of a given strain gauge.

The horizontal distance was calculated as:

$$\text{Distance} = \sum_{i=1}^{n-1} \sqrt{(x_{i+1}-x_i)^2 + (y_{i+1}-y_i)^2} \times \frac{1}{dt}, \quad (3)$$

where n is the total number of coordinate pairs, x_i and y_i are the x- and y-coordinates in mm of the ith instantaneous position, and dt is the interval between consecutive samplings, i.e. 0.0125 s.

2.6. Horizontal distance correction and background subtraction

When long-lasting measurements (>10 h) are performed with mice, evaporation induces mass change that generates an error on the distance results. The error can be seen as a significant drift in minimum minute distances per hour. Assuming that the minimum distance covered in a minute in any given hour is inactivity, these values should be similar and stable. The distance data was corrected minute by minute using correction coefficients derived from formula describing second order regression line fitted into minimum distance values (minimum minutes per hour). The median of minimum minute distances, analyzed hour by hour from corrected data, was used as the background value and it was finally subtracted from data.

2.7. Validation measurements

The accuracy and repeatability of activity index and activity time analyses were measured by producing triangle wave shaped force changes onto the force plate with a solenoid (electromagnet). The solenoid was fixed to its own rigid support, which did not have any contact to the base of the force plate. The magnetic force (amplitude) was adjusted to 0.94 N by tuning the distance between the solenoid and the iron cylinder that was affected on the plate. The selected amplitude represented the average amplitude that was detected in force signals containing clear reaction forces of moving mouse. Thus, the amplitude of force change was selected to mimic reaction forces induced by a moving mouse. The frequency was regulated by a low frequency oscillator set to 4 Hz. Because the facts about frequencies of reaction forces induced by mice were not available, the frequency of 4 Hz was selected just based on the frequency content of the force signal (i.e. the 4 Hz frequency was clearly present in a 12 h measurement of mice without a running wheel) and the capabilities of the system and calibration device. Each validation measurement lasted 65 min. Four different durations of force changes were used in separate measurements: 3600, 900, 225 and 57 s (each repeated 3 times). Activity indexes and activity times were then analyzed and the results were compared to true values. The true activity times were known (described above). To obtain activity index true values, activity index analyses were performed to synthetic triangle wave signals with the same amplitude, frequency and duration than the induced force changes.

The validation of distance analysis was performed by using a custom made device that can move a certain amount of water from one measuring glass to another and back without external force affecting the force plate (Fig. 2.). The force changes that were induced during this calibration represented simple slow back and forth horizontal movement of mouse weighing 40 g. The calibration device consisted of measuring glasses that were fixed exactly 125 mm apart from each other and they were connected by a tube from the lowest part of the glasses. The outfall of one glass was open but the outfall of other glass was sealed with tubed lid. One tube was attached to an air compressor and the other tube was in the water bottle. Just before the measurement, water was added to the glass system so that both glasses contained 200 ml water. Then all sensors of the force plate were set to zero and 40 ml (simulating the weight of a mouse) of extra water was added to the system. Next, the air compressor was turned on and the tube in the water bottle was fixed to the depth where hydrostatic pressure equals the pressure needed to shift exactly 40 ml of water from the sealed glass to the other. When the air compressor was turned off, the water volumes returned to normal. During the described cycle, 40 g of water traveled a distance of 250 mm. In validation measurements, four different traveling distances were induced during a 65 min reaction force measurement: 1.5, 5.5, 11.25 and 44.5 m. The measurements were repeated three times with all four distances. Distances were analyzed from reaction force data and the results were compared to true traveling distances (described above).

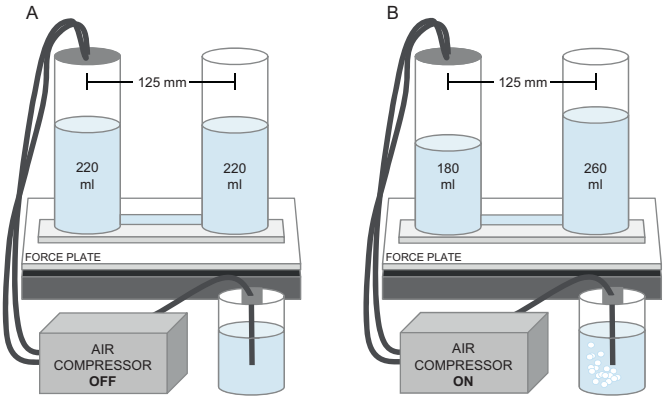

Fig. 2. Distance analysis was tested with a calibration device that transferred water from one measuring glass to another by using air pressure. (A) When the air compressor was off there was an equal amount of water in both glasses. (B) When the air compressor was set on, 40 ml of water moved from the left glass into the right glass. When the air compressor was turned off again, the water volumes returned to normal. In validation measurements, the water was transferred back and forth inducing four different traveling distances during 65 min reaction force measurement: 1.5, 5.5, 11.25 and 44.5 m, and all the measurements were repeated three times.

2.8. Mouse experiment

To test our system in situ, we conducted an experiment with twelve 6-months-old male C57BL/6 mice (Harlan Laboratories, Inc., The Netherlands). Before the experiment, the mice were housed in groups of four in standard conditions (temperature 22 °C, humidity 50 ± 10%, lights on from 8 AM to 8 PM) and received food pellets ((R36, 4% fat, 55.7% carbohydrate, 18.5% protein, 3 kcal/g; Labfor, Stockholm, Sweden) and tap water ad libitum.

To enhance the well-being of mice, the environment of cages were enriched with aspen nesting material (Tapvei, Kaavi, Finland). Two weeks before the start of activity measurements, the mice housed in same cage, were separated into individual cages (Makrolon 3) and they were also allocated to two groups: control group (C, $n = 4$) and running group (R, $n = 8$). At the first experiment week all the mice were housed in similar cages. During this week, basal activity measurement of each animal was performed. The measurement was conducted in the animal's own cage and in the same room with the other mice in this experiment. The measurement protocol was as follows: the cage without the mouse was positioned on top of the force plate, and the force levels of all force sensors were adjusted to zero. The mouse was inserted in the cage and the activity measurement of a 48 h period was collected. After the basal measurement, custom made vertical running wheels (stainless steel, diameter 24 cm, width 8 cm) were added into the cages of the running group (Fig. 1B). The running wheels were fixed to the lid of the cage and the lid did not have other supports than the cage. Therefore, all the reaction forces produced by the mouse whether the mouse is moving inside or outside the running wheel affect also the force plate beneath the cage. Because the system detects all vertical reaction forces, produced activity variables are measures of total activity and cannot directly separate the running activities from other activities.

The mice had continuous free access to running wheels. Total wheel revolutions were recorded daily with running wheel controlling system comprising magnetic reed sensors (MK04-1A71B-500 W, Standex-Meder Electronics, Cincinnati, OH, USA), data acquisition device (National instruments, Austin, TX, USA) and data acquisition software (developed in house). Total running distance per day was determined by multiplying the number of wheel rotations by the circumference of the wheel. For the next four weeks, the same activity measurement protocol was repeated once a week for all animals. After the final measurements, the running wheels were removed and, one week after that, post-exercise activity measurements were performed. The final result of activity index, activity time and intensity were calculated from mean of the first and second halves of the 48 h-measurement. The distance result was analyzed from the first 24 h. The mice were weighed with laboratory scale at the beginning of experiment and before and after every activity measurement (at intervals of one week). This study was approved by the National Animal Experiment Board, Finland (Permit number ESAVI-2010-07989/Ym-23).

2.9. Statistical analysis

The results are presented as mean ± SE if not stated otherwise. The Shapiro–Wilk test was used to investigate the within-group normality for a given parameter of interest. Levene's test was conducted to assess the homogeneity of the variance assumption. When the assumptions were met, ANOVA was used to determine the differences between the time points within groups and the paired t-test with Holm-Bonferroni correction was used for the post hoc comparisons. When the normality or equality of variance assumptions were not met, logarithm transformations were conducted. If these parameters still did not meet the assumptions, non-parametric Friedman's two way ANOVA by ranks test was used to determine differences between time points within groups. Wilcoxon signed-rank test was used for the post hoc analysis. Differences between the groups were determined using the Mann–Whitney U test. The similarity of the measured activity variables and the true values were assessed with Pearson correlation coefficient and Bland–Altman plots (Bland and Altman, 1986). LOA was calculated using the formula: mean ± 2 × standard deviation (Bland and Altman, 1986). As a measure of repeatability, the average root-mean-square coefficient of variation (CV_{rms}) was calculated from repeated measurements. The significance level was set at $p < 0.05$. All statistical analyses were carried out using IBM SPSS statistics 20software (IBM corporation, Armonk, NY, USA).

3. Results

3.1. Validation experiment

The association was very strong between measured activity index values and true values ($R^2 = 1$, $p < 0.01$, Fig. 3A). The absolute measured activity index values were 9.7% (95%LOA, −28.6 to 9.4%) smaller than true values. The accuracy data is presented as Bland–Altman-plot in Fig. 3B. The CV_{rms} of activity index analysis in the validation measurement was 2.6%.

There was a very strong association between the measured activity time and the true time ($R^2 = 1$, $p < 0.01$, Fig. 4A). The measured activity time values were similar to true values (Fig. 4B). The mean difference was +0.9% (95% LOA, −1.2 to 3.0%) and the CV_{rms} of the measurement 0.52%.

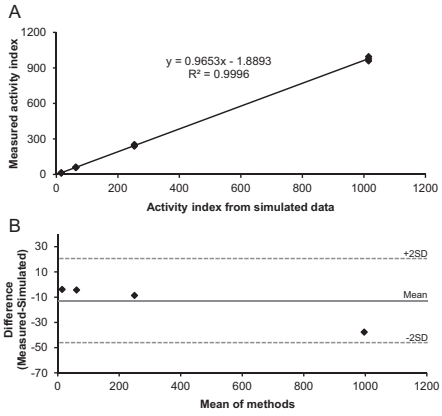

Fig. 3. (A) The relationship between activity indexes calculated from the simulated and measured data. (B) Bland–Altman-plot for activity index calculated from the simulated and measured data. Values are index values without units.

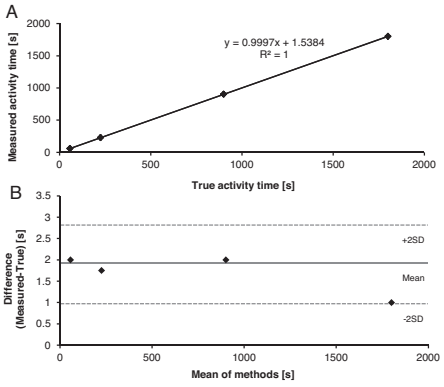

Fig. 4. (A) The relationship between measured activity time and true activity time. (B) Bland–Altman-plot for measured activity time and true activity time.

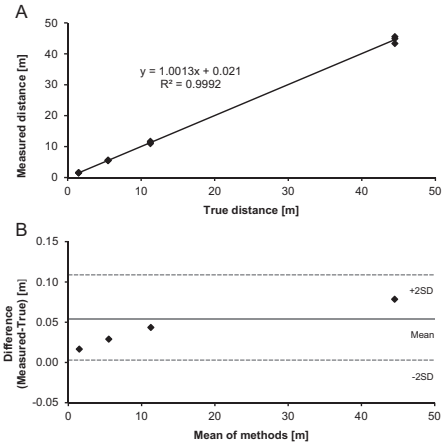

Fig. 5. (A) The relationship between measured distance and true distance. (B) Bland–Altman-plot for measured distance and true distance.

A very strong association was also found between measured distance and true distance ($R^2 = 1$, $p < 0.01$, Fig. 5A). The measured distances were similar to true distances (Fig. 5B). The distances analyzed from the force plate data were 0.7% (95% LOA, −4.6 to 6.0%) higher than true distances. The CV_{rms} of distance measurement was 2.81%.

3.2. Mouse experiment

The activity measurement system was tested in situ by measuring spontaneous activities of the mice with or without running wheels. The absolute value results are presented in Table 1 and the relative changes compared to baseline values in Fig. 6.

On average, the mice in the running group ran 1634 ± 336 meters per day. The running distances increased from week1 and peaked at week 3. The body mass of the mice decreased by 6.8 ± 1.3% ($p < 0.01$) during 4 weeks of running. The running wheels increased activity time by 39 ± 3%, intensity by 94 ± 16% and activity index by 211 ± 40%(Fig. 6A–C). The differences were significant when compared to the baseline values and also to the respective control group values at all time points. The running wheel induced changes were similar between different time points. However, similarly with running distances, activity index and intensity values peaked after 3 weeks of running. The running wheels did not have a clear effect on distance values (Fig. 6D). Compared to the baseline values, distances were increased only at the time point of 3 weeks (43 ± 20%, $p < 0.05$), when the running distances were at their highest level. Activity index ($R^2 = 0.982$, $p < 0.01$), activity time ($R^2 = 0.618$, $p < 0.01$), intensity ($R^2 = 0.920$, $p < 0.01$) and distance ($R^2 = 0.405$, $p < 0.01$) were significantly associated to running distance (Fig. 7A–D).

4. Discussion

The primary finding of the present study was that the developed spontaneous activity measurement method was valid and precise. Moreover, the in situ experiment indicated that the method is applicable in practice, quantifying a tripling of total physical activity with the introduction of a running wheel.

Table 1
The absolute results of the mouse experiment.

	Baseline, mean (SE)		Wk 1, mean (SE)		Wk 2, mean (SE)		Wk 3, mean (SE)		Wk 4, mean (SE)		POST, mean (SE)	
	Control ($n=4$)	Running ($n=8$)	Control ($n=4$)	Running ($n=8$)	Control ($n=4$)	Running ($n=8$)	Control ($n=4$)	Running ($n=8$)	Control ($n=4$)	Running ($n=8$)	Control ($n=4$)	Running ($n=8$)
Body mass (g)	33.0 (1.3)	32.5 (1.2)	32.5 (1.6)	31.5 (1.1)[a]	31.8 (1.1)	30.8 (1.2)[aa]	32.0 (1.6)	30.5 (0.9)[a]	31.5 (1.3)	30.3 (1.1)[aa]	31.0 (1.5)	31.1 (1.0)[a]
Running distance 24 h (m)	–	–	–	1182 (602)	–	1497 (653)	–	2061 (876)	–	1797 (613)	–	–
Activity index	392 (15)	342 (15)	382 (29)	867 (265)[a,b]	377 (29)	1054 (320)[a,bb]	361 (10)	1322 (413)[a,b]	401 (23)	1196 (279)[a,bb]	417 (30)	398 (23)[a]
Distance (m)	201.5 (7.6)	170.5 (19.2)	153.7 (5.5)	167.5 (18.3)	171.0 (16.4)	194.0 (28.1)	167.2 (9.6)	224.6 (42.1)[a]	171.7 (23.2)	198.2 (46.9)	211.6 (24.7)	186.1 (30.8)
Activity time (min)	296.5 (24.9)	249.8 (15.0)	289.6 (37.4)	336.1 (18.1)[aaa]	282.5 (41.7)	347.1 (23.7)[aa]	267.5 (16.0)	348.4 (26.5)[aa]	290.1 (19.4)	348.5 (20.3)[aaa]	286.8 (24.3)	265.8 (13.7)
Intensity (index/min)	0.87 (0.02)	0.88 (0.02)	0.88 (0.03)	1.41 (0.25)[a,bb]	0.87 (0.02)	1.6 (0.27)[a,bb]	0.87 (0.04)	1.90 (0.34)[a,bb]	0.89 (0.04)	1.89 (0.28)[a,bb]	0.94 (0.05)	0.94 (0.03)[a]

[a] $p<0.05$ vs. baseline.
[aa] $p<0.01$ vs. baseline.
[aaa] $p<0.001$ vs. baseline.
[b] $p<0.05$ vs. control.
[bb] $p<0.01$ vs. control.

The developed system measures three different variables from force data: activity index (total activity), activity time and distance, which were tested in specific validation measurements. The system also quantifies the mean intensity of activity, which is calculated from the activity index and activity time data. The function of an intensity variable was not separately validated. Activity index was originally developed for spontaneous activity measurements of rats (Biesiadecki et al., 1999). In the present study, activity index analysis was modified for measuring activity of mice with the developed system. The mass correction was added to the analysis to remove the effect of body mass on results. In addition, the resolution of analysis was enhanced with background subtraction. High resolution is crucial when the activities of small animals like mice are measured.

The validation data showed that the activity index values associated very strongly with the true values and the precision was adequate indicating that our method is valid to measure relative differences. However, the measured absolute values were on average 9.7 percent lower than the actual true values. Because the detection of relative difference is the main task of activity index values, we did not correct these values in any way. However, this could be done by using a linear regression equation. The accuracy and precision of activity time measurements were excellent. The calibration measurements indicated that distance analysis was accurate and precise. However, during analysis of the mouse experiment, we observed that water evaporation causes significant drift in distances leading to overestimated results during long measurements (>10 h). After applying several correction methods, it was found that the best method is to correct the distances minute by minute using correction coefficients derived from the equation describing second order regression line fitted into minimum distance values (minimum minutes per hour) of each individual data. The drift was corrected during the first 24 h but after 48 h the loss of mass and the resulting error were mostly so significant that the correction was no longer reliable. Based on the calibration and animal tests, the distance analysis is valid when the continuous measurement does not last over 24 h.

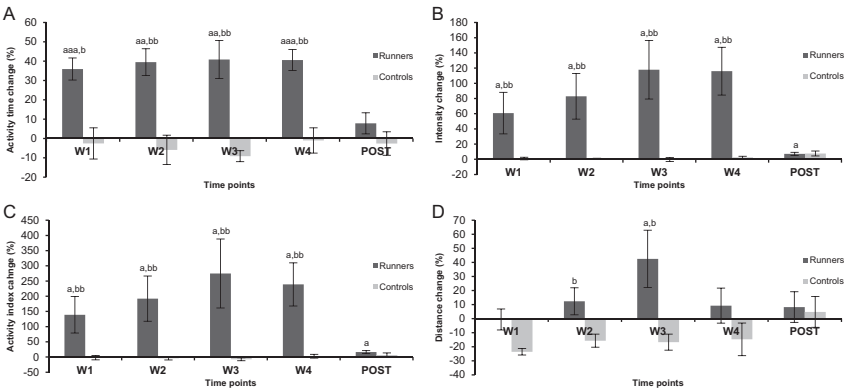

Fig. 6. (A) Activity time changes (%) compared to baseline. (B) Intensity changes (%) compared to baseline. (C) Activity index changes (%) compared to baseline. (D) Distance changes (%) compared to baseline. W1–W4 are time points in weeks after baseline measurement, and the time point POST is one week after removing the running wheel. Results are means ± SE. Running group $n=8$, Control group $n=4$. a $p<0.05$ vs. baseline, aa $p<0.01$ vs. baseline, aaa $p<0.001$ vs. baseline, b $p<0.05$ vs. control, bb $p<0.01$ vs. control, bbb $p<0.001$ vs. control.

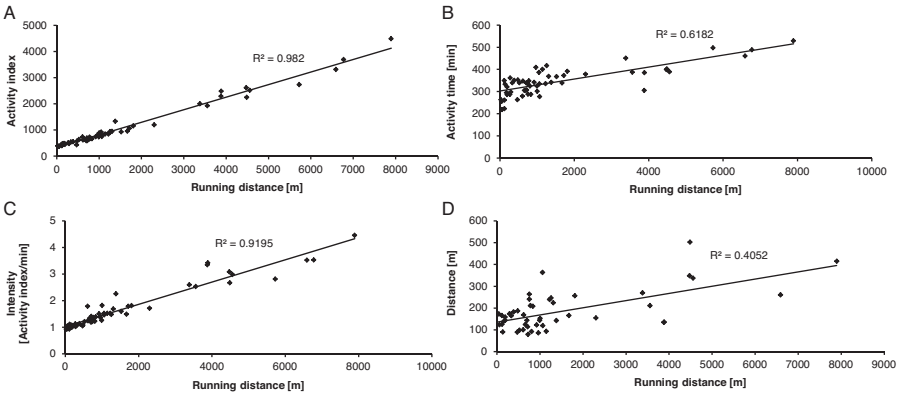

Fig. 7. The relationship of activity index (A), activity time (B), intensity (C) and distance (D) to running distance.

It has been shown earlier, that access to running wheels decreases the amount of other normal activities like climbing and grooming (Harri et al., 1999). This may attenuate the effect of running wheels on total activity of mice. However, our results clearly show that the running wheels nearly double the intensity of activity ($94 \pm 16\%$) and also increase significantly the time of activity ($39 \pm 3\%$). These changes resulted in over 200% increase in total activity. This result is in agreement with findings by de Visser et al., 2005 (de Visser et al., 2005). They showed with the same strain of mice (females) that wheel running increased total horizontal activity time even if the cage floor activity time was simultaneously decreased (absolute 24 h activity time results were not presented).

The strong associations between the measured activity variables and the running distance confirm that running clearly affects the total physical activity of mice. Running seems to boost total activity, especially by increasing the intensity of physical activity. The strong associations also confirm that the activity time, activity index and activity intensity analyses are reliable in actual measurement conditions and that these variables can be used in the quantitation of physical activity of mice with or without running wheels. The distance analysis is not sensitive to wheel running, thus, its use is limited to cages without running wheels. This was expected, because the distance analysis is based on the measured changes of the center of force. Running in a wheel occurs mostly in one place and, therefore, does not induce marked changes in the location of the center of force.

Unlike other activity measurement systems, the force-plate system was developed and validated specifically for voluntary running studies. The system provides comparable measures for total physical activity of both voluntary running mice and sedentary mice, which is not possible without appropriate activity measurement system. Wheel running distances cannot be used because the wheel running is only one part of the daily activity and the running distances are unavailable for sedentary mice. Total activity data enables the determination of activity differences between voluntary running and sedentary groups and the variability of activity within groups. In addition to the system presented here, there are only a few activity measurement systems that could be used for measuring physical activity from both cages with and without running wheels. The force-plate actometer method developed by Biesiadecki et al. (1999) could be used if the validity of the system was first proven for mouse measurements (developed for rats). The other available systems are usually measuring physical activity occurring in one plane, such as the horizontal plane (total distance and activity time), by combining the running wheel data with cage floor activity data, which is usually measured using video tracking (e.g. Phenotyper/Etho Vision, Noldus, The Netherlands) or infrared photo-beam system (e.g. Phenomaster/Actimot2, TSE systems, Germany). If both vertical and horizontal movements are not included in the measurement, the results cannot be considered total activity. However, the advantage of these last mentioned systems is that they are very versatile and consequently suitable especially for behavioral studies. Contrary to novel video tracking methods e.g. (Brodkin et al., 2014), the system presented here, cannot recognize different behavior patterns or separate the type of activity (running or floor activity). However, the advantage of the validated force-plate system is that instead of measuring total activity as a movement in one certain plane, the sensitive force-plate system quantitates all the activity inducing vertical reaction forces. In addition to movements in vertical and horizontal plane, it also detects stationary movements (e.g. eating, drinking and grooming). Contrary to tracking and photo-beam systems, running wheels or other environmental enrichments do not disturb the measurement in any way and they can be placed inside the home cage. Thus, the cage and running wheel do not have to be certain specific type to be measured with the system. The force-plate system is an economical option especially for those scientists who already have voluntary running system but lack a method for recording total activity. Similarly with other activity measurement systems, the activity measurements produce a large amount of data. In order to make data analysis simple and convenient, an open source Java-based analysis program was developed. The source code is free to be used and modified by anyone who is interested in building their own force-plate system.

The validation measurements revealed that when sensitive force plates are used, efficient data filtering and background subtraction procedures are needed to enable adequate resolution. The disadvantage of data filtering is that it may lead to loss of some real activity signals. We were able to conduct dynamic validation measurements that allowed the variable specific optimization of data filtering and background subtraction procedures. This is crucial because physical activity induced dynamic force changes are much more challenging to measure compared to stationary situations. Since man-made calibration devices can never perfectly

mimic real animal movements and, since individual animals differ in their behavior, it is probable that filtering is not always optimal and a small part of the movements are not recorded. The activity time measurement is based on activity index analysis and threshold value. The threshold defines the level of force changes that must be reached to consider force changes as physical activity. Based on tests with calibration data and mouse data, three times the background value was selected as the threshold value. This should exclude continuous force changes (e.g. breathing) and short flinches of activity. The threshold method worked perfectly with validation data but with real mouse data the threshold selection can have a significant impact on absolute activity time values, because there is a continuum from small force changes to large ones. Thus, the interpretation of activity time and intensity (activity time dependent) results should concentrate more on relative differences than absolute values.

5. Conclusions

Calibration measurements and actual long-term measurements of mouse movements proved that the developed system is valid for the quantitation of total physical activity of mice housed in cages with or without running wheels. The activity index and activity time are the most valid measures for these conditions. The distance analysis is acceptable when the maximum measuring time is 24 h and there is no running wheel in the cage. The mouse experiment showed that wheel running triples the mean total activity of mice. The main part of this effect is explained by the increases of the intensity of activity and the activity time. The developed method is compatible with all types of cages and running wheels and it causes minimal disturbance to the experimental animals. Therefore, it can be considered well-suited for estimating total physical activity in various research paradigms.

Acknowledgements

The study was financially supported by the Finnish Ministry of Education and Culture (50/627/2010), Finnish Cultural Foundation and the Academy of Finland (125209). Support from the National Doctoral Program of Musculoskeletal Disorders and Biomaterials (TBDP) is also acknowledged. Dr. Rantalainen was supported by an Alfred Deakin Postdoctoral Research Fellowship during the preparation of the manuscript. We are grateful to Jouni Tukiainen, Seppo Seppälä and Terho Kaipio-Sarja for their expertise and patience in building the activity measurement system.

References

Beninger RJ, Cooper TA, Mazurski EJ. Automating the measurement of locomotor activity. Neurobehav Toxicol Teratol 1985;7:79–85.
Biesiadecki BJ, Brand PH, Koch LG, Britton SL. A gravimetric method for the measurement of total spontaneous activity in rats. Proc Soc Exp Biol Med 1999;222:65–9.
Bland JM, Altman DG. Statistical methods for assessing agreement between two methods of clinical measurement. Lancet 1986;1:307–10.
Brodkin J, Frank D, Grippo R, Hausfater M, Gulinello M, Achterholt N, et al. Validation and implementation of a novel high-throughput behavioral phenotyping instrument for mice. J Neurosci Methods 2014;224:48–57.
Chiesa JJ, Araujo JF, Diez-Noguera A. Method for studying behavioural activity patterns during long-term recordings using a force-plate actometer. J Neurosci Methods 2006;158:157–68.
Coletti D, Berardi E, Aulino P, Rossi E, Moresi V, Li Z, et al. Substrains of inbred mice differ in their physical activity as a behavior. Sci World J 2013;2013:237260.
de Visser L, van den Bos R, Spruijt BM. Automated home cage observations as a tool to measure the effects of wheel running on cage floor locomotion. Behav Brain Res 2005;160:382–8.
Dielenberg RA, Halasz P, Day TA. A method for tracking rats in a complex and completely dark environment using computerized video analysis. J Neurosci Methods 2006;158:279–86.
Eisenmann JC, Wickel EE, Kelly SA, Middleton KM, Garland T Jr. Day-to-day variability in voluntary wheel running among genetically differentiated lines of mice that vary in activity level. Eur J Appl Physiol 2009;106:613–9.
Fowler SC, Birkestrand BR, Chen R, Moss SJ, Vorontsova E, Wang G, et al. A force-plate actometer for quantitating rodent behaviors: illustrative data on locomotion, rotation, spatial patterning, stereotypies, and tremor. J Neurosci Methods 2001;107:107–24.
Harri M, Lindblom J, Malinen H, Hyttinen M, Lapvetelainen T, Eskola S, et al. Effect of access to a running wheel on behavior of C57BL/6J mice. Lab Anim Sci 1999;49:401–5.
Kao SD, Shaw FZ, Young MS, Jan GJ. A new automated method for detection and recording of animal moving path. J Neurosci Methods 1995;63:205–9.
Lightfoot JT, Turner MJ, Daves M, Vordermark A, Kleeberger SR. Genetic influence on daily wheel running activity level. Physiol Genomics 2004;19:270–6.
Ma H, Torvinen S, Silvennoinen M, Rinnankoski-Tuikka R, Kainulainen H, Morko J, et al. Effects of diet-induced obesity and voluntary wheel running on bone properties in young male C57BL/6J mice. Calcif Tissue Int 2010;86:411–9.
Martin B, Ji S, Maudsley S, Mattson MP. "Control" laboratory rodents are metabolically morbid: why it matters. Proc Natl Acad Sci USA 2010;107:6127–33.
Meijer JH, Robbers Y. Wheel running in the wild. Proc Biol Sci 2014;281:10, 1098/rspb.2014.0210.
Pan WH, Lee CR, Lim LH. A new video path analyzer to monitor travel distance, rearing, and stereotypic movement of rats. J Neurosci Methods 1996;70:39–43.
Rantalainen T, Silvennoinen M, Kainulainen H, Sievanen H. Vertical ground reaction force measurements and video measurements provide comparable estimates of distance moved by mice during artificial light and dark periods. J Neurosci Methods 2011;197:104–8.
Rinnankoski-Tuikka R, Silvennoinen M, Torvinen S, Hulmi JJ, Lehti M, Kivela R, et al. Effects of high-fat diet and physical activity on pyruvate dehydrogenase kinase-4 in mouse skeletal muscle. Nutr Metab (Lond) 2012;9(53), 7075-9-53.
Silvennoinen M, Rinnankoski-Tuikka R, Vuento M, Hulmi JJ, Torvinen S, Lehti M, et al. High-fat feeding induces angiogenesis in skeletal muscle and activates angiogenic pathways in capillaries. Angiogenesis 2013;16:297–307.
Teicher MH, Andersen SL, Wallace P, Klein DA, Hostetter J. Development of an affordable hi-resolution activity monitor system for laboratory animals. Pharmacol Biochem Behav 1996;54:479–83.

IV

PGC-1 ISOFORMS AND THEIR TARGET GENES ARE EXPRESSED DIFFERENTLY IN HUMAN SKELETAL MUSCLE FOLLOWING RESISTANCE AND ENDURANCE EXERCISE

by

Silvennoinen M, Ahtiainen J, Hulmi JJ, Pekkala S, Taipale R, Nindl B, Laine T, Häkkinen K, Selänne H, Kyröläinen H, Kainulainen H. 2015.

Physiological Reports 3(10), e12563

Physiological Reports

Open Access

Physiological Reports ISSN 2051-817X

ORIGINAL RESEARCH

PGC-1 isoforms and their target genes are expressed differently in human skeletal muscle following resistance and endurance exercise

Mika Silvennoinen[1], Juha P. Ahtiainen[1], Juha J. Hulmi[1], Satu Pekkala[2], Ritva S. Taipale[1], Bradley C. Nindl[3], Tanja Laine[1], Keijo Häkkinen[1], Harri Selänne[4,5], Heikki Kyröläinen[1] & Heikki Kainulainen[1]

1 Department of Biology of Physical Activity, University of Jyväskylä, Jyväskylä, Finland
2 Department of Health Sciences, University of Jyväskylä, Jyväskylä, Finland
3 The Military Performance Division, The Unites States Army Research Institute of Environmental Medicine, Natick, Massachusetts
4 Jyväskylä Central Hospital, Jyväskylä, Finland
5 LIKES Research Center for Sport and Health Sciences, Jyväskylä, Finland

Keywords
PGC1-1β, *PGC-1α*, physical activity, splice variant.

Correspondence
Mika Silvennoinen, Department of Biology of Physical Activity, University of Jyväskylä, P. O. Box 35, FIN-40014 University of Jyväskylä, Jyväskylä, Finland.
Tel: +358 40 733 8864
Fax: +358 14 260 2071
E-mail: mika.m.silvennoinen@jyu.fi

Funding Information
This work was financially supported by a grant from the Scientific Advisory Board for Defence, the David Sports Ltd., and the Finnish Cultural Foundation Central Fund (Kainulainen). Support from the National Doctoral Programme of Musculoskeletal Disorders and Biomaterials (TBDP) is also acknowledged.

Received: 2 September 2015; Accepted: 6 September 2015

doi: 10.14814/phy2.12563

Physiol Rep, 3 (10), 2015, e12563, doi: 10.14814/phy2.12563

Abstract

The primary aim of the present study was to investigate the acute gene expression responses of PGC-1 isoforms and PGC-1α target genes related to mitochondrial biogenesis (*cytochrome C*), angiogenesis (*VEGF-A*), and muscle hypertrophy (myostatin), after a resistance or endurance exercise bout. In addition, the study aimed to elucidate whether the expression changes of studied transcripts were linked to phosphorylation of AMPK and MAPK p38. Nineteen physically active men were divided into resistance exercise (RE, $n = 11$) and endurance exercise (EE, $n = 8$) groups. RE group performed leg press exercise (10 × 10 RM, 50 min) and EE walked on a treadmill (~80% HR_{max}, 50 min). Muscle biopsies were obtained from the vastus lateralis muscle before, 30 min, and 180 min after exercise. EE and RE significantly increased the gene expression of alternative promoter originated *PGC-1α* exon 1b- and 1b'-derived isoforms, whereas the proximal promoter originated exon 1a-derived transcripts were less inducible and were upregulated only after EE. Truncated *PGC-1α* transcripts were upregulated both after EE and RE. Neither RE nor EE affected the expression of *PGC-1β*. EE upregulated the expression of *cytochrome C* and *VEGF-A*, whereas RE upregulated *VEGF-A* and downregulated *myostatin*. Both EE and RE increased the levels of p-AMPK and *p*-MAPK p38, but these changes were not linked to the gene expression responses of *PGC-1* isoforms. The present study comprehensively assayed *PGC-1* transcripts in human skeletal muscle and showed exercise mode-specific responses thus improving the understanding of early signaling events in exercise-induced muscle adaptations.

Introduction

Skeletal muscle comprises about 40–50% of body mass in humans (lean) and plays significant roles in locomotion, heat production, and whole-body metabolism. Skeletal muscle has an outstanding capability to adapt to a variety of external stimuli that explains, in part, the marked differences observed in physical performance (e.g., endur-

ance and strength) and health profiles between individuals (Hawley et al. 2014). The question remains, Which specific mechanisms are involved in the response to different types of physical activities? Because the effects are so diverse, mechanisms comprise multiple signaling cascades that form a complex network with each other (Egan et al. 2010). Yet, there have been attempts to identify single signaling cascades or molecules that could work as a master regulator for controlling exercise-specific adaptations (Atherton et al. 2005; Baar and Esser 1999). In recent years, the transcriptional coactivator peroxisome proliferator-activated receptor-γ coactivator (PGC)-1α has been under a thorough investigation. PGC-1α has been identified as a regulator of mitochondrial biogenesis, angiogenesis, antioxidant defense, and inflammatory proteins (Olesen et al. 2010).

A single bout of prolonged endurance exercise transiently increases *PGC-1α* mRNA content in human and rat skeletal muscle (Pilegaard et al. 2003; Gidlund et al. 2015; Baar et al. 2002; Chinsomboon et al. 2009). Furthermore, other types of physical activity (e.g., sprint and resistance exercise) can also result in an increase in the gene expression of *PGC-1α* (Gibala 2009; Ydfors et al. 2013). There are several intracellular signaling pathways that may contribute to eliciting the exercise-induced *PGC-1α* gene expression response including calcium signaling, AMPK and MAPK signaling, ROS-mediated regulation, and β-adrenergic signaling (Olesen et al. 2010).

Recently the existence of several different splice variants of *PGC*-1α has been found in skeletal muscle. The splice variants differ from their starting exon (exon 1a, exon 1b, and exon 1b'/1c) and via alternative 3′ splicing, which produce either full-length PGC-1α protein (PGC-1α) or shorter N-truncated protein (NT-PGC-1α). Exon 1a-derived *PGC-1α* mRNAs are transcribed from the canonical proximal promoter, while exon 1b- and 1b'-derived mRNAs are transcribed from an alternative promoter ~14-kb upstream from the canonical one (Ruas et al. 2012; Zhang et al. 2009). Lately, the roles of different splice variants of *PGC-1α* in the initial signaling events of exercise-induced skeletal muscle adaptations have been under heavy investigation. Ruas et al. (2012) showed that the expression of *PGC-1α4*, exon 1b originated N-truncated *PGC-1α* transcript, results in robust skeletal muscle hypertrophy in vitro and in vivo. The study suggested that PGC-1α4 is preferentially induced in mouse and human muscle during resistance exercise, and this would lead to muscle hypertrophy via induced expression of IGF1 and repressed expression of myostatin. However, the studies of Lundberg et al. (2014) and Ydfors et al. (2013) have questioned the preferential induction of *PGC-1α4* expression after resistance exercise by showing that also endurance exercise has effects on the response of this transcript in human skeletal muscle. In fact, the effects of endurance exercise were shown already in the study of Ruas et al. (2012). Interestingly, the study of Thom et al. (2014) showed that hypoxia specifically induces truncated forms of *PGC-1α* (*NT-PGC-1α* and *PGC-1α4*), which induces *VEGF* expression and angiogenesis, while having only a little effect on mitochondrial genes. Previous studies have also shown that both resistance and endurance exercise are able to induce expression of alternative and proximal promoter originated *PGC-1α* transcripts, the alternative promoter originated transcripts being much more inducible compared to proximal promoter originated transcripts (Lundberg et al. 2014; Ydfors et al. 2013).

Exact primer design is an essential part of studies measuring mRNA levels of different splice variants. Since the most of the previous studies (Lundberg et al. 2014; Norrbom et al. 2011; Ydfors et al. 2013) investigating exercise-induced acute gene expression responses of different *PGC-1α* splice variants in human skeletal muscle did not report exact primer sequences, it was impossible to evaluate the specificity of the used primers. To increase knowledge of early signaling events that drive the exercise mode-specific adaptations, and to confirm previous findings with well-defined primers, the present study aimed to investigate the acute gene expression responses of different *PGC-1* isoforms after a single bout of high-load resistance exercise (leg press protocol) or moderate intensity endurance exercise (uphill walking on treadmill) in human skeletal muscle. In addition, we aimed to determine how these two different exercise protocols affect the expression of a selection of known PGC-1α target genes related to mitochondrial biogenesis, angiogenesis, and muscle hypertrophy. Furthermore, we wanted to elucidate whether the expression changes of studied transcripts were linked to phosphorylation changes of known *PGC-1α* regulators AMPK and p38 MAPK.

Materials and Methods

Ethical approval

The study was conducted according to the Declaration of Helsinki, and ethical approval was granted by the ethics committees of the University of Jyväskylä and the Central Finland Health Care District, Jyväskylä, Finland. Each subject was carefully informed of all potential risks and discomforts and, thereafter, signed an informed consent document.

Study subjects

Two different experimental setups were included in the study: resistance and endurance exercise. The studies were linked to the larger military research project. A total of 22

healthy male reservists, who were physically active but not endurance or strength athletes, were recruited for the present investigation. Two subjects withdrew from the endurance exercise group and one subject was excluded from this group because of inadequate muscle samples. Therefore, the final study groups included 11 subjects in resistance exercise group (RE) and eight in endurance exercise group (EE). The general characteristics of the groups, which have been partly published previously (Ahtiainen et al. 2015), were as follows (mean ± SD): RE (n = 11, 26.0 ± 4.6 years, 182 ± 8 cm, 78.6 ± 11.7 kg, MVC 339.7 ± 99.7 kg, CMJ 34.0 ± 3.8 cm, 1RM 207.0 ± 26.6 kg, VO_{2max} 59.9 ± 5.3 $mL \cdot kg^{-1} \cdot min^{-1}$) and EE ($n$ = 8, 27.0 ± 3.6 years, 181 ± 9 cm, 72.5 ± 11.5 kg, MVC 221.8 ± 33.2 kg, CMJ 30.9 ± 3.6 cm, 1RM 167.3 ± 33.6 kg, VO_{2max} 65.3 ± 5.2 $mL \cdot kg^{-1} \cdot min^{-1}$).

Exercise protocols

The protocols and equipment used with both exercise modes have been described in detail elsewhere (Ahtiainen et al. 2015). In brief, RE was a single high-load hypertrophic type of resistance exercise consisting 10 sets of 10 repetition maximum (10 × 10 RM) using a bilateral leg press device (David 210, David Health Solutions Ltd., Helsinki, Finland). The starting load was 70% of 1RM. Thereafter, the loads were adjusted so that each subject would be able to perform a maximum of 10 repetitions for each set. The recovery between the sets was 2 min, except a 10 min rest that was applied between the fifth and sixth set. EE consisted of 50 min of strenuous walking on a treadmill. To increase exercise load additional weight (16.5 kg) were carried in backpack (OJK-1, Telineyhtymä, Kotka, Finland). At minutes 0:00–5:00 and 40:00–45:00, the speed of the treadmill was 4.5 $km \cdot h^{-1}$ and the slope 4.0 degrees. At minutes 5:00–10:00 and 45:00–50:00, the speed was 7.0 $km \cdot h^{-1}$ and the slope 4.0 degrees. During the minutes 10:00–40:00, the walking speed was individually controlled and adjusted in 5-min intervals by heart rate (HR) and blood lactate measurements. The criteria for walking speed included (1) blood lactate concentration approximately 4.0 $mmol \cdot L^{-1}$; and (2) HR between 75% and 85% of the individual HR maximum (HR_{max}) that was determined by a maximal endurance capacity test before the study.

The subjects were familiarized with the upcoming exercises and testing protocols 4–5 days before the study. To control effects of nutrition and hydration status, the subjects fasted for 12 h before the first (PRE) biopsy. Immediately after the biopsy, the subjects ate an energy bar (170 kcal, protein 7 g, carbohydrate 21 g, and fat 5.5 g) and drank 0.5 L of water. Two hours after the exercise loading, the subjects were allowed to eat again an energy bar and drink water (ad libitum). The energy bars and water were given to avoid lack of energy and disturbance of fluid balance during the measurement day lasting 8.5 h. Moreover, the amount of given energy was selected so that we could minimize the known effects of caloric restriction, fasting, and feeding on exercise responses (Ranhotra 2010; Canto et al. 2010). The subjects were asked to refrain from vigorous physical activity for 2 days before the study.

Muscle strength and explosive power

To assess basal strength characteristics and muscular fatigue produced by exercise, the following measurements were performed before and after exercise: maximal voluntary bilateral isometric force (MVC) of leg extensor muscles (electromechanical dynamometer, Department of Biology of Physical Activity, University of Jyväskylä, Jyväskylä, Finland) (Ahtiainen et al. 2015), maximal dynamic bilateral 1RM leg press (David 210, David Health Solutions Ltd, Helsinki, Finland), and countermovement jump (CMJ).

Blood lactate

In both EE and RE, fingertip blood lactate samples were collected before and immediately after exercises into capillary tubes, which were placed in a 1-mL hemolyzing solution and analyzed automatically (EKF diagnostic, Biosen, Barleben, Germany). To adjust speeds in EE, blood lactate was monitored (Lactate Pro LT-1710 analyser 35, Arkray Inc., Kyoto, Japan) during the exercise in 5-min intervals.

Muscle biopsy procedure

The first (PRE) muscle biopsy was obtained from VL (right leg) 3 h before exercise. Biopsies were taken with a 5-mm Bergström biopsy needle together with suction, midway between the patella and greater trochanter. Muscle depth was kept constant in different biopsies within subject by markings on the needle. The muscle sample was cleaned of any visible connective and adipose tissue as well as blood and frozen immediately in liquid nitrogen (−180°C) and stored at −80°C. The postexercise biopsy samples were taken from VL (left leg) after 30 and 180 min of recovery. The recovery protocol was identical in both exercise groups. The subjects were physically passive during the recovery.

Western blot analysis

Muscle biopsy specimens were hand-homogenized in ice-cold buffer (20 $mmol \cdot L^{-1}$ HEPES [pH 7.4], 1 $mmol \cdot L^{-1}$

EDTA, 5 mmol·L^{-1} EGTA, 10 mmol·L^{-1} $MgCl_2$, 100 mmol·L^{-1} b-glycerophosphate, 1 mmol·L^{-1} Na_3PO_4, 2 mmol·L^{-1} DTT, 1% Triton X-100, 0.2% sodium deoxycholate, 30 μg·mL^{-1} leupeptin, 30 μg·mL^{-1} aprotinin, 60 μg·mL^{-1} PMSF, and 1% phosphatase inhibitor cocktail; P 2850; Sigma, St. Louis, MO) at a dilution of 15 μL·mg^{-1} of wet weight muscle. Homogenates were rotated for 30 min at 4°C, centrifuged at 10,000 *g* for 10 min at 4°C to remove cell debris, and stored at −80°C. Total protein content was determined using the bicinchoninic acid protein assay (Pierce Biotechnology, Rockford, IL).

Aliquots of muscle lysate, containing 30 μg of total protein, were solubilized in Laemmli sample buffer and heated at 95°C for 10 min to denature proteins, and were then separated by SDS-PAGE for 90 min at 200 V using 4–20% gradient gels on Criterion electrophoresis cell (Bio-Rad Laboratories, Hercules, CA). All samples from each subject were run on the same 18-sample gel. Proteins were transferred to PVDF membranes at 350 mA constant current for 3 h on ice at 4°C. Membranes were blocked in TBS with 0.1% Tween 20 (TBS-T) containing 5% nonfat dry milk for 1 h and then incubated overnight at 4°C with rabbit polyclonal primary antibodies. Antibodies recognizing phosphorylated p38MAPK$^{Thr180/Tyr182}$ and AMPKα^{Thr172} were purchased from Cell Signaling Technology (Danvers, MA) and these primary antibodies were diluted 1:2000 in TBS-T containing 2.5% nonfat dry milk. For measuring protein levels of nontruncated full-length splice variants of PGC-1α, the antibody (1:3000, Calbiochem, Merck KGaA, Darmstadt, Germany) against C-terminus of protein (amino acids 777–797) was used. Membranes were then washed (5 × 5 min) in TBS-T, incubated with secondary antibody (horseradish peroxidase-conjugated anti-rabbit IgG; Cell Signaling Technology) diluted 1:25,000 in TBS-T with 2.5% milk for 1 h followed by washing in TBS-T (5 × 5 min). Proteins were visualized by ECL according to the manufacturer's protocol (SuperSignal west femto maximum sensitivity substrate, Pierce Biotechnology) and quantified (band intensity × volume) using a ChemiDoc XRS in combination with Quantity One software (version 4.6.3. Bio-Rad Laboratories).

The uniformity of protein loading was confirmed by staining the membrane with Ponceau S. Our earlier studies and preliminary experiments confirmed a proportional linear relation between the protein loaded and the strongest band in Ponceau S at ~42 kDa in quantification between 5 and 60 μg of total protein loaded (Hulmi et al. 2012). A less well proportional and linear relationship was found between GAPDH, α-actin, and staining of myosin heavy chain left in the gel after blotting. Therefore, all of the results were normalized to the corresponding Ponceau S staining value at ~42 kDa. In addition, to reduce gel-to-gel variation, the results of all samples within the gel were normalized to the mean value of all PRE samples within the gel. Quantification of p-p38 MAPKThr180/Tyr182 was based on the average of two visible bands at 42 and 44 kDa. Phosphorylated AMPKαThr172 was quantified using the visible band at 62 kDa and nontruncated PGC-1α using the band at 100 kDa.

RNA extraction and cDNA synthesis

Total RNA was isolated from the muscle biopsy with Trizol reagent (Life Technologies, Carlsbad, CA) according to the manufacturer's instructions. Muscle samples were homogenized with a FastPrep FP120 (Thermo Fisher Scientific, Waltham, MA) tissue homogenizer by using Lysing Matrix D FP120 (Thermo Fisher). The quality of RNA was confirmed by spectrophotometry (NanoDrop; Thermo Fisher Scientific) and agarose gel electrophoresis. Reverse transcription of mRNA was performed from total RNA (5 μg) by using anchored oligo(dT)$_{20}$ primers (Oligomer, Helsinki, Finland) and a SuperScript III Reverse Transcriptase kit (Life Technologies) according to the manufacturer's instructions. The cDNA samples were stored in −20°C.

Real-time quantitative PCR

Cytochrome C (*CYC*), *glyceraldehyde-3-phosphate dehydrogenase* (*GAPDH*), and *vascular endothelial growth factor A* (*VEGF-A*) mRNAs were quantified using TaqMan primers and hydrolysis probes (Assay IDs: *CYC*: Hs01588974_g1; *GAPDH*: Hs03929097_g1; *VEGF-A*: Hs00900055_m1), TaqMan Gene Expression Master Mix (Life Technologies), and ABI 7300 Real-Time quantitative PCR System (Life Technologies). The PCR cycle parameters used were: +50°C for 2 min, +95°C for 10 min, 40 cycles at +95°C for 15 sec, and +60°C for 1 min. The other studied transcripts (*PGC-1α* exon 1a-, 1b- and 1b' -derived mRNAs, total *NT-PGC-1α*, total *PGC-1α*, *PGC-1β*, and *myostatin*) were quantified using iQ SYBR Supermix (Bio-Rad Laboratories) and CFX96 Real-Time PCR Detection System (Bio-Rad Laboratories). The PCR cycle parameters used with this system were as follows: +95°C for 10 min, 40 cycles at +95°C for 10 sec, at gene-specific annealing temperature (61°C, except 56 for total *NT-PGC-1α*) for 30 sec and at +72°C for 30 sec, followed by 5 sec at +65°C.

The primer sequences recognizing total *NT-PGC-1α* and *PGC-1α* exon 1a-derived transcripts were copied from Ruas et al. (2012) and *myostatin* from Kim et al. (2007). Other primers were designed with Primer3 (web version 4.0.0) software (Koressaar and Remm 2007;

Untergasser et al. 2012). The structure of 5′ region of the human *PGC-1α* gene is illustrated in Figure 1A. In addition, the detailed description of exon structure and primer design of measured *PGC-1α* transcripts is presented in Figure 1B. The sequences of primer sets used with the SYBR green method are listed in Table 1. Following pilot RT-qPCR runs performed with the SYBR green method, the specificity of each primer set was monitored by the melting curves and by agarose gel (3%) electrophoresis (Fig. 2). In addition, optimal gene-specific annealing temperatures were determined. The amplification efficiencies for each gene were between 95% and 105%.

Each sample was analyzed in duplicate, and a nontemplate control was included in each run. Relative gene expression levels of all target transcripts were normalized using RNA:cDNA hybrid concentrations which were measured using a Quant-iT™ PicoGreen® assay (Life Technologies) according to the manufacturer's recommendations. This method of normalization has been validated especially for human exercise studies and muscle biopsy samples (Lundby et al. 2005). The stability of RNA:cDNA hybrid concentrations was compared to stability of *GAPDH*, one of the most common reference genes used in exercise studies. The average differences between time points in both exercise modes were similar in *GAPDH* and RNA:cDNA hybrid concentrations. However, the variation within time points in both exercise modes were lower in RNA:cDNA hybrid concentrations compared to *GAPDH* levels. The RNA:cDNA hybrid concentrations are presented in (Fig. 3G). The normalized relative gene expression results (R) of each sample were expressed in relation to PRE average and calculated using following formula:

$$R = \frac{2^{-(\text{Cq sample}-\text{Cq PRE average})} \times \text{RNA: cDNA hybrid conc. PRE average}}{\text{RNA: cDNA hybrid conc. sample}}$$

Statistical analyses

Conventional statistical methods were used to obtain means, standard deviations (SD), medians, interquartile ranges (IQR), and percentiles. The Shapiro–Wilk test was used to test the normality of the variables and the Levene's test was used to analyze the homogeneity of variances. Due to the small sample size and random violations in the normal distribution assumption and the homogeneity of the variance assumption, a nonparametric Friedman's two-way ANOVA by ranks test was used to determine differences between time points (PRE, 30′ and 180′) within groups (RE and EE). Wilcoxon matched-pair signed-rank test with Holm–Bonferroni correction was used for the post hoc analysis. A Spearman's rank correlation test was used to test if the changes in p38 MAPKThr180/Tyr182 or AMPKαThr172 phosphorylation were associated with exercise-induced gene expression changes. The significance level was set at $P < 0.05$. All statistical analyses were carried out using IBM SPSS statistics 20 software (IBM Corporation, Armonk, NY).

Results

The effects of exercise bouts

RE led to a decrease of 45 ± 16% ($P < 0.01$) in MVC and 17 ± 24% (NS, $P = 0.07$) in CMJ from pre- to postexercise. Blood lactate increased to 11.1 ± 3.0 mmol·L^{-1} ($P < 0.01$) immediately after RE. During the loading in EE, averaged treadmill speed was 6.2 ± 0.4 km·h^{-1} and the slope 4.1 ± 0.8 degrees, the blood lactate was 4.2 ± 1.0 mmol·L^{-1} and HR was 83 ± 8% of the HR_{max}. Immediately after EE, MVC was 9 ± 14% (NS, $P = 0.06$) and CMJ 7 ± 6% ($P < 0.05$) lower than before the exercise, and blood lactate was 2.4 ± 1.5 mmol·L^{-1} ($P < 0.01$). These results (except CMJ) have been previously published (Ahtiainen et al. 2015).

Gene expression responses of *PGC-1* transcript variants after RE and EE

The average basal state (PRE) C_q values (all subjects) for studied *PGC-1* transcripts were as follows: *PGC-1α* exon 1a-derived transcripts 25.6 ± 1.2, *PGC-1α* exon 1b-derived transcripts 31.3 ± 3.1, *PGC-1α* exon 1b'-derived transcripts 33.8 ± 1.7, total *NT-PGC-1α* 29.7 ± 1.4, total *PGC1α* 24.1 ± 1.2, and *PGC1β* 30.0 ± 1.6. The expression of *PGC-1α* exon 1a-derived transcripts increased by 1.7-fold ($P < 0.05$, Fig. 3A) 30 min after EE. After RE no significant response was detected. The expression of *PGC-1α* exon 1b-derived transcripts was significantly increased in response to both RE and EE (Fig. 3B), while the peak changes were detected 180 min after exercise. At this time point, the average gene expression change was 170-fold ($P < 0.05$) after EE and 997-fold ($P < 0.01$) after RE. The expression of *PGC-1α* exon 1b'-derived transcripts were low in the present basal conditions. In the RE group, the transcripts were detected in six PRE samples from 11 and in EE group in three PRE samples from eight. However, after RE and EE the expression of *PGC-1α* exon 1b'-derived transcripts was substantially increased (Fig. 3C).

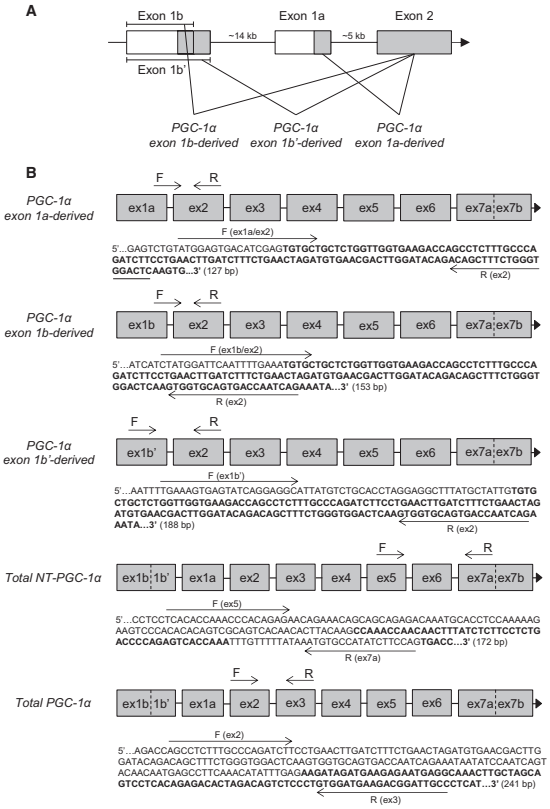

Figure 1. (A) The schematic structure of the 5′ region of the human *PGC-1α* gene (Miura et al. 2008). White boxes indicate untranslated exon regions and gray boxes translated coding regions. Straight lines between boxes indicate introns. When mRNA is formed from the gene, two completely distinct first exons of *PGC-1α* (exon 1a and 1b) can be spliced to the common exon 2. Furthermore, exon 1b can be spliced to the common exon 2 in two different ways producing either *PGC-1α* exon 1b- or 1b′-derived transcripts. In addition to differences in the starting exon, the splice variants of *PGC-1α* differ via alternative 3′ splicing. The exon subsequent to exon 6 may be either exon 7a (ex7a) or exon 7b (ex7b). Ex7a is the exon insert, which contains an in-frame stop codon resulting in the shorter N-truncated proteins (*NT-PGC-1α*). Ex7b is present in nontruncated full-length *PGC-1α* proteins, which are translated using all 13 exons of *PGC-1α*. The proximal promoter drives the transcription of *PGC-1α* exon 1a-derived transcripts (truncated and nontruncated) and the alternative promoter the transcription of *PGC-1α* exon 1b and 1b′-derived transcripts (truncated and nontruncated). (B) Detailed descriptions of primer pairs and their possible cDNA targets are presented. Primer pairs for detecting *PGC-1α* exon 1a-, 1b-, 1b′-derived transcripts are specific for different first exons, but do not separate truncated and nontruncated *PGC-1α* splice variants. Primer pair for total *NT-PGC-1α* is specific for truncated *PGC-1α* splice variants, but do not separate differences in first exon. The total *PGC-1α* primer pair was designed to detect all truncated and nontruncated splice variants of *PGC-1α*. The possible exon structures of mRNA targets for each primer pair are illustrated with gray boxes. The structure is presented only from the first exon to Ex7a or Ex7b because the mRNA structure is common in following exons (Ex8–Ex13). Binding sites of target specific forward (F) and reverse (R) primers are pointed out by arrows drawn next to the cDNA sequence in question. The sequences of all primers are also listed in Table 1. The sequences are amplicon sequences plus five nucleotides in the 3′ and 5′ end. The sequences of every other exon are bolded to separate subsequent exons from each other. The sequences were constructed by using human PGC-1α cDNA sequence (Ensembl: ENST00000264867), human PGC-1α gene sequence with its upstream regions (NCBI, Gene ID: 10891), and published cDNA structures of murine PGC-1α splice variants (Wen et al. 2014; Ruas et al. 2012).

Table 1. RT-qPCR primers used with the SYBR green method

Transcript	Strand	Sequence 5′–3′
PGC-1α exon 1a derived	Forward	ATGGAGTGACATCGAGTGTGCT
	Reverse	GAGTCCACCCAGAAAGCTGT
PGC-1α exon 1b derived	Forward	CTATGGATTCAATTTTGAAATGTGC
	Reverse	CTGATTGGTCACTGCACCAC
PGC-1α exon 1b′ derived	Forward	TGAAAGTGAGTATCAGGAGGCA
	Reverse	CTGATTGGTCACTGCACCAC
Total *NT-PGC-1α*	Forward	TCACACCAAACCCACAGAGA
	Reverse	CTGGAAGATATGGCACAT
Total *PGC-1α*	Forward	AGCCTCTTTGCCCAGATCTT
	Reverse	GGCAATCCGTCTTCATCCAC
PGC-1β	Forward	GAGTCAAAGTCGCTGGCATC
	Reverse	AACTATCTCGCTGACACGCA
Myostatin	Forward	CTACAACGGAAACAATCATTACCA
	Reverse	GTTTCAGAGATCGGATTCCAGTAT

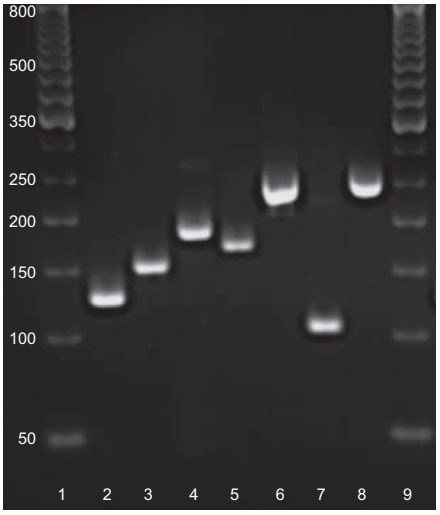

Figure 2. RT-qPCR products on agarose gel. The bands correspond to the calculated amplicon sizes: *PGC-1α* exon 1a- (127 bp, lane 2), 1b- (153 bp, lane 3), 1b′ (188 bp, lane 4)-derived transcripts, total *NT-PGC-1α* (172 bp, lane 5), total *PGC-1α* (241 bp, lane 6), *PGC-1β* (104 bp, lane 7), and *myostatin* (243 bp, lane 8). 50-bp DNA ladder at lanes 1 and 9.

When PRE values below the detection limit (C_q value before of which amplification was repeatable and specific) were replaced with the detection limit values (C_q 34.9), the average change was 67-fold at 180 min after RE ($P < 0.01$) and ninefold at 180 min after EE ($P < 0.05$). The expression of truncated *PGC-1α* transcripts (total *NT-PGC-1α*) (Fig. 3D) was increased at 180 min after RE (fivefold, $P < 0.01$) and 30 min after EE (1.7-fold, $P < 0.01$). The expression of total *PGC1α* (all truncated and nontruncated splice variants together) (Fig. 3E) was increased at 180 min after RE (fourfold, $P < 0.01$) and 30 min after EE (1.8-fold, $P < 0.05$). *PGC1β* had no significant gene expression response to either of the exercises (Fig. 3F).

Gene expression responses of PGC-1α-regulated genes after RE and EE

The gene expression of mitochondrial marker *cytochrome c* was increased at 30 min after EE (1.7-fold, $P < 0.05$, Fig. 4A), but there were no responses to RE. However, the gene expression of angiogenesis regulator *VEGF-A* was increased both after EE (threefold, $P < 0.05$) and RE (twofold, $P < 0.05$). EE-induced response was significant already 30 min after exercise, but RE-induced response did not appear until 180 min after exercise (Fig. 4B). RE decreased (2.5-fold, $P < 0.05$) the gene expression of *myostatin*, the known inhibitor of muscle growth, without response to EE (Fig. 4C).

The level of PGC-1α proteins, p-p38 MAPK$^{Thr180/Tyr182}$ and p-AMPKα^{Thr172}, and their associations with studied gene expression changes

The protein level of full-length nontruncated PGC-1α was increased at 180 min after RE (2.3-fold, $P < 0.05$, Fig. 5A) without changes after EE ($n = 7$). The results of phosphorylated p38 MAPK$^{Thr180/Tyr182}$ and AMPKα^{Thr172} have been previously published from pre to post 30 min (Ahtiainen et al. 2015). The present study adds to that study a new time point (180 min) and because of this, the data were reanalyzed using different statistics, and the gel-to-gel variation was normalized differently. The level of the active phosphorylated form of p38 MAPK$^{Thr180/Tyr182}$ was increased by ninefold ($P < 0.05$, Fig. 5B) at 30 min after RE, but not after 180 min or EE. The level of p-AMPKα^{Thr172} was increased by fourfold at 30 min after RE (Fig. 5C), but not anymore after 180 min. There was also a trend ($P = 0.07$) for increased levels of p-AMPKα^{Thr172} at 30 min after EE.

There were no strong associations between the exercise-induced changes in p-p38 MAPK$^{Thr180/Tyr182}$ or p-AMPKα^{Thr172} levels and the gene expression responses of *PGC-1* isoforms, *PGC-1β*, and *myostatin* in either of the exercise groups. However, the level change of p-*AMPKα*^{Thr172} (ratio 30′/PRE) associated with the corresponding changes in *VEGF-A* ($r_s = 0.821$, $P = 0.023$) and *CYC* ($r_s = 0.75$, $P = 0.052$) at 30 min after EE. Similar associations were

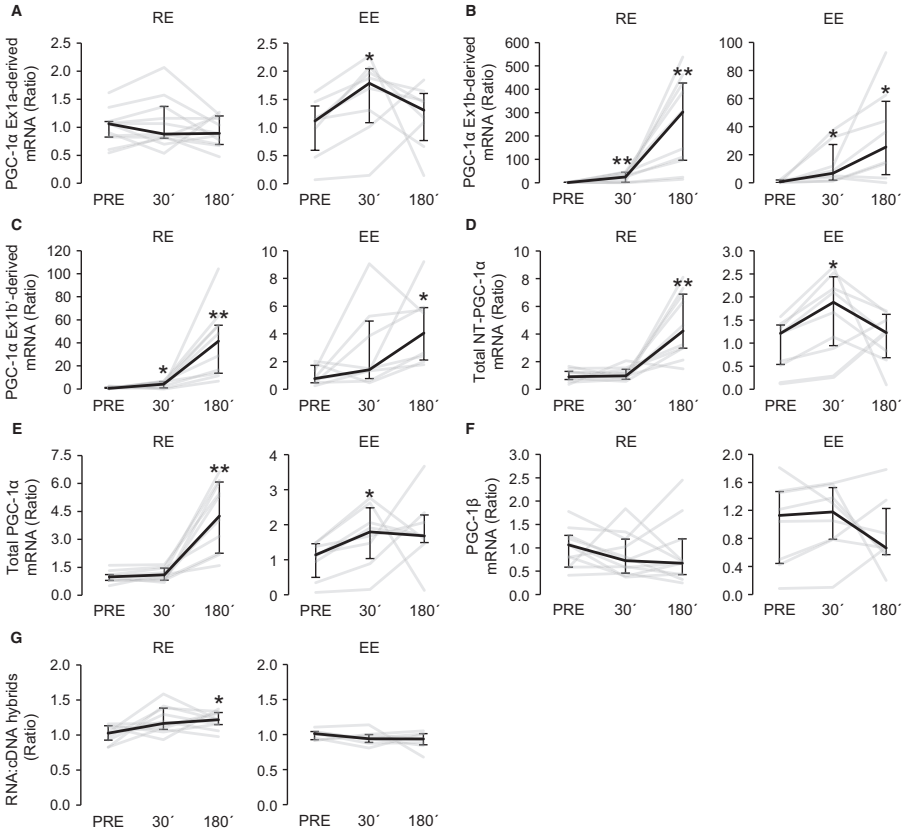

Figure 3. The expression profiles of *PGC-1α* exon 1a-derived transcripts (A), *PGC-1α* exon 1b-derived transcripts (B), *PGC-1α* exon 1b'-derived transcripts (C), total *NT-PGC-1α* (D), total *PGC-1α* (E), and *PGC1β* (F) at 30 min (30′) and 180 min (180′) after resistance (RE, $n = 11$) and endurance (EE, $n = 8$) exercises. The gene expression data of each sample are normalized to corresponding relative concentration value of RNA:cDNA hybrids (G). The gene expression changes are presented in relation to PRE average. Black lines represent median responses to exercise and gray lines represent individual responses. Error bars represent interquartile range. *Wilcoxon matched pairs signed-rank test with Holm–Bonferroni correction $P < 0.05$ versus PRE, **$P < 0.01$ versus PRE.

also found after EE when the both time points after exercise were pooled (ratio 30′/PRE and ratio 180′/PRE) and analyzed together (*VEGF-A*: $r_s = 0.608$, $P = 0.036$; *CYC*: $r_s = 0.601$, $P = 0.039$).

Discussion

The main findings of this study were that (1) both EE and RE induced significant increase in the gene expression of alternative promoter originated *PGC-1α* exon 1b- and 1b'-derived isoforms, whereas the proximal promoter originated *PGC-1α* exon 1a-derived transcripts were less inducible and were upregulated only after EE; (2) truncated *PGC-1α* transcripts were upregulated markedly after RE and slightly after EE; (3) based on the marker gene expression changes, EE induced responses typical for angiogenesis and mitochondrial biogenesis, while RE induced responses typical for angiogenesis and muscle

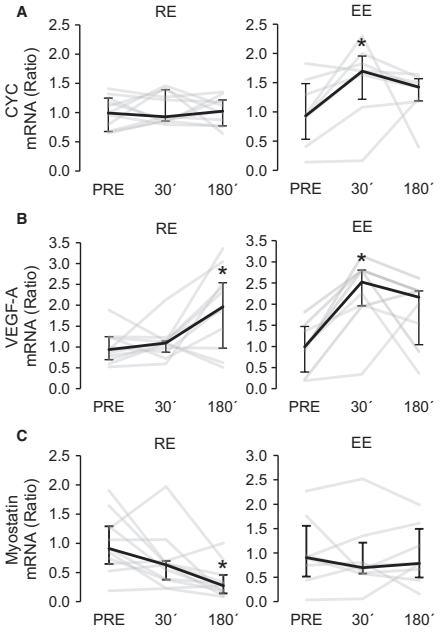

Figure 4. Gene expression changes of known PGC-1α target genes *cytochrome C* [(A), *CYC*], *VEGF-A* (B), and *myostatin* (C) at 30 min (30′) and 180 min (180′) after resistance (RE, $n = 11$) and endurance (EE, $n = 8$) exercises. The gene expression changes are presented in relation to PRE average. Black lines represent median responses to exercise and gray lines individual responses. Error bars represent interquartile range. *Wilcoxon matched pairs signed-rank test with Holm–Bonferroni correction $P < 0.05$ versus PRE, **$P < 0.01$ versus PRE.

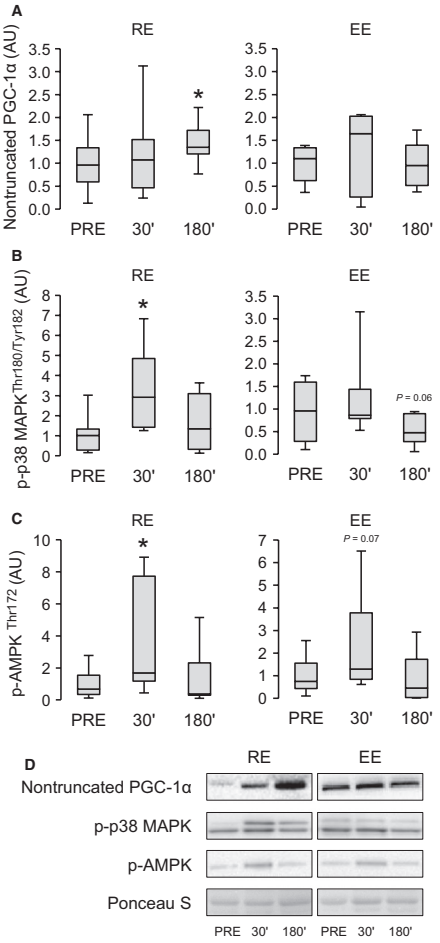

Figure 5. The effect of endurance (EE, $n = 7$) and resistance (RE, $n = 9$) exercises on levels of nontruncated PGC-1α proteins (A), p-p38-MAPK (B), and p-AMPK (C) at 30 min (30′) and 180 min (180′) after exercise. The results are presented in relation to PRE average and the box plots show minimum–maximum values, interquartile ranges, and medians. *Wilcoxon matched pairs signed-rank test with Holm–Bonferroni correction $P < 0.05$ versus PRE. Representative immunoblot images of one individual (D).

hypertrophy; (4) both EE and RE increased the levels of phosphorylated p38 MAPK and AMPKα, but these changes were not linked to the gene expression responses of *PGC-1* isoforms.

The primary aim of the present study was to investigate the acute mRNA responses of different *PGC-1* isoforms after high-load resistance exercise and moderate intensity endurance exercise. The RE and EE protocols used in the present study differed significantly from protocols used in other human studies with a similar aim. The RE protocol was designed to represent common hypertrophic RE for leg muscles. It consisted of significantly more sets (10 vs. 4) and had shorter recovery periods (2 vs. 5 min) between sets compared to study of Ydfors et al. (2013) who also used leg press loading in their study. Other studies (Lundberg et al. 2014; Norrbom et al. 2011) have used knee extension ergometers in the RE loading. The present EE protocol consisted of strenuous walking on

treadmill. Even though being common recreational exercise mode, the effects of walking exercises on expression of *PGC-1* isoforms have not been studied earlier. All previous studies (Popov et al. 2014; Ydfors et al. 2013; Gidlund et al. 2015) investigating *PGC-1* splice variant responses have used a bicycle loading for EE. The tests of maximal strength (MVC), explosive strength (CMJ), and lactate levels indicated that RE was anaerobic exercise that predictably induced significant fatigue. As intended, the intensity of EE was close to the onset of blood lactate accumulation ($4.0\ mmol{\cdot}L^{-1}$) and EE induced lesser muscular fatigue in leg extensors compared to RE.

The current results together with previous studies (Lundberg et al. 2014; Ydfors et al. 2013; Norrbom et al. 2011; Gidlund et al. 2015) showed clearly that the expression of alternative promoter driven *PGC-1α* transcripts (exon 1b and 1b'-derived) are strongly induced after different types of RE and EE, whereas transcripts originating from proximal promoter (*PGC-1α* exon 1a-derived) are much less inducible. In the present study, proximal promoter driven transcripts were induced only after EE and the magnitude of the response was slight compared to strong responses seen in alternative promoter-driven transcripts after EE (Fig. 4A–C). Our study is the first that reports the RE-induced responses of *PGC-1α* exon 1b'-derived transcripts in human skeletal muscle. Popov et al. (2014) have reported earlier the responses of these transcripts after EE, but the reverse primer used in the detection of these transcripts contained two mismatch nucleotides, which may have impaired the specificity and function of this primer pair. The same primer pair with mismatch nucleotides was used earlier also in the study of Ruas et al. (2012) for detection of *PGC-1α3*. The rodent studies have shown that alternative promoter originated *PGC-1α* isoforms, which were also induced in the present study, promote angiogenesis (Chinsomboon et al. 2009), mitochondrial biogenesis, and improve fatty acid oxidation capacity in skeletal muscles (Miura et al. 2008). Despite different exercise modes and protocols, both RE and EE increased the expression of truncated *PGC-1α* transcripts (total *NT-PGC-1α*) similarly to earlier studies (Gidlund et al. 2015; Popov et al. 2014; Ydfors et al. 2013). Interestingly, it has been shown recently that hypoxia specifically induces truncated forms of *PGC-1α* (*NT-PGC-1α* and *PGC-1α4*), which induces *VEGF* expression and angiogenesis, while having only a little effect on mitochondrial genes (Thom et al. 2014). In this study, neither RE nor EE modulated the expression of *PGC-1β* thus supporting the assumption that PGC-1β is not transcriptionally regulated after exercise (Meirhaeghe et al. 2003).

According the conventional dogma, chronic EE (low-intensity to high-volume loading) favors skeletal muscle adaptations (e.g., mitochondrial biogenesis, angiogenesis and improved β-oxidation) enhancing oxidative capacity with modest effect on muscle size (Holloszy and Booth 1976). Conversely, RE (high–intensity to low-volume loading) increases protein accretion promoting muscle hypertrophy and force (Hawley et al. 2014). The present increased gene expression of mitochondrial marker *cytochrome c* by EE but not RE suggests that mitochondrial adaptation was induced preferentially by EE. In contrast, angiogenic response seemed to be stimulated by both EE and RE because both exercise types increased the mRNA expression of angiogenesis regulator *VEGF-A*. As expected, RE decreased the gene expression of *myostatin*, the known target of PGC-1α4 (Ruas et al. 2012) and an inhibitor of muscle growth, but the EE did not have any effect. The downregulation of *myostatin* may be a part of hypertrophic response induced by RE (Hulmi et al. 2007). Yet, the importance of the role of myostatin in hypertrophic response to RE in humans is still unclear and needs further experimental evidence.

To check whether the activation changes of known signaling molecules regulating *PGC-1α* expression would explain the expression changes of specific isoforms of *PGC-1*, the levels of p-p38 MAPKThr180/Tyr182 and p-AMPKαThr172 were measured. The levels of p-p38 MAPK were increased after RE and levels of p-AMPKα after both RE and EE. However, the phosphorylation changes of these signaling molecules were not associated with the gene expression responses of *PGC-1* isoforms. This result is not fully consistent with the study of Norrbom et al. (2011), which indicated that AMPK is a major regulator of *PGC-1α* transcripts from the proximal promoter, but the expression of transcripts from an alternative promoter are regulated by *β*-adrenergic signaling in combination with AMPK. Even if AMPK activation did not explain *PGC-1* isoform responses, we found that *VEGF-A* and *CYC* responses 30 min after EE were associated with a corresponding change in the level of p-AMPKα suggesting that AMPK activation may partly explain *VEGF-A* and *CYC* responses seen after EE.

There were some limitations in our study. Because two separate exercise groups were used instead of a crossover design, the experimental setup did not allow direct comparison of gene expression responses between RE and EE. This study included walking endurance exercise, and it should be noted that another type of endurance exercise than continuous strenuous walking might induce different kind of cellular signaling responses in the front thigh muscles. It is also acknowledged that the time point: immediately after exercise could have been more optimal for detecting peak AMPK and p38 MAPK phosphorylation responses. However, the phosphorylation of these signaling proteins may not drop dramatically during the

first 30 min after exercise (Bartlett et al. 2012; Sriwijitkamol et al. 2007). The present and previous studies (e.g., Bartlett et al. 2012; Lundberg et al. 2014; Popov et al. 2014; Gidlund et al. 2015) have shown that the studied transcripts seem to peak during the first 3 h after exercise. Thus, the selected time points can be considered justified and valid for the gene expression response detection of the studied genes. Our setup measured only acute exercise responses without physiological outcome variables of long-term training effects, which could be connected to measured acute exercise responses.

In conclusion, this study comprehensively assayed *PGC-1* transcripts in human skeletal muscle and showed specific response profiles after the present RE and EE. The study established that both alternative promoter originated *PGC-1α* exon 1b- and 1b'-derived transcripts are strongly induced after EE and RE, whereas the proximal promoter originated *PGC-1α* exon 1a-derived transcripts are less inducible and were upregulated only after EE. Truncated *PGC-1α* transcripts were upregulated both after EE and RE, thus there was no clear exercise-type specificity observed in the responses of these transcripts. The expression changes of marker genes suggested that EE induced responses typical for angiogenesis and mitochondrial biogenesis, while RE induced responses typical for angiogenesis and muscle hypertrophy. Our results improve the understanding of exercise-type specific early signaling events and support the idea that gene expression responses of *PGC-1α* isoforms may have an important role in exercise-induced muscle adaptations. However, future studies are still required to verify the roles of different *PGC-1α* isoforms in the mechanisms of muscle adaptation.

Acknowledgements

The authors thank Ms. Sheila Gagnon, M.Sc., Opri Jokelainen, M.Sc., Suvi Pulkkinen, M.Sc., Sira Karvinen, M.Sc., Mira Tuovinen, Mr. Risto Puurtinen, and Mrs. Aila Ollikainen for their work in data collection and analyses.

Conflict of Interests

None declared.

References

Ahtiainen, J. P., S. Walker, M. Silvennoinen, H. Kyröläinen, B. C. Nindl, K. Häkkinen, et al. 2015. Exercise type and volume alter signaling pathways regulating skeletal muscle glucose uptake and protein synthesis. Eur. J. Appl. Physiol. 115:1835–1845.

Atherton, P. J., J. Babraj, K. Smith, J. Singh, M. J. Rennie, and H. Wackerhage. 2005. Selective activation of AMPK-PGC-1alpha or PKB-TSC2-mTOR signaling can explain specific adaptive responses to endurance or resistance training-like electrical muscle stimulation. FASEB J. 19:786–788.

Baar, K., and K. Esser. 1999. Phosphorylation of p70(S6k) correlates with increased skeletal muscle mass following resistance exercise. Am. J. Physiol. 276:C120–C127.

Baar, K., A. R. Wende, T. E. Jones, M. Marison, L. A. Nolte, M. Chen, et al. 2002. Adaptations of skeletal muscle to exercise: rapid increase in the transcriptional coactivator PGC-1. FASEB J. 16:1879–1886.

Bartlett, J.D., C. Hwa Joo, T. S. Jeong, J. Louhelainen, A. J. Cochran, M. J. Gibala, et al. 2012. Matched work high-intensity interval and continuous running induce similar increases in PGC-1alpha mRNA, AMPK, p38, and p53 phosphorylation in human skeletal muscle. J. Appl. Physiol. (1985) 112:1135–1143.

Canto, C., L. Q. Jiang, A. S. Deshmukh, C. Mataki, A. Coste, M. Lagouge, et al. 2010. Interdependence of AMPK and SIRT1 for metabolic adaptation to fasting and exercise in skeletal muscle. Cell Metab. 11:213–219.

Chinsomboon, J., J. Ruas, R. K. Gupta, R. Thom, J. Shoag, G. C. Rowe, et al. 2009. The transcriptional coactivator PGC-1alpha mediates exercise-induced angiogenesis in skeletal muscle. Proc. Natl. Acad. Sci. U. S. A. 106:21401–21406.

Egan, B., B. P. Carson, P. M. Garcia-Roves, A. V. Chibalin, F. M. Sarsfield, N. Barron, et al. 2010. Exercise intensity-dependent regulation of peroxisome proliferator-activated receptor coactivator-1 mRNA abundance is associated with differential activation of upstream signalling kinases in human skeletal muscle. J. Physiol. 588:1779–1790.

Gibala, M. 2009. Molecular responses to high-intensity interval exercise. Appl. Physiol. Nutr. Metab. 34:428–432.

Gidlund, E. K., M. Ydfors, S. Appel, H. Rundqvist, C. J. Sundberg, and J. M. Norrbom. 2015. Rapidly elevated levels of PGC-1alpha-b protein in human skeletal muscle after exercise: exploring regulatory factors in a randomized controlled trial. J. Appl. Physiol. (1985) 119:374–384.

Hawley, J. A., M. Hargreaves, M. J. Joyner, and J. R. Zierath. 2014. Integrative biology of exercise. Cell 159:738–749.

Holloszy, J. O., and F. W. Booth. 1976. Biochemical adaptations to endurance exercise in muscle. Annu. Rev. Physiol. 38:273–291.

Hulmi, J. J., J. P. Ahtiainen, T. Kaasalainen, E. Pöllänen, K. Häkkinen, M. Alen, et al. 2007. Post exercise myostatin and activin IIb mRNA levels: effects of strength training. Med. Sci. Sports Exerc. 39:289–297.

Hulmi, J. J., S. Walker, J. P. Ahtiainen, K. Nyman, W. J. Kraemer, and K. Häkkinen. 2012. Molecular signaling in muscle is affected by the specificity of resistance exercise protocol. Scand. J. Med. Sci. Sports 22:240–248.

Kim, J. S., J. K. Petrella, J. M. Cross, and M. M. Bamman. 2007. Load-mediated downregulation of myostatin mRNA is not sufficient to promote myofiber hypertrophy in humans: a cluster analysis. J. Appl. Physiol. (1985) 103:1488–1495.

Koressaar, T., and M. Remm. 2007. Enhancements and modifications of primer design program Primer3. Bioinformatics 23:1289–1291.

Lundberg, T. R., R. Fernandez-Gonzalo, J. Norrbom, H. Fischer, P. A. Tesch, and T. Gustafsson. 2014. Truncated splice variant PGC-1alpha4 is not associated with exercise-induced human muscle hypertrophy. Acta Physiol. (Oxf) 212:142–151.

Lundby, C., N. Nordsborg, K. Kusuhara, K. M. Kristensen, P. D. Neufer, and H. Pilegaard. 2005. Gene expression in human skeletal muscle: alternative normalization method and effect of repeated biopsies. Eur. J. Appl. Physiol. 95:351–360.

Meirhaeghe, A., V. Crowley, C. Lenaghan, C. Lelliott, K. Green, A. Stewart, et al. 2003. Characterization of the human, mouse and rat PGC1 beta (peroxisome-proliferator-activated receptor-gamma co-activator 1 beta) gene in vitro and in vivo. Biochem. J. 373:155–165.

Miura, S., Y. Kai, Y. Kamei, and O. Ezaki. 2008. Isoform-specific increases in murine skeletal muscle peroxisome proliferator-activated receptor-gamma coactivator-1alpha (PGC-1alpha) mRNA in response to beta2-adrenergic receptor activation and exercise. Endocrinology 149:4527–4533.

Norrbom, J., E. K. Sallstedt, H. Fischer, C. J. Sundberg, H. Rundqvist, and T. Gustafsson. 2011. Alternative splice variant PGC-1alpha-b is strongly induced by exercise in human skeletal muscle. Am. J. Physiol. Endocrinol. Metab. 301:E1092–E1098.

Olesen, J., K. Kiilerich, and H. Pilegaard. 2010. PGC-1alpha-mediated adaptations in skeletal muscle. Pflugers Arch. 460:153–162.

Pilegaard, H., B. Saltin, and P. D. Neufer. 2003. Exercise induces transient transcriptional activation of the PGC-1alpha gene in human skeletal muscle. J. Physiol. 546:851–858.

Popov, D. V., A. V. Bachinin, E. A. Lysenko, T. F. Miller, and O. L. Vinogradova. 2014. Exercise-induced expression of peroxisome proliferator-activated receptor gamma coactivator-1alpha isoforms in skeletal muscle of endurance-trained males. J. Physiol. Sci. 64:317–323.

Ranhotra, H. S. 2010. Long-term caloric restriction up-regulates PPAR gamma co-activator 1 alpha (PGC-1alpha) expression in mice. Indian J. Biochem. Biophys. 47:272–277.

Ruas, J. L., J. P. White, R. R. Rao, S. Kleiner, K. T. Brannan, B. C. Harrison, et al. , et al. 2012. A PGC-1alpha isoform induced by resistance training regulates skeletal muscle hypertrophy. Cell 151:1319–1331.

Sriwijitkamol, A., D. K. Coletta, E. Wajcberg, G. B. Balbontin, S. M. Reyna, J. Barrientes, et al. 2007. Effect of acute exercise on AMPK signaling in skeletal muscle of subjects with type 2 diabetes: a time-course and dose-response study. Diabetes 56:836–848.

Thom, R., G. C. Rowe, C. Jang, A. Safdar, and Z. Arany. 2014. Hypoxic induction of vascular endothelial growth factor (VEGF) and angiogenesis in muscle by truncated peroxisome proliferator-activated receptor gamma coactivator (PGC)-1alpha. J. Biol. Chem. 289:8810–8817.

Untergasser, A., I. Cutcutache, T. Koressaar, J. Ye, B. C. Faircloth, M. Remm, et al. 2012. Primer3–new capabilities and interfaces. Nucleic Acids Res. 40:e115.

Wen, X., J. Wu, J. S. Chang, P. Zhang, J. Wang, Y. Zhang, et al. 2014. Effect of exercise intensity on isoform-specific expressions of NT-PGC-1 alpha mRNA in mouse skeletal muscle. Biomed. Res. Int. 2014:402175.

Ydfors, M., H. Fischer, H. Mascher, E. Blomstrand, J. Norrbom, and T. Gustafsson. 2013. The truncated splice variants, NT-PGC-1alpha and PGC-1alpha4, increase with both endurance and resistance exercise in human skeletal muscle. Physiol. Rep. 1:e00140.

Zhang, Y., P. Huypens, A. W. Adamson, J. S. Chang, T. M. Henagan, A. Boudreau, et al. 2009. Alternative mRNA splicing produces a novel biologically active short isoform of PGC-1alpha. J. Biol. Chem. 284:32813–32826.